HALOCOMPLEXES OF NIOBIUM AND TANTALUM IN REDUCED OXIDATION STATES

by

Dinsukh Lal

A thesis submitted in partial fulfillment of the requirements for the degree of Doctor of Philosophy (Chemistry)

to

the School of Graduate Studies of

the University of Ottawa

September 1973

To

Anne, Kieran and Anita

ABSTRACT

This work deals with magnetic, spectroscopic and thermochemical aspects of the chemistry of halogen compounds of niobium and tantalum in the quadrivalent state.

Studies were made of A_2MX_6 (A = alkali metal, M = Nb, Ta; X = Cl, Br, I) prepared by heating stoichiometric quantities of starting materials at the melting point of the alkali halides, also by heating at 300°C and by precipitation from concentrated hydrochloric acid. Single crystals of K_2NbCl_6 were prepared by cooling a melt consisting of stoichiometric quantities of KCl and $NbCl_4$ through a steep temperature gradient.

The magnetic investigations showed that the susceptibility data were influenced by the conditions of preparation. Plots of susceptibility against 1/T for the hexahaloniobates prepared at high temperatures were found to be curved, contrary to expectation for a d^1 system. Cs_2NbCl_6 prepared at 300°C and the salts having non-cubic symmetry gave linear plots. A dilute solid solution of K_2NbCl_6 and K_2ZrCl_6 also gave a linear plot. The curved nature of certain plots of molar susceptibility is attributed to a mixed valence nature of the A_2NbCl_6 systems i.e. the niobium is assumed to be present as a mixture of Nb^V, Nb^{IV} and either Nb^{III} or Nb^{II}. Plots of χ_m versus 1/T for K_2TaCl_6 were linear. The electronic

spectra indicate that K_2TaCl_6 is probably similar to K_2NbCl_6 in containing a mixture of ion types. The magnetic behaviour is "normal" however and could be explained as being due to the Ta(IV) alone.

Electronic spectra of the various solid complexes were studied by reflectance spectroscopy. Cs_2NbCl_6 prepared at 300°C had fairly strong bands at 10 kK and 25 kK which suggests that a considerable quantity of the cluster compound $Cs_4Nb_6Cl_{18}$ had been formed at 300°C. The intense band at ~ 19 kK in the spectra of alkali-metal hexahaloniobates appeared only as a shoulder in $(Pyh)_2NbCl_6$. Its greatly reduced intensity suggests that it is not a feature of the spectrum of the $NbCl_6^{2-}$ ion. Spectral examination of $K_2(Nb,Zr)Cl_6$ crystals provided further evidence that the 19 kK band is not due to a d-d transition. It is suggested rather that this band is due to an intervalence charge transfer transition.

Upon examination of the infrared spectra of powdered single crystals of K_2NbCl_6 and other A_2NbCl_6 polycrystalline systems, several bands were found in the 200-400 cm^{-1} region, more than the number of bands predicted by theory for octahedral systems. A band at ~ 310 cm^{-1} is assigned to the Nb(IV)-Cl

stretch in these systems. Weak shoulders are attributed to Nb(V)-Cl and Nb(II)-Cl or Nb(III)-Cl stretching.

The systems "K_2NbCl_5" and "K_2NbCl_4" which have been reported in the literature were also examined. The former is shown to be a mixture of K_2NbCl_6, $K_4Nb_6Cl_{18}$ and other impurities. "K_2NbCl_4" is in fact found to be the cluster compound $K_4Nb_6Cl_{18}$ mixed with KCl and Nb.

The enthalpies of reactions of the type:

$$2AX(c) + MX_4(c) \rightarrow A_2MX_6(c)$$

were measured calorimetrically and the values used to obtain heats of reaction for the processes:

$$2AX(g) + MX_4(g) \rightarrow A_2MX_6(c)$$

Considerations of these partial gas phase enthalpies suggests that niobium exhibits some degree of class (b) character.

The chlorozirconates were found to be slightly more stable than chloroniobates. This is rationalized on the basis of chlorine to metal π-bonding.

The decomposition pressures of niobium tetrabromide according to the process

$$(5-x)NbBr_4(s) \rightleftharpoons NbBr_x(s) + (4-x)NbBr_5(g)$$

were measured by a dew point technique and the existence region of the various bromide phases obtained.

Acknowledgements

Numerous people have helped towards completion of this work and I would especially like to mention the following:

- to Dr. Alan Westland for supervising this work with interest and concern. I wish to thank him particularly for his understanding and patience in the early stages of this work and for invaluable advise and guidance in the later stages of this work. His readiness in help with experimental work and to discuss various aspects of the problems were more than welcome. To him, I offer my heartfelt thanks.
- to Isabelle Boisclair and Francois Sarrazain, for their invaluable help in preparation of the diagrams for this thesis; to Jerome Bezaire for proofreading sections of this thesis.
- to Dr. W. Rank (National Research Council, Ottawa) for carrying out the study of mixed crystal systems mentioned in this thesis.
- to Liza Siemsen for assistance with magnetic and x-ray work; to Larrie Thomson for helping with calorimetric work.
- to Edward Hearns (Department of Geology, University of Ottawa) for many hours of assistance with microscope work.
- to Dr. A. Manoogian (Department of Physics, University of Ottawa) for recording the e.s.r. spectra; to Dr. Wyn Gilbert (National Research Council) for recording the Raman Spectra.

- to the technical staff of the Department and especially to Mr. Egon Kristoff for his assistance with many difficult aspects of glassblowing and also with the design and fabrication of the apparatus.

- to Janet Savage for typing services beyond the call of duty.

- to National Research Council for research grant under the name of Dr. Westland and to the Ontario Government for the Ontario Graduate Fellowship for the years 1970, 1971 and 1972.

I would also like to thank my families in Fiji Islands and Dunedin (New Zealand). I am deeply grateful for their moral support.

Finally I would like to extend my deep gratitude to my wife, Anne, son Kieran and daughter Anita for their patience and understanding throughout the course of this work.

CONTENTS

LIST OF FIGURES

LIST OF TABLES

Abbreviations

(PyH) = C_5H_5NH

F.C.C. = face centred cubic

F.C.T. = face centred tetragonal

Fus. = fusion

Trans = transformation

Ghz = 10^9 Hertz

kK = kilokayser = 1000 cm^{-1}

CHAPTER 1

INTRODUCTION

Niobium and tantalum are very much alike chemically and are therefore closely associated in nature. Their discovery occurred almost simultaneously, i.e. in 1801 and 1802 respectively, but the similarity of their chemical properties caused great difficulty in establishing their individual identity. For many decades, the elements remained comparatively obscure and the principal contribution to their chemistry was that of Marignac (1) who discovered in 1865 that these metals could be separated by utilizing the marked difference in the solubilities of their double fluorides of potassium.

Interest in niobium revived in the decade following the year 1960 owing in part to the discovery of large deposits of niobium minerals. In Canada, pyrochlore deposits are mined in three principal areas: in the Oka district near Montreal, on the Manitoulin Islands near North Bay, Lake Nipissing, and in the Trout Lake area north-west of Sudbury. Reserves may total 135 million tons averaging 0.35 percent Nb_2O_5. Canada's only producer of niobium oxide, St. Lawrence Columbium Corporation, increased its output of Nb_2O_5 by nearly 50% in 1969 to maintain Canada's position as the non-communist world's

second largest producer. Initial Canadian shipments of tantalite concentrates were made from Bernic Lake, Manitoba in 1970.

The expanded production of these minerals has been occasioned by the increased use of niobium for modern technology. One of the important recent uses of niobium, which takes advantage of its high melting point and its resistance to heat, is the production of heat-resistent alloys for high-speed tools, jet engines, gas turbines and rocketry equipment. Niobium is also used as a fabricating material in nuclear technology.

The present study can be loosely divided into two sections:

(A) Magnetic and spectroscopic properties of the complex halides of these metals in low oxidation states.

(B) Thermochemical studies of some simple and complex halides of these metals.

(A) In general, much more is known about the chemistry of elements in the first transition series than of those in the remaining periods. This is particularly true of the elements in the titanium and vanadium sub groups. For example, vanadium commonly exhibits oxidation states of +5, +4, +3 and +2 and the states +1, 0, and -1 are known as well.

By contrast, investigations into the chemistry of niobium and tantalum have largely been confined to studies of these elements in their maximum oxidation states.

Prior to 1960, only a few well characterized compounds containing niobium and tantalum in oxidation states less than five were known. These include the tetravalent and trivalent halides, the cluster compounds containing the $Nb(Ta)_6X_{12}^{++}$ ion, the tetravalent oxides and some nitrides and sulphides etc. All of these compounds were prepared by high temperature reduction of pentavalent niobium compounds.

Many of the studies of the lower oxidation states of these elements were carried out in aqueous solution. Some workers (2-6) have attempted to devise methods for the volumetric determination of these metals by zinc reduction. However, there is much disagreement regarding the extent and reproducibility of the reduction.

In most of these solution studies there was a failure to isolate any well characterized species. The main difficulty in isolating compounds from solution is in large measure a result of the very limited conditions under which solutions of these highly acidic compounds are stable.

Many synthetic methods have been employed in order to prepare compounds in low oxidation states. A number of studies of the structure and chemical properties of niobium and tantalum cluster compounds have been reported (7-12).

A number of workers have prepared six-coordinate adducts of niobium and tantalum tetrahalides having nitrogen, oxygen, and sulphur as donor atoms (13-17). In some cases the tetrahalides were used as starting materials but in other cases pentahalides were found to be reduced by excess ligand to produce the tetravalent complex.

The existence of hexahaloniobates (IV) and hexahalotantalates (IV) was first demonstrated by Russian workers, from phase equilibrium studies of niobium and tantalum tetrachloride-alkali metal chloride systems (18-20). The most complete characterization of these salts was carried out by Torp (21a, 21b) who studied their spectral and magnetic properties. Torp found that for hexahalo-niobates, plots of molar susceptibility against 1/T were somewhat curved, contrary to expectation for d^1 systems. Similar plots for tantalum analogues were linear. The

behaviour of the niobium salts remained unexplained. The relative order of susceptibility for salts of the various alkali elements was believed to afford some slight evidence of superexchange interaction.

In a series of investigations of the magnetic properties of ions of the type MeX_6^{n-} where Me is an element from the second or third transition series, Westland et al. showed that compounds crystallizing with the K_2PtCl_6 structure were not magnetically dilute when the central ion is Re, Os or Ir (22, 23). On the other hand, Ru and Rh analogues were essentially free of superexchange interactions (24, 25). Since these examples were chosen from near to the right hand end of the respective series. it seemed desirable to extend the study to the d^1 systems, $NbCl_6^{2-}$ and $TaCl_6^{2-}$, i.e. from nearer the left hand side of the series. Moreover, the curvature in plots of susceptibilities against reciprocal temperature for the hexahaloniobates aroused our curiousity and prompted us to search for its origin.

Since the study by Torp, there have been several reports of work on hexahaloniobates and tantalates (26-29). It became clear that there were discrepancies and unexplained bands in the infrared and visible spectra reported by various workers including Torp. In view of these discrepancies it

was considered desirable to repeat the earlier studies as carefuily as possible and to clarify these anomalies.

(B) The thermochemical studies were carried out for several reasons.

(i) Possibly the most widely used technique for the preparation of lower halides of second and third transition series including niobium and tantalum has been a flow technique. Although at first sight this method seems very simple, it is capable of producing significantly different products by subtle variation of such conditions as temperature, flow rate, dilution with inert carrier gas, etc.

Early attempts at preparation of niobium tetrachloride involved passing hydrogen over the pentachloride maintained at 450°. The product was a mixture of tetrachloride and trichloride. This method is now seldom used because of the difficulty of controlling the composition of the product.

Transport in a thermal gradient has been fully exploited by Schäfer and his co-workers (30-33). Reduction of pentahalide is carried out in an evacuated tube. Metal is heated to a moderately high temperature at one end of the tube and the pentahalide is heated to a temperature that generates a vapour pressure sufficient to cause a reaction. The centre portion of the tube is maintained at a temperature

intermediate between that of the two ends, and the temperature is adjusted so that the product sublimes from the hottest zone to the centre compartment. If the product is a compound that tends to undergo thermal decomposition into one or both of the reactants, the decomposition can be avoided by adjustment of the temperature gradient. The diffusion of gases in a thermal gradient is such that the equilibrium conditions in the tube strongly favour formation of the required product, and removal of the product as a solid phase drives the reaction to completion.

The design of effective procedures of this type is facilitated by a knowledge of saturation vapour pressures and decomposition pressures. The niobium chlorides have received thorough attention (30,34) but information about the bromides is relatively lacking. For this reason, an investigation of the disproportionation of $NbBr_4$ was undertaken. An attempt was also made to measure the saturation vapour pressure of this compound. Owing to its tendency to decompose, the compound had to be examined in the presence of $NbBr_5$ vapour. The experimental difficulty of measuring the small partial pressure of the tetrabromide vapour caused this work to be discontinued.

(ii) There have been no reports of thermochemical studies of ternary niobium salts. It therefore seemed desirable to initiate work in this area. The enthalpy of formation of potassium hexachlorotantalate (IV) has been reported (35).

(iii) Further thermochemical investigation of niobium and tantalum compounds may have a fairly direct significance on the technology of these metals. Their broadening use in metallurgy has called for the development of new processes for producing these metals in high purity. The electrolysis of chlorides of niobium, tantalum and zirconium and other refractory metals in a melt of alkali chloride or in a mixture of alkali chlorides is one of the promising methods of producing these metals. Complexes, such as K_2NbCl_6 and K_2ZrCl_6 for example, may be intermediates in a chain of chemical reactions proceeding in electrolytic cells. Thus a study of such intermediates and the clarification of the possibility of using complex halides of these metals in lower oxidation states as electrolytes may require further basic knowledge

The following summary outlines the broad objectives of the work described in this thesis.

(a) An investigation of the magnetic properties of halocomplexes of niobium and tantalum. In particular it was sought to determine if a superexchange mechanism operates in these systems.

(b) Examination of the electronic and far infrared spectra of these complexes to account for the unexpected bands observed by previous workers.

(c) Measurement of thermochemical data which are needed for the bromides of the second and third transition series. Decomposition and saturation vapour pressures of niobium tetrabromide were of particular interest in view of the fact that similar studies on chloride systems had already been performed.

(d) Determination of the heats of formation of hexahalometallates of niobium, tantalum and zirconium by solution calorimetry and interpretation of the results in terms of periodicity relationships and current concepts of bonding.

CHAPTER 2

REVIEW OF PREVIOUS WORK

Since it is only a few years ago that halocomplexes of niobium(IV), tantalum(IV) and zirconium(IV) began to receive attention, the volume of literature is not large. Each publication will be reviewed here in some detail but initially, attention will be limited to methods and experiments rather than results. In the following chapters the results of the various workers will be compared with those obtained in the present work.

This chapter will be divided into two sections, although there will be some overlap:

A. Magnetic, spectroscopic and structural studies.

B. Thermochemical studies.

A. As stated earlier, Torp (21) has done the most extensive magnetic, spectral and x-ray work on the hexahalo salts of niobium(IV) and tantalum(IV). The compounds were prepared by heating a stoichiometric mixture of alkali metal chloride and metal tetrachioride in one end of an evacuated, sealed quartz tube which had been filled in the dry box. The tube was held at the melting point of the alkali metal halide for one to three hours in a resistance furnace. A temperature gradient was maintained with the end containing the material

ca. 50° cooler than the other end to prevent sublimation of metal tetrahalide from the reaction zone. Torp found that x-ray patterns of all the hexahalo complexes could be indexed on the basis of a cubic unit cell with the exception of K_2NbBr_6 which crystallized with a unit cell which was similar but which was distorted tetragonally.

The lattice parameters for the A_2MX_6 complexes are given below in Table I.

Table I. Lattice parameters of A_2MX_6 Complexes (21)

Complex	Lattice Type	Refined Lattice Parameters (Å)
K_2NbCl_6	FCC	$a_o = 9.97 \pm 0.01$
Rb_2NbCl_6	"	$a_o = 10.10 \pm 0.01$
K_2NbBr_6	FCT	$a_o = 10.38 \pm 0.01$
		$c_o = 10.86 \pm 0.01$
Rb_2NbBr_6	FCC	$a_o = 10.63 \pm 0.01$
Cs_2NbI_6	"	$a_o = 11.54 \pm 0.01$
K_2TaCl_6	"	$a_o = 9.96 \pm 0.01$
Rb_2TaCl_6	"	$a_o = 10.11 \pm 0.01$
Rb_2TaBr_6	"	$a_o = 10.62 \pm 0.01$

A point to note is the similarity in the unit cell dimensions of niobium and tantalum analogues. This is because the covalent radii of niobium(IV) and tantalum(IV) are almost

identical due to the lanthanide contraction experienced by elements in the third transition series.

Torp showed that K_2NbCl_6 is isomorphous with K_2PtCl_6. Since all of the cubic alkali metal hexahalo complexes of Nb(IV) and tantalum(IV) exhibit similar trends in the relative positions and intensities of x-ray diffraction lines, they evidently have the same structure.

The K_2PtCl_6 structure for these salts was confirmed by Smirnova and Vasil'kova (36). However, these authors later reported new isomorphs for some of these hexachlorometallates; in some cases the symmetry of tantalum compounds is not the same as that previously reported in spite of similar methods of preparation. The new parameters are given in Table II (37).

It is interesting to note that alkali metal hexahalometallates(IV) of the second and third transition series usually adopt the potassium hexachloroplatinate structure, which may be related to the CaF_2 type lattice by considering the complex anion as a single unit occupying the calcium positions of that structure.

Table II: New lattice parameters of A_2MCl_6 complexes (37)

Compound	Symmetry	Parameters (Å)
Rb_2NbCl_6	Cubic	a = 10.25
Cs_2NbCl_6	Cubic	a = 10.31
K_2TaCl_6	Tetragonal	a = 9.01 c = 12.43
Rb_2TaCl_6	Tetragonal	a = 10.67 c = 9.07
Cs_2TaCl_6	Cubic	a = 10.32

Torp has reported the diffuse reflectance spectra and magnetic properties of the hexahalo complexes. The compounds were examined in the solid state as no solvent could be found to dissolve the compounds without reaction. Torp also obtained a solution spectrum for $NbCl_4$ in molten pyridinium chloride and found it to be essentially similar to that of the solid state spectra of alkali hexachloroniobates.

The magnetic susceptibilities were measured by the Gouy method from 100°K to 300°K.

Horner et al. (26) have prepared Cs_2NbCl_6 and Cs_2TaCl_6 by interaction of correct proportions of the pentachlorides and caesium chlorides in the presence of red phosphorous. Alternately, $CsTaCl_6$ may be used as the starting material. The method involved heating mixtures of red phosphorous and metal chloride in a closed tube. By this

method they also prepared Cs_2MoCl_6 and Cs_2WCl_6.

Tyree's research group (27) has prepared Cs_2NbX_6 and Cs_2TaX_6 (X = Cl, Br) by heating a mixture of CsI and $CsMX_6$ (M = Nb, Ta) in a sealed tube. The temperature required for reaction in the several cases were: Cs_2NbCl_6 (200°) Cs_2TaCl_6 (300°), Cs_2NbBr_6 (250°). and Cs_2TaBr_6 (310°).

They also prepared the chloro salts by reaction of CsI with $CsNbCl_6$ or $CsTaCl_6$ in hexabutadiene An equimolar mixture of the reagents were suspended in 30 ml. of dry solvent, and the mixture was refluxed for several days. Their analytical results for chlorine and bromine were slightly low.

The electronic spectra of these salts were determined on samples which had been ground with freshly fused KCl and pressed into pellets. It was found that the charge transfer bands of MX_6^{1-} and MX_6^{2-} salts corresponded quite closely. Such a similarity of energies implies that the more electronegative pentavalent metal simply abstracts more electronic charge from the surrounding ligands, so that the effective nuclear charge on the metal is nearly the same for MX_6^{1-} and MX_6^{2-}. Certain other bands were assigned to d-d $^2T_{2g} \longrightarrow {}^2Eq$ transitions.

The room temperature magnetic moments and corrected susceptibilities are listed in Table III.

Table III: Magnetic data for A_2MX_6 complexes (27)*

Complex	Moments, (B.M.)	Molar susceptibility χ_m (e.m.u. mole^{-1})
Cs_2NbCl_6 (C_4Cl_6 suspension)	1.24	
Cs_2NbCl_6	1.24	
Cs_2NbBr_6	1.18	
Cs_2TaCl_6		97×10^{-6}
Cs_2TaBr_6		145×10^{-6}

*Measured at 20°C.

These authors were the first to report the infrared spectra of some of these salts in the low energy end of the infrared region.

Fowles et al. (28) have reported the preparation and properties of $[(C_2H_5)_4N]_2NbX_6$ (X = Cl or Br). The preparative method involved mixing the appropriate acetonitrile complex $NbX_4 \cdot 2CH_3CN$ and tetraethyl-ammonium halide using chloroform-acetonitrile (9:1 volume) as solvent. The reaction mixture was heated under gentle reflux for 2 weeks after which time reaction product was separated by filtration and dried. The magnetic and spectral studies of $[(C_2H_5)_4N]_2NbX_6$ (X = Cl Br) were reported.

Prior to Fowles' publication, Benzinger (29) had studied the electrochemical reduction of $[(C_2H_5)_4N]NbCl_6$ in acetonitrile and determined what products were formed and the potentials needed for their formation. The electrochemical reduction produced several species in oxidation states (IV) and (III). Orange crystals of $[(C_2H_5)_4N]_2NbCl_6$ separated from solution during the reduction.

The infrared spectrum showed a strong band at 920 cm^{-1} which is characteristic of metal-oxygen stretching. Benzinger was unable to obtain the spectrum in the 300 cm^{-1} region because $[(C_2H_5)_4N]_2NbOCl_5$ has a strong, broad absorption which extends from about 370 cm^{-1} to the instrumental cut-off at 260 cm^{-1}. A determination of the oxidation state of Nb in this compound supported the conclusion that the contaminant was $[(C_2H_5)_4N]_2NbOCl_5$.

The electronic spectrum and magnetic susceptibility of this compound were also recorded.

The magnetic susceptibility of $[(C_2H_5)_4N]_2NbCl_6$ was determined by the Faraday method. Since it was shown that the compound was contaminated with $[(C_2H_5)_4N]_2NbOCl_5$ values of susceptibility were then corrected for the presence of 25% non-paramagnetic material. The resultant paramagnetic susceptibilities were used for the calculation of the effective

magnetic moment. The results are given in Fig. 1(a). There is only a rough correlation between experimental and theoretical curves, and it can be seen that the theory does not completely account for the observed magnetic properties of the compound. Consideration of other magnetic parameters, viz. k (electron delocalization factor) and v (axial distortion) gave calculated curves that gave better agreement with the experimental ones. Results are given in Fig. 1(b).

Benzinger's attempt to obtain an e.s.r. spectrum of $[(C_2H_5)_4N]_2NbCl_6$ in acetonitrile solution failed This is not surprising since the lowest state in the $NbCl_6^{2-}$ ion is a non-magnetic state. However he did obtain a complicated 10 line spectrum from a solid sample, (a ten line spectrum is expected for a single electron localized on a niobium nucleus, which has a nuclear spin of $^9/_2$ with a g value of 1.96).

The fact that an e.s.r. spectrum could be obtained with a solid sample but not with a solution sample was explained as follows. The ions with a T ground state and perfect octahedral symmetry have a short spin-lattice relaxation time at room temperature and therefore it is difficult to obtain a spectrum of such ions. Solid $[(C_2H_5)_4N]_2NbCl_6$ has already been shown to be distorted from octahedral symmetry. However, in solution this distortion was assumed

Fig. 1: Magnetic data reported by Benzinger (ref. 29).

Fig. 1(a) Variation of effective magnetic moment with absolute temperature.

(a) experimental curve when $\lambda = 750\ cm^{-1}$

(b) experimental curve when $\lambda = 600\ cm^{-1}$

(c) experimental curve when $\lambda = 500\ cm^{-1}$

(d) theoretical curve according to Kotani formula.

Fig. 1(b): Variation of effective magnetic moment with absolute temperature including effects of electron delocalization (k) and axial distortion (v). Dashed lines are theoretical curves. Solid lines are experimental curves.

(a) $k = 0.8$; $v = 1$

(b) $k = 1$; $v = 1$

(c) $k = 0.8$; $v = 0$

(d) $\lambda = 600\ cm^{-1}$

(e) $\lambda = 500\ cm^{-1}$

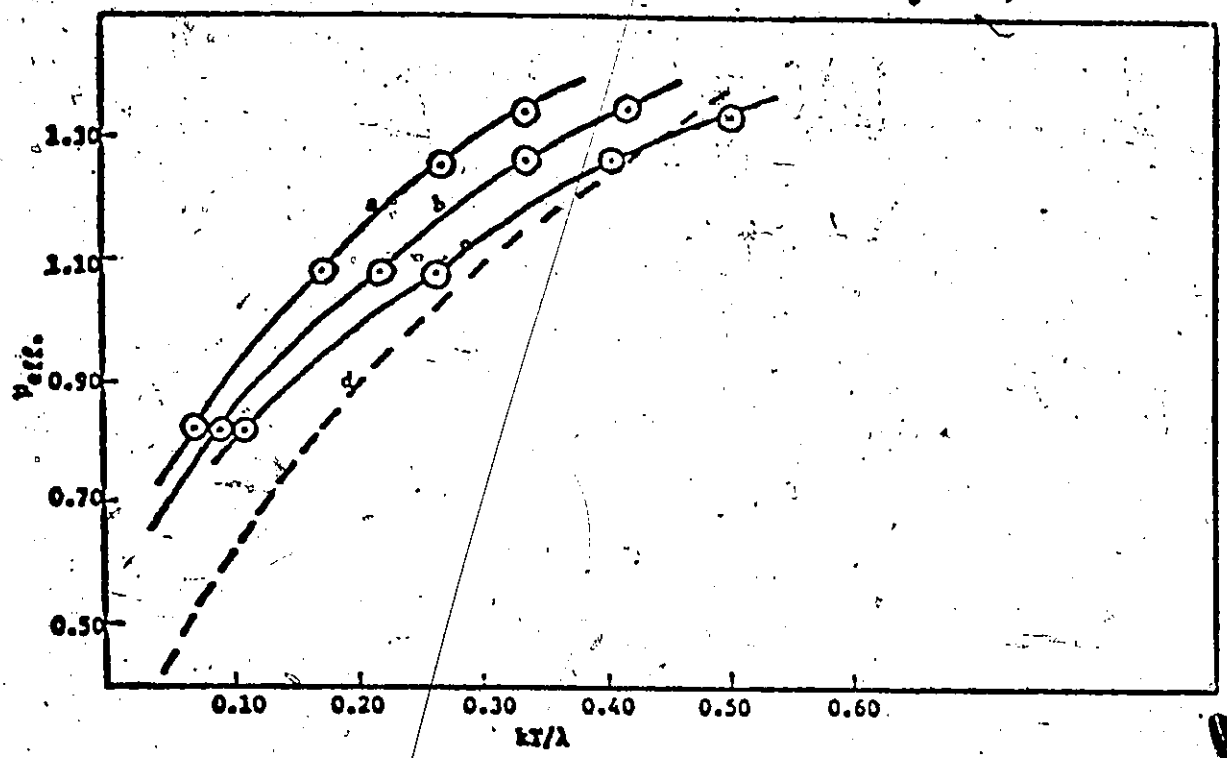
1.30
1.10
0.90
0.70
0.50
$p_{eff.}$
a
b
c
0.10
0.20
0.30
0.40
0.50
0.60
kT/λ

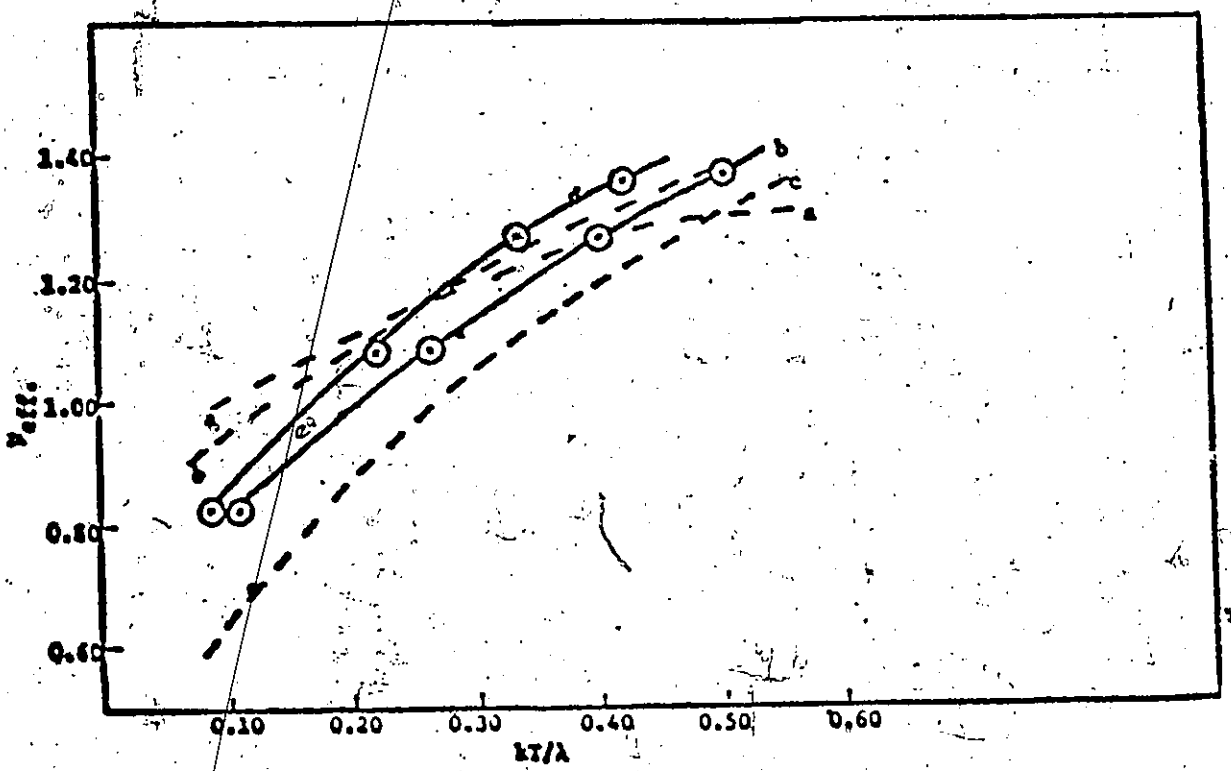
1.40
1.20
1.00
0.80
0.60
$p_{eff.}$
a
b
c
0.10
0.20
0.30
0.40
0.50
0.60
kT/λ

to be less or entirely absent. It was proposed that in the solid state, the distortion is apparently large enough to cause a sufficient decrease in the spin-lattice relaxation time so that a spectrum can be obtained.

There have been other attempts to record the e.s.r. spectrum of Nb(IV) species. Fedetov (38) et al. have examined the e.s.r. spectrum of Nb(IV) in ethanol prepared by reduction with zinc and HCl. They obtained a frozen glass spectrum but no solution spectrum. The same group repeated their experiments in aqueous HCl and obtained significantly different parameters. Larden and Günthard (39) examined the e.s.r. spectrum of Nb(IV) in HCl - alcohol mixture obtained by electrolytic reduction. Maniv (40) et al. have examined Nb(IV) in Cs_2ZrCl_6 and found it to be tetragonally distorted.

More recently Johnson and Bereman (41) have reported e.s.r. studies of Cs_2NbCl_6. They prepared these salts by (i) reacting stoichiometric quantities of starting materials in a sealed tube at 480° and (ii) by precipitation from 12NHCl.

They found that no electron spin resonance signal could be obtained at 297° or 110° K from the solid Cs_2NbCl_6 by either preparative method. This suggests a very short

spin-lattice relaxation time which is consistent with an octahedral configuration. Similar results have been found for VCl_6^{2-} in solution and in the solid state (42).

However Johnson did obtain a spectrum from solutions of $NbCl_4$ in 12N HCl and 10N HCl. He assigned these spectra to the species Cs_2NbOCl_4. This compound had been isolated earlier (43) and the behaviour of the frozen glass spectrum of $NbCl_4$ in HCl strongly suggests that the $NbOCl_4(H_2O)^{2-}$ ion is the predominant species. Johnson postulated the following equilibria existing in 12N HCl:

$$NbCl_4 + 2Cl^- \rightleftharpoons NbCl_6^{2-}$$

$$NbCl_6^{2-} + H_2O \rightleftharpoons NbOCl_4^{2-} + 2HCl$$

$$NbOCl_4^{2-} + Cl^- \rightleftharpoons NbOCl_5^{3-}$$

Furthermore when solutions of Nb(IV) in ethanol or in HCl are obtained by reduction of Nb(IV) chloride with Zn, Johnson found it was impossible under all conditions to isolate the $NbCl_6^{2-}$ species. This is probably due to the fact that the $NbCl_4$ was hydrolysed to the oxo species, i.e. $NbOCl_4^{2-}$.

The optical spectra obtained for the species investigated are given below.

Table IV: Band maxima reported by Johnson and Bereman

Compound	Band Position (cm^{-1})	
Cs_2NbCl_6 (Mull)	18,600 (broad and symmetrical)	
$NbOCl_4(H_2O)^{2-}$ (10N HCl)	15,400	19,600
Nb(IV) in 10N HCl	14,200	20,000

McCullough and Meites (44) have also postulated the presence of several niobium species in electrochemical reduction of Nb(V) in aqueous HCl solution. Their results led to the suggestion that Nb(V) is a dimer in high concentrations of HCl. They felt that the niobium(V) dimer was reduced to a niobium(IV) dimer which disproportionated into a Nb(V) - Nb(III) adduct. The latter was further reduced to a Nb(IV) - Nb(III) adduct. The niobium dimers were presumed to be involved in dissociation equilibria with the respective monomers. It was presumed that the monomeric Nb(IV) was reduced to Nb(II) which reacted with monomeric Nb(IV) to produce a monomeric Nb(III) species as a final product.

B. (i) Nb(IV), Ta(IV) and Zr(IV) Complexes

As stated earlier, Russian workers (18-20) were the first to report the existence of the complex salts A_2MCl_6

where A = Na, K, Rband Cs, M = Nb and Ta. The compounds were identified by phase equilibrium studies. They performed their experiments in quartz glass vessels which were sealed under vacuum or filled with argon and then heated. The potassium, rubidium and caesium salts were found to be congruently melting with high melting points (Table V).

TABLE V

Melting Points and Transformation Temperatures of A_2MCl_6 Complexes

Compound	m.p. °C	Transformation Temperature °C
Na_2NbCl_6	582	365
K_2NbCl_6	782	548
Rb_2NbCl_6	802	
Cs_2NbCl_6	822	
K_2TaCl_6	732	
Rb_2TaCl_6	756	322
Cs_2TaCl_6	796	352

The phase studies also indicated that the melts contained $[NbCl_5]^-$ and $[NbCl_6]^{2-}$ whereas $[TaCl_6]^{2-}$ seemed to be the only ionic tantalum species.

Morozov and Lipatova (45) obtained compounds of $NbCl_4$ with alkali metal and ammonium chlorides by precipitation from hydrochloric acid solutions. The niobium tetrachloride was dissolved in concentrated hydrochloric acid and alkali chlorides and ammonium chlorides were dissolved in 10% hydrochloric acid. They obtained crystalline precipitates when solutions containing the chlorides were saturated with hydrogen chloride gas and mixed. Potassium chloride did not give a solid under these conditions.

The decomposition pressures of A_2NbCl_6 complexes have been determined by Safanov's group (46). They assumed that the decomposition proceeded as given by the following equation:

$$2A_2NbCl_6 = 2ACl + NbCl_5 + A_2NbCl_5$$

The $NbCl_5$ formed as a result of the reaction was drawn off by a stream of argon into the condensation portion of the apparatus, from which it was dissolved out with methanol for subsequent quantitative determination.

Tsintsius and Smirnova (35) have measured the enthalpies of formation of K_2TaCl_6 by calorimetry. They used 0.03% H_2O_2 solution as calorimetric liquid.

More recently the Russian workers (47-48) have reported the study of hydrogen reduction of $AMCl_6$ complex between the temperatures 20-900°C. The reduction was studied by x-ray diffraction, chromatography and analysis. In the case of niobium, the reaction was reported to proceed as:

$$ANbCl_6 \longrightarrow A_2NbCl_6 \longrightarrow A_2NbCl_5 \longrightarrow A_2NbCl_4 \longrightarrow Nb + MCl$$

The tantalum analogue showed a much more complex behaviour

The oxychloride complexes of Nb(IV) and Ta(IV) have been reported for the first time by Morozov and co-workers (45,49). Rubidium and caesium oxotetrachloroniobates (IV) were prepared by reduction of the corresponding oxopentachloro niobate(V) with stannous chloride in an argon stream at 450-550°C. The x-ray diffraction patterns of these complexes were found to be essentially the same as that of the alkali metal hexahaloniobates(IV).

The alkali metal oxotetrachlorotantalates(IV) were obtained by the interaction of potassium, rubidium and caesium hexachlorotantalates(IV) with antimony trioxide at 180-580°C in an inert atmosphere of argon. The x-ray diffraction photographs of A_2TaOCl_4 and A_2TaCl_6 showed that they have different structures. The oxotetrachlorotantalates (IV) do not have cubic structures.

Morozov and Sun Yn'Chzhu (50) have reported the thermal analysis on reactions of $ZrCl_4$ and $HfCl_4$ and alkali chlorides. The phase diagrams showed the existence of compounds $A_2Zr(Hf)Cl_6$. They found that Na_2ZrCl_6 undergoes a polymorphic transformation. These authors have also reported decomposition pressures of these compounds (51).

Zvara and Tarasov (52) have studied the same system with the aid of a radioactive indicator and reported the heats of formation of these salts.

More recently Flengas et al. (53-56) have studied these systems extensively. Some of the thermodynamic data reported by these authors for these compounds are shown in Table VI.

TABLE VI

Thermodynamic Properties of Hexachlorozirconates

Property	Li_2ZrCl_6	Na_2ZrCl_6	K_2ZrCl_6
m.p.(°C)	535	646	800
H_{fus} (kcal/mole)	9.30	4.00	5.50
S_{fus} (kcal/mole)	10.6	5.0	5.1
Transition (°C)		353	620
H_{Trans} (kcal/mole)		7.00	4.50
S_{Trans} (cal/degree)		10.9	5.0

(ii) Nb(III) and Nb(II) complexes

There have been few reports on the "A_2NbCl_5" and A_2TaCl_5 complexes (57-59). Safonov and co-workers have studied the interaction of alkali metal chlorides and $TaCl_3$. They isolated the thermally stable, red pentachloro-tantalates(III). No compound could be detected in the sodium chloride - tantalum trichloride system. The same group have reported the preparation of A_2NbCl_5 complexes. The preparative methods were similar to those used for the tantalum analogues.

Some of the properties of these salts are given in Table VII.

TABLE VII

Melting Points and Transition Temperatures of A_2MCl_5 Complexes

Compound	m.p.°C	Transition Temperature °C
K_2TaCl_5	560	263
Rb_2TaCl_5	642	360
Cs_2TaCl_5	710	346
"Na_2NbCl_5"		362
"K_2NbCl_5"	718	590
"Rb_2NbCl_5"	753	
"Cs_2NbCl_5"	763	

Clusters containing Nb atoms in oxidation state (III) have also been reported (60). $Cs_3Nb_2X_9$ (X=Cl, Br, I) and $Rb_3Nb_2X_9$ have been prepared by the reaction of CsX or RbBr, respectively with Nb_3X_8 in a temperature gradient. The magnetic properties were observed to correspond to two unpaired electrons at 200-500° K.

The potassium salt of the type $K_4[(Nb_6Cl_{12})Cl_6]$ has been prepared by solid state reactions of Nb_6Cl_4 and KCl (61), or by Nb_3Cl_{18} with KCl (62) at high temperatures where disproportionation occurs to form also K_2NbCl_6. The tetraethyl ammonium analogue has been obtained from Nb_6Cl_{18}, $8H_2O$ in ethanol saturated with HCL (63). The x-ray, magnetic and spectral properties of this cluster will be discussed in appropriate sections.

Safonov et al. (64) have studied "K_2NbCl_4", "Rb_2NbCl_4" and "Cs_2NbCl_4" complexes. No similar sodium salts seem to exist. They reported that these compounds are optically isotropic. Melting points of these complexes are recorded in Table VIII.

TABLE VIII

Melting Points of A_2NbCl_4

Compound	m.p. °C
"K_2NbCl_4"	695
"Rb_2NbCl_4"	718
"Cs_2NbCl_4"	725

(iii) Niobium and tantalum tetrahalides

It is characteristic of many intermediate halides of the elements of groups (IV), (V) and (VI) that they undergo thermal disproportionation to a higher halide and a lower

halide or a metal itself in some cases. Some typical examples are given in Table IX.

TABLE IX

Decomposition Products of Some Halides

Reactant	Product
$ZrCl_3$	$ZrCl_4 + ZrCl_2$
$MoCl_4$	$MoCl_5 + MoCl_3$
$TaCl_4$	$TaCl_5 + TaCl_3$
$NbCl_4$	$NbCl_5 + NbCl_{2.67-3.13}$
WCl_4	$WCl_5 + WCl_2$
$NbBr_4$	$NbBr_5 + NbBr_{2.67-3.03}$
NbI_5	$NbI_4 + \frac{1}{2} I_2$

Reference has already been made to the vapour pressure and decomposition pressure studies of $NbCl_4$ (30,34).

The decomposition pressures of TaX_4 (X = Cl, Br) have been reported by Schäfer and co-workers (65,66). The dissociation pressures of $TaCl_5$ over solid chlorides is given by the equation:

$$\log p^{\circ}_{m.m.} = 13.2 - \frac{5700}{T} \qquad [1]$$

The decomposition pressures of $TaBr_4$ is given by the following equation:

$$\log p_{m.m.} = 9.83 - \frac{6145}{T} \qquad [2]$$

McCarley and Boatman (67) have recently reported detailed phase equilibrium studies of the tantalum-bromine systems, from which they concluded that $TaBr_4$ melts incongruently at 392°.

Seabough and Corbett (68) have done a complete niobium-iodine phase analysis. The tetraiodide appears to be trimorphic, although the α-NbI_4 to β-NbI_4 transition at 348° is characterized by only a small endothermic effect. The α and β phases of NbI_4 give similar x-ray powder diffraction patterns. On the other hand, the β-NbI_4 to γ-NbI_4 transition at 417° is clearly a phase transformation.

In contrast to some of the other niobium and tantalum lower halide systems, the niobium-iodine system is simple in that only one phase lower than niobium tetraiodide is observed in the phase diagram, namely Nb_3I_8. As in the case of the chlorides and bromides, NbI_3 is probably not a thermodynamically stable phase - at least it has not been detected in the phase diagram studies.

Like the niobium analogue, the tantalum-iodine system is simple. McCarley and coworkers (57,69) have shown that TaI_4 and $[Ta_6I_{12}]I_2$ are the only equilibrium phases in the Ta, I system.

c. Organic analogues of A_2MX_6 complexes

Recently there has been a brief mention in the literature of the complexes of the type $K_2[Nb(NCS)_6]$ (70). The synthesis and characterization of these organic analogues of the halocomplexes of the type studied in this thesis should provide an interesting diversification in the study of $A_2M^{IV}Y_6$ (Y = halogen and organic ligands) type of complexes.

CHAPTER 3

EXPERIMENTAL

Since all of the simple halides and their derivatives were extremely susceptible to hydrolysis and oxidation by air, vessels which were sealed and evacuated or filled with inert atmospheres, were used throughout all preparations and experiments. In addition, all materials used in the preparations were rigorously dried and stored in evacuated containers. Certain substances, notably the volatile materials were purified immediately before use.

A dry box and glass transferring apparatus were employed in storage and handling of all the solid materials. A frequent flow of dry nitrogen was maintained through the box and an abundent supply of freshly exposed phosphorus pentoxide was kept in the box to remove excess moisture. A typical sample transferring apparatus is shown in Fig. 2. The apparatus was connected to a vacuum line, evacuated and flamed to ensure complete dryness. Dried nitrogen was then admitted The 24/40 joint was disconnected while nitrogen was passing through, and a nitrogen filled tube containing the sample was broken over the opening and the sample poured in, the ground was cap replaced and the assembly evacuated again. At this stage, if the properties of the materials

Fig. 2: An all-glass sample transfering apparatus.

A and B = seal-off points

C = connection to vacuum system and nitrogen supply

D = 24/40 ground glass cap.

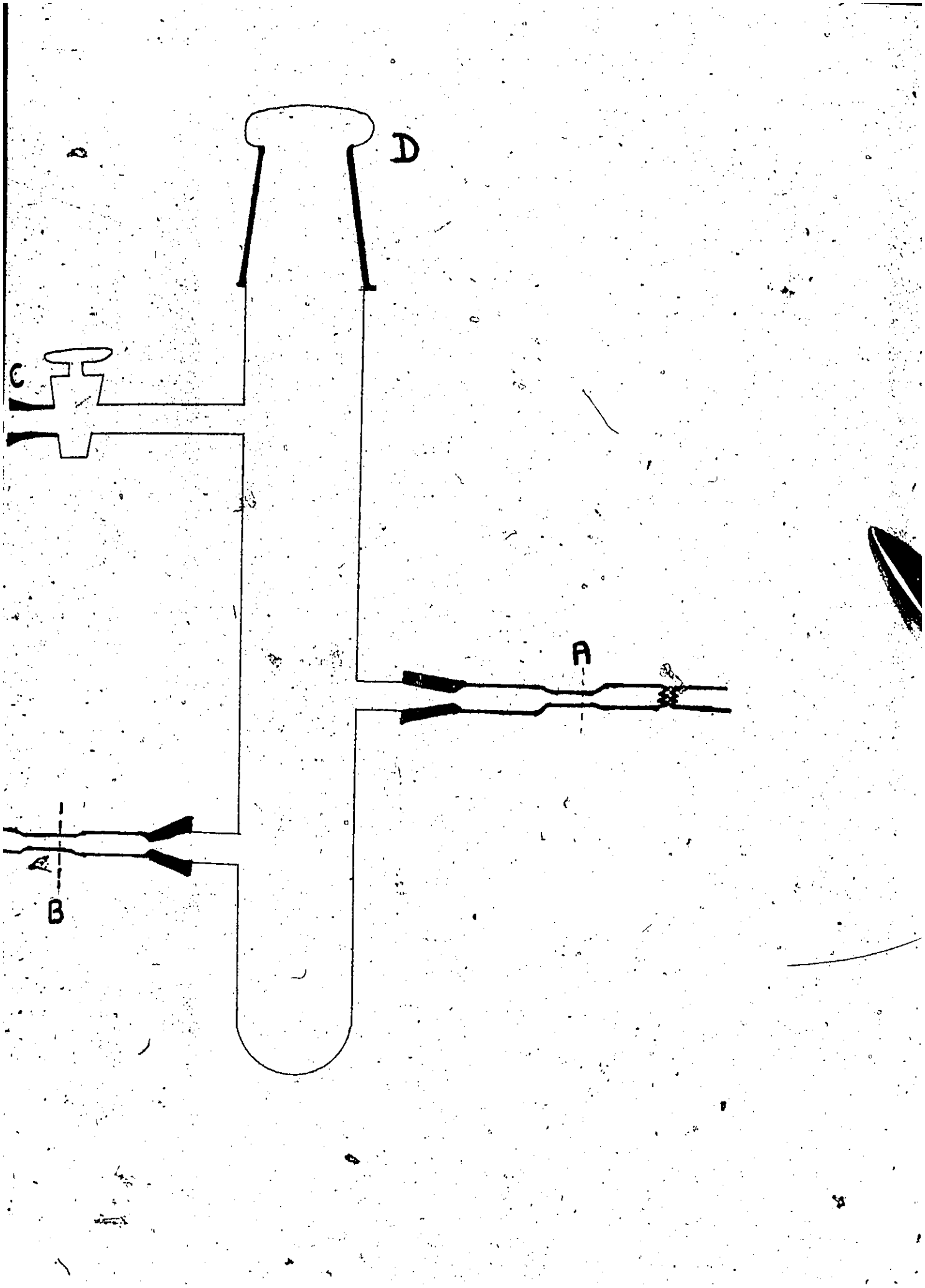
A
C
A
A
B

permitted, these substances were heated under vacuum to ensure complete dryness. The stopcock was closed and the apparatus was removed from the vacuum line. The sample was then transferred to the reaction tubes (A and B in the diagram) and subsequently sealed off at the points indicated, either under a dynamic vacuum or under a flow of nitrogen.

1. MATERIALS

Metals. High purity niobium(99.95%), and tantalum sheet (99.95%) were used in all preparations of their respective halides. The niobium and tantalum metals were obtained from Fansteel Inc.,Metals Division, Maryland, U.S.A.

The niobium powder (99.95%), niobium oxide (99.5%), and zirconium metal (99.999%), were supplied by Research Organic/Inorganic Chemical Co., Sun Valley, California, U.S.A.

Halogens. Research grade chlorine was obtained from the Matheson Company, Whitby, Ontario.

Bromine (J.T. Baker Analysed Reagent) was first dried over P_2O_5 for several days in a well dried nitrogen-filled container and distilled immediately prior to use.

Iodine (J.T. Baker Analysed Reagent) was purified by sublimation and then outgassed in a vacuum.

Hydrogen chloride and hydrogen bromide gases were also supplied by the Matheson Company.

Organic Reagents. Organic reagents used were of spectrograde quality obtained from either the Eastman Company or British Drug Houses. The liquids were purified by standard procedures(71).

Alkali Metal Halides. The alkali metal halides used in the preparations of the complexes were obtained from two sources. The potassium salts were J.T. Baker Analysed Reagent grade material. They were purified by recrystallizing twice from doubly distilled water. The other alkali halides (99.9%) were supplied by K. and K. Laboratories of Holywood, California and were used without further purification other than drying.

All alkali metal halides were dried by heating in a vacuum immediately prior to use.

Acids. Hydrochloric acid and hydrobromic acid were supplied by McArthur Chemical Co. Ltd. of Montreal, Canada.

2. ANALYTICAL METHODS

Several different analytical techniques were used depending upon the type of compound being analysed. In some cases, two or more different techniques were used to analyse a given compound.

Niobium(IV), tantalum(IV) and zirconium(IV) halides

The tetrahalides were hydrolysed in dilute aqueous ammonia or sodium hydroxide solution which was heated to

ensure complete reaction. The solution was cooled, the hydrated metal oxide separated by filtration, and the filtrate diluted to 250 ml in a volumetric flask.

For the determination of the metal, the filter paper containing the hydrated Nb(V), Ta(V) or Zr(IV) oxide was placed in a tared silica crucible. After converting the sample to anhydrous oxide by igniting at 900° and reweighing the crucible, the percent metal was calculated in the usual manner. To check the above method, the metal content of a solid compound was determined by direct ignition to oxide.

Halide was determined, after hydrolyzing the sample as described above, either by the Volhard method or by potentiometric titration.

When it was necessary to determine the amount of Nb(IV) in the sample - as in the case of vapour pressure studies of $NbBr_4$ - an oxidimetric method was used. The sample was oxidized to Nb(V) with an excess of acidic iron(III) sulfate solution in an inert atmosphere. The iron(II) formed was subsequently titrated with standard cerium(IV) sulfate solution with ferroin indicator.

Schäfer's "H-tube" method was also used [72]. The apparatus, with approximate dimensions, is shown in Fig. 3.

Fig. 3: "H-tube" for determination of chlorine and metal

A = quartz sample vessel.

B = vessel containing $AgNO_3$ and HNO_3

C and D = seal-off points.

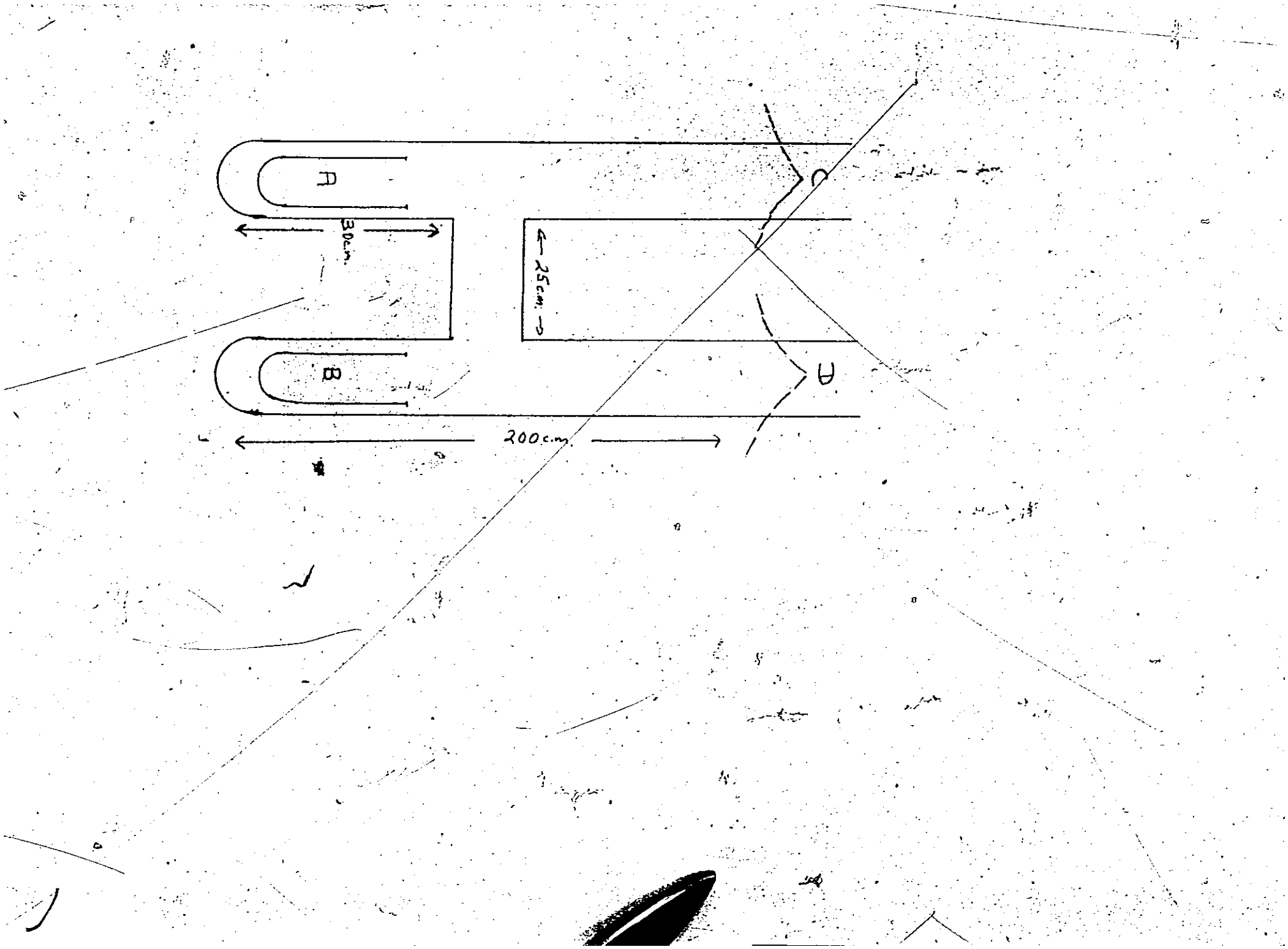
A
B
C
D
30cm.
25cm.
200cm.

This consisted of quartz crucibles A and B. Crucible A was heated to constant weight. Approximately 100 m.g. of the sample to be analysed was transferred to crucible A and the tube above it sealed at C. Crucible B contained silver nitrate (excess of stoichiometric quantity to react with the sample to form AgCl) and a few ml. concentrated nitric acid. A seal was made at D. The sealed tube was then heated to 130°-140° for twenty-four hours. After reaction was complete the tube was cooled and crucible B removed. The weight of silver chloride was determined by leaching the contents of B with hot water, filtering and weighing the AgCl in a tared crucible. Crucible A containing the Nb_2O_5 was heated at 900°C.

The method worked well for the chlorides. However, an attempt to analyse NbI_4 by this method was unsuccessful. Iodine, rather than HI, was formed.

The following compounds were analysed by the H-tube method: $NbCl_4$, $NbCl_3$, $NbCl_{2.67}$ and Cs_2NbCl_6.

$NbCl_3$

The H-tube method proved to be the most satisfactory method of analysis for $NbCl_3$.

Analysis of this compound was also attempted by carbonate fusion as suggested by Bruebaker and Young (73). We found that the results were invariably low in chlorine.

This was probably due to volatilization of the alkali halide at the temperature of fusion of K_2CO_3 (900°). To prevent volatilization, we found that the low melting 1:1 mixture of sodium and potassium carbonate was satisfactory. The compound was intimately ground with carbonates and heated in a platinum crucible over a Meker burner. The mixture was heated for 15 minutes with swirling after which the cooled product was dissolved in water. These solutions were acidified with 1:1 nitric acid-water. The pentoxide was precipitated with ammonia and filtered. Elemental determinations then followed the usual procedures.

Results of Carbonate Fusion

	Found	Calc.
Nb:	46.0	46.6
Cl:	52.9	53.4

$NbCl_2$

This compound was too refractory to be analysed by the H-tube method. $NbCl_2$ could not be oxidized even after four days at a temperature of 160°.

Schäfer's method ([72]) involved dissolving a sample in a mixture of concentrated H_2SO_4 and concentrated HNO_3 until a clear solution was obtained. The oxide was precipitated with ammonia and the usual procedure followed thereafter.

In our hands, this method consistently gave low results for chlorine. This was not surprising in view of the fact that concentrated HNO_3 oxidizes the chloride ion.

We also attempted to use the Parr Bomb Combustion technique (74). In this method about 0.200 grams of the sample was put into a 22 ml. nickel bomb and immediately mixed with 0.3 grams powdered lactose and 15 grams of sodium peroxide This was mixed thoroughly and ignited with a small hot flame After igniting the charge, the bomb was cooled rapidly to room temperature by immersing it in water. The contents of the bomb were dissolved in 100 mls. of water and neutralized by adding 1:1 nitric acid-water. Chloride was then determined potentiometrically.

This method also gave low results for chlorine. Even prolonged heating in an open nickel container with peroxide gave poor results. It appeared that carbonate fusion, as in the case of $NbCl_3$, was the most suitable method.

$(PyH)_2Nb(Ta)Cl_6$

Samples were dissolved in dilute nitric acid and chloride was determined potentiometrically. The metal content was determined by direct ignition.

The C, H and N analysis were done by Bernhardt Mikroanalytisches Laboratorium Elback, West Germany.

3. SYNTHETIC METHODS

Simple Chlorides and Bromides of Niobium and Tantalum

Standard procedures for preparations of these halides have been described by several workers (30,33,75,77). The procedures described here are slight modifications of these. In addition, in the case of niobium(IV) chloride, new synthetic routes were attempted.

$NbCl_4$

(i) The preparation of $NbCl_4$ from the metal was carried out in two steps. The apparatus is shown in Fig. 4.

The whole apparatus was thoroughly outgassed by flaming under vacuum. Chlorine was then passed over the metal M_1 which was heated to 220°C. At this temperature the metal reacted slowly, without inflaming, to produce the yellow pentachloride. Our observations showed that if the metal was allowed to burst into flame the product often became contaminated with white oxychloride. Trace amounts of oxychloride were invariably formed because the oxide on the metal surface initially reacted with chlorine to produce the oxychloride. However we feel that inflaming of the metal generates enough heat to cause a reaction between $NbCl_5$ and silica:

$$2NbCl_5 + SiO_2 \longrightarrow 2NbOCl_3 + SiCl_4$$

Fig. 4: Apparatus for preparation of MCl_4

A and B = seal-off points

C = connection to vacuum line and gas outlet

M_1 = metal for preparation of $NbCl_5$

M_2 = metal for reduction of $NbCl_5$ to $NbCl_4$

D = furnace

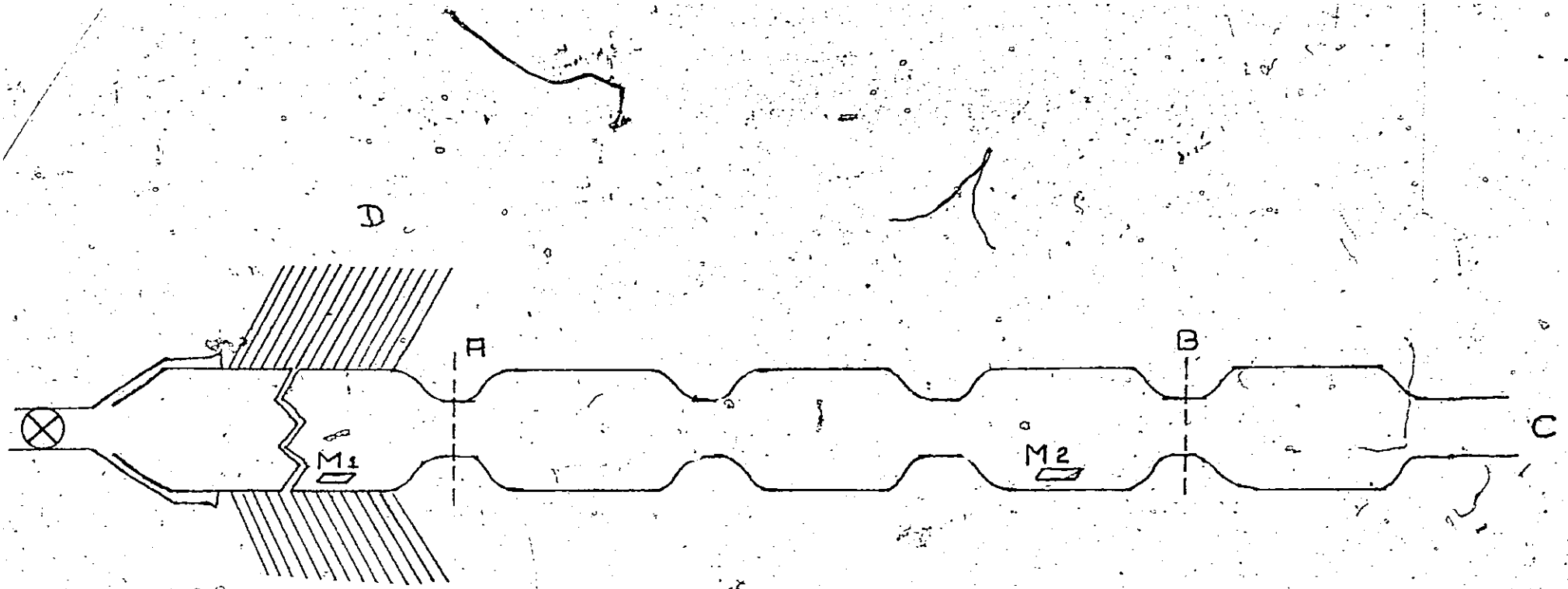
D
A
B
C
M1
M2

The $NbCl_5$ was then reduced by the metal M_2 in a temperature gradient obtained by placing two aluminum block furnaces end to end in a slanted position.

By carrying out these two steps in a single system, transference from one system to another was avoided and this eliminated any danger of hydrolysis.

Analytical Results:

Calc. for $NbCl_4$: Nb, 39.6 Cl, 60.4

Found for several samples: Nb; 39.5, 39.6, 39.2

Cl; 60.5, 60.7, 60.2.

(ii) Schäfer and Pietruck (78) have prepared very pure $NbCl_5$ by reaction of Nb_2O_5 and CCl_4 in a sealed tube. Using the same technique we attempted to prepare $NbCl_4$ by heating a mixture of NbO_2 and CCl_4 at 200°. After several days the product obtained was $NbCl_5$.

(iii) Pure $MoCl_4$ has been prepared by Shchukarev and co-workers (79) using a modification of the reaction of oxide with CCl_4. A modification of their apparatus which is shown in Fig. 5 was used in an attempt to prepare $NbCl_4$.

NbO_2 prepared by reduction of Nb_2O_5 with H_2 was mixed with activated charcoal (Norit-A) in the ratio of five parts of the former to one part of the latter and heated to

Fig. 5: Modification of Shchukarev's apparatus used for attempted preparation of $NbCl_4$

A = nitrogen inlet

B = CCl_4 container

C = furnace

D = boat containing NbO_2 and charcoal

E = sample collector

F = spiral condenser

G = phosgene outlet

H = connection to vacuum line

I = liquid nitrogen trap

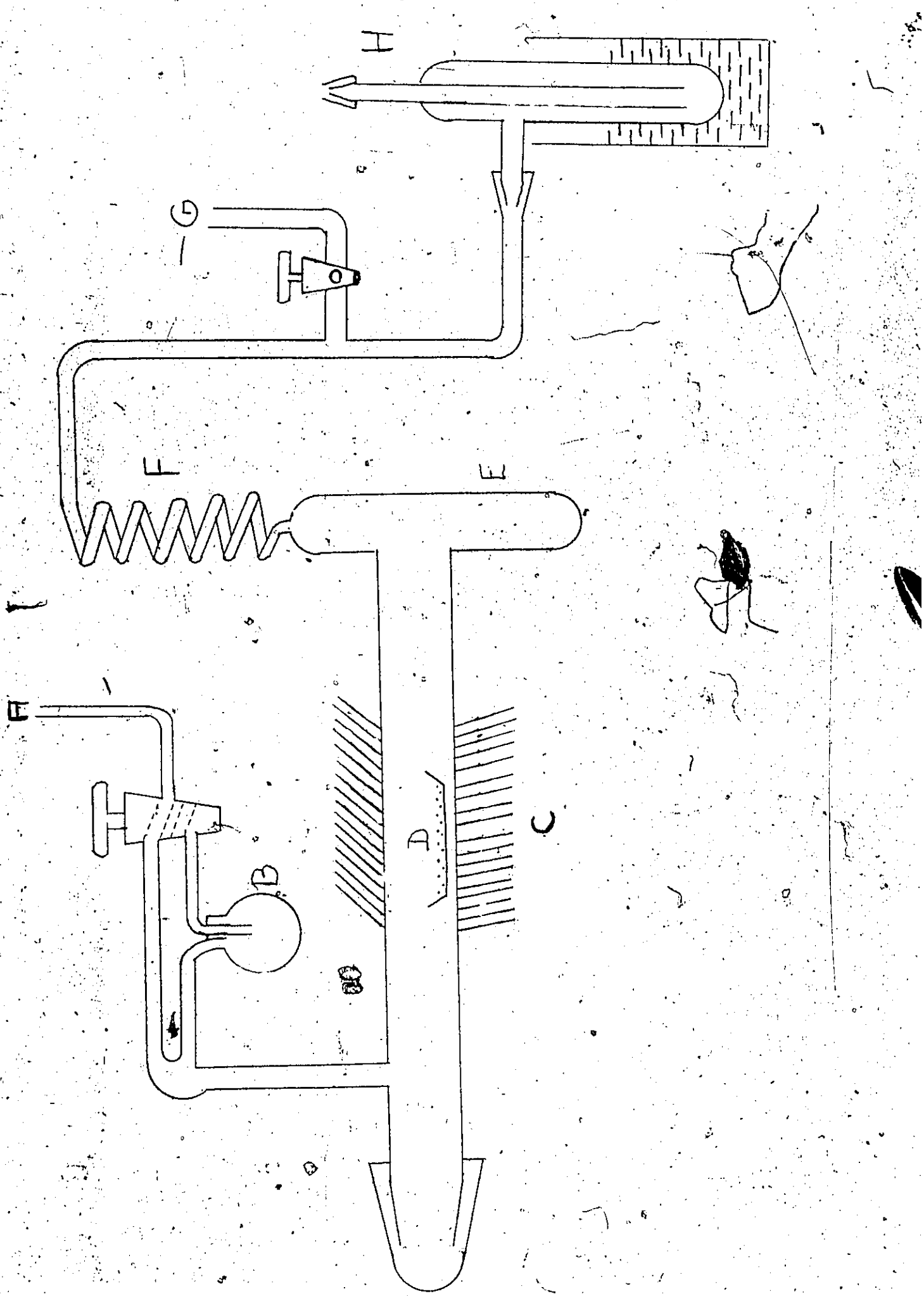
H
I
F
E
D
A
C
B

about 250-300° in a stream of nitrogen saturated at room temperature with carbon tetrachloride vapour. A vertical spiral tube at the outlet end replaced a condenser recommended by Shchukarev et al. for it was found to be more effective in collecting the fine powdered product. The powder descended the spiral tube into a receiver when the former was tapped gently.

Under these conditions only a mixture of $NbCl_5$ and $NbOCl_3$ was obtained.

$NbBr_4$

$NbBr_4$ was prepared in a process similar to that employed for $NbCl_4$. It appears that complete elimination of oxybromide formation is virtually impossible. There may be several reasons for this: firstly that bromine is difficult to dry and moreover oxide on the metal surface may initially react with niobium bromide to produce the oxybromide. In view of this difficulty, we decided to improve on the method of McCarley and Torp (75). Our apparatus is shown in Fig. 6.

Bromine which had been kept over phosphorus oxide for a long period of time was directly distilled into the flask A, which contained phosphorus V oxide and which had

Fig. 6: Apparatus for preparation of $NbBr_4$

A and B = bromine containers

C = connection to vacuum system

D and E = cold baths

F = break seal

M_2 = niobium foil for $NbBr_5$ preparation

M_1 = niobium foil for $NbBr_5$ reduction

X, Y and Z = seal-off points

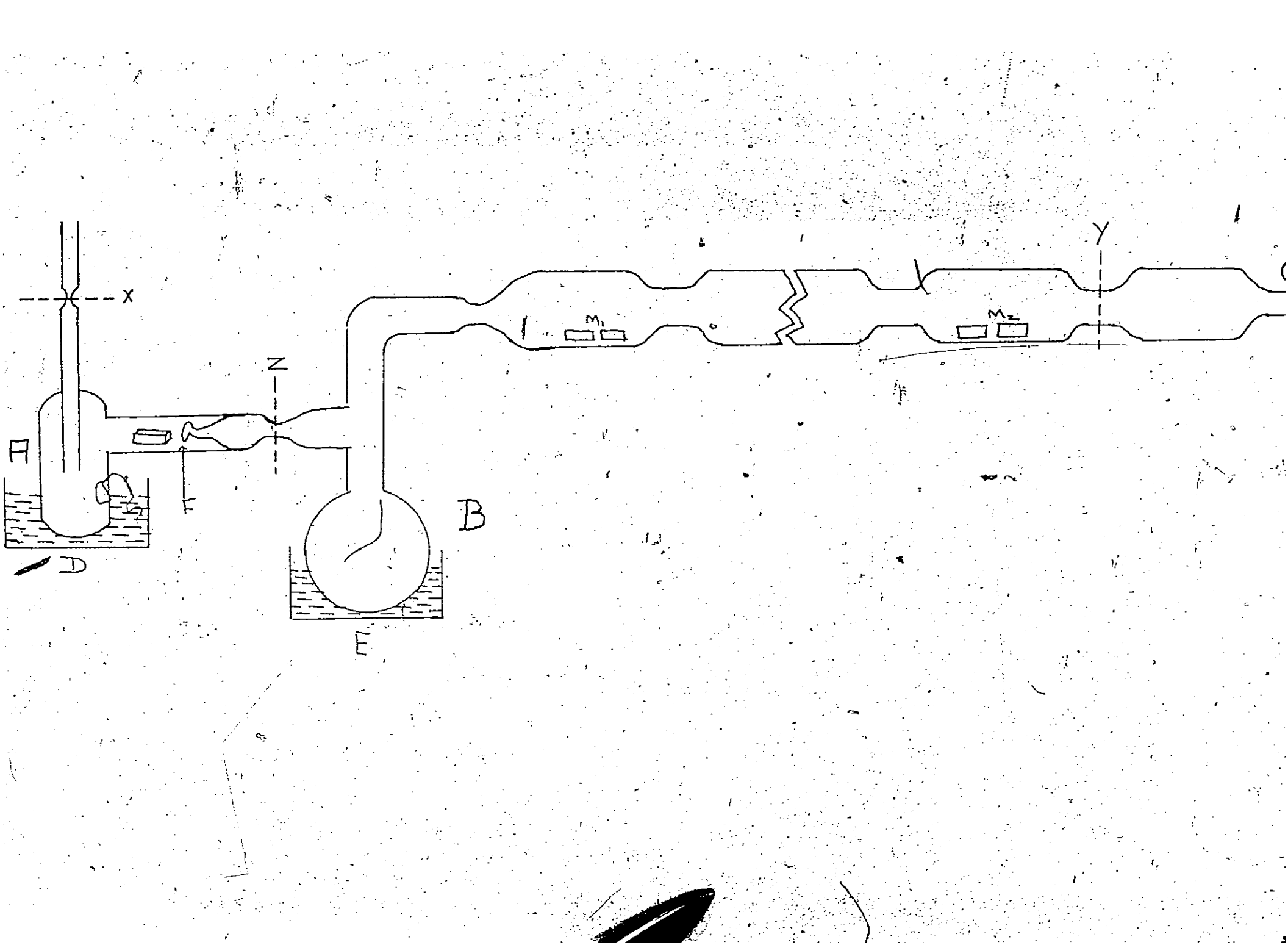
X
Y
Z
A
B
D
E
F
M1
M2

been evacuated, flamed and flushed with nitrogen. When sufficient bromine was distilled, the apparatus was sealed off at x. Meanwhile, the part on the right hand side of the break seal was thoroughly evacuated and flamed. It was then sealed off at y. The seal was then broken and bromine was distilled into flask B with the aid of liquid nitrogen while flask A was kept at 0° in an ice bath. When the required amount of bromine was distilled into B, the apparatus was sealed at z. $NbBr_5$ was then prepared by reaction of bromine vapour with niobium metal at 400° for several days.

Our observations showed that the niobium oxybromide comes from the reaction of bromine with surface oxide on the metal. When reaction first began the metal strips were covered with yellow product which soon disappeared and deposited on the cool part of the tube. After this initial reaction, no further oxybromide was seen to form.

However, the amount of niobium oxybromide was not present in very large quantities and appeared not to interfere with the preparation of tetrabromide.

The tetrabromide was then prepared by a temperature gradient technique.

Analytical Results

Calc. for $NbBr_4$: Nb, 22.5; Br, 77.5

Found for several samples: Nb; 22.2 22.6, 22.7

Br; 77.2 77.1, 77.8

NbI_4

NbI_4 was prepared by the method of Rolston (80). The pentaiodide was prepared by reaction of the metal with iodine that was sublimed directly into the reaction vessel similar to the type described in Fig. 4. The iodine was then outgassed. The reaction tube was placed in a slightly inclined position - with the niobium metal at the higher and the iodine at the lower end. The iodine was first heated to 180° and then to 250°. For the niobium end the suggested temperature was 300°. We found that at this temperature the pentaiodide was not readily transported from the hot zone into the intermediate zone. Moreover the product was only slowly formed. By raising the temperature to 350°, the pentaiodide was found in the intermediate zone and reaction was completed in 24 hours. After cooling the furnaces, the excess iodine was sublimed to one end of the tube. The reaction tube was opened and the pentaiodide rinsed with dry hexane until adhering iodine was removed. The NbI_4 was then synthesized by decomposition of the pentaiodide as described by Rolston (80).

Since the tetraiodide is likely to have free iodine adhering to the surface, the product was washed with dry hexane. This step was found to be essential if the product was to be used for subsequent preparations of the complex.

Analytical Results

Calc. for NbI_4: Nb, 15.5 I, 84.5

Found for several samples: Nb; 15.1, 15.2

I; 83.7, 83:8

$TaCl_4$

Chlorination of tantalum gave a product that was pale yellow. Pure $TaCl_5$ is white. The yellow colour was probably due to the presence of trace amounts of impurities, probably other metal chlorides.

The $TaCl_5$ was first prepared in a reaction tube similar to the one described in Fig. 4. In place of metal M_2, about 250 mg. of tantalum powder was used. After chlorination the tube was sealed off at A and B and the whole reactor was heated to 400° for four days with crude pentachloride at one end and tantalum powder at the other. The product was then sublimed. Pure white crystals of $TaCl_5$ were obtained. The preparation of $TaCl_4$ was then carried out by the temperature gradient method.

$TaCl_4$ was much more difficult to prepare in comparison with $NbCl_4$. The temperature control had to be fairly precise - fluctuations in the temperature were kept to a minimum. Best results were obtained by having more than two constrictions on the hotter side of the tube. This may have helped to reduce the convection of gases that could disturb

the equilibrium which favours the formation of $TaCl_4$.

Analytical Results

Calc. for $TaCl_4$: Ta, 56.0 Cl, 44.0

Found for several samples: Ta; 55.8, 55.6

Cl; 43.6, 43.4

$ZrCl_4$

$ZrCl_4$ was prepared by chlorination of pure metal in the apparatus shown in Fig. 4.

Analytical Results

Calc. for $ZrCl_4$: Zr, 39.1 Cl, 60.9

Found for several samples: Zr; 39.8, 39.1

Cl; 61.3, 61.0

A_2MX_6 (A = Na, K, Rb, Cs; M = Nb, Ta, Zr; X = Cl, Br, I)

(i) High temperature preparations: The A_2MX_6 complexes were prepared by heating stoichiometric mixtures of AX and MX_4 in a sealed quartz tube with 5 mm. inside diameter as described by Torp (21). The tube was held at the melting point of the alkali metal halide for 1-3 hours.

Unlike Torp, no temperature gradient was maintained to prevent sublimation. Instead, the following procedure was used to prevent separation of tetrahalide to one side of the tube. The length of the tube (~ 6 cm) was sufficiently

short so that the temperature was essentially constant along the entire length. The vessels were always nearly filled so that very little free space was available for sublimation.

On cooling, dark coloured, sintered solids were obtained which indicated that the complexes have melting points above the reaction temperature.

Completeness of the reaction was shown by x-ray diffraction patterns which showed no lines that could be attributed to either of the starting materials.

(ii) Low temperature preparations: Some of the complexes were also prepared at low temperatures. Stoichiometric quantities of intimately ground starting materials were sealed in a 7 cm. outside diameter pyrex tube of short length. The various temperatures which were used and the length of time and cooling periods for the reactions are given in Table X.

TABLE X

Temperature and Time Data for Preparation of A_2MX_6 Complexes

Compound	Temperature °C	Days	Cooling period (Hours)
K_2NbCl_6	300	20	36
Rb_2NbCl_6	300	17-20	36
Cs_2NbCl_6	300	14	72
Cs_2NbCl_6	275	21	24
Cs_2NbI_6	400	20	24

To facilitate reaction, the samples were ground several times during the course of the heating and the progress of the reaction followed by x-ray diffraction. If the samples were quenched, a yellow product ($NbCl_5$?) was seen on the inner walls of the tube although it was not seen if the samples were cooled over several days.

In the preparation of Cs_2NbCl_6 at 300°, a very small amount of solidified melt was observed. The reason for this is not known. No such melts could be seen in the other preparations.

(iii) Aqueous preparations of Cs_2NbCl_6 and Cs_2NbBr_6: Aqueous preparations of A_2NbCl_6 (A = Cs, Rb) were carried out using the procedure reported by Morozov and co-workers (45). Solutions containing starting materials were first saturated with gaseous HCl and mixed. One hour was allowed for precipitation of the product which was subsequently separated by pressure filtration in the apparatus shown in Fig. 7. The contents of the reaction vessel were poured into the filtering vessel A, and immediately connected to a pressure system by a 24/40 joint secured tightly by rubber bands. The mercury column in the apparatus was raised by HCl gas supplied by a rubber bulb pump connected to a gas cylinder.

Fig. 7: Pressure filtering apparatus

A = fritted disc

B = mercury container and column

C = HCl supply

D = rubber bulb provided with check valves

E = rubber connection

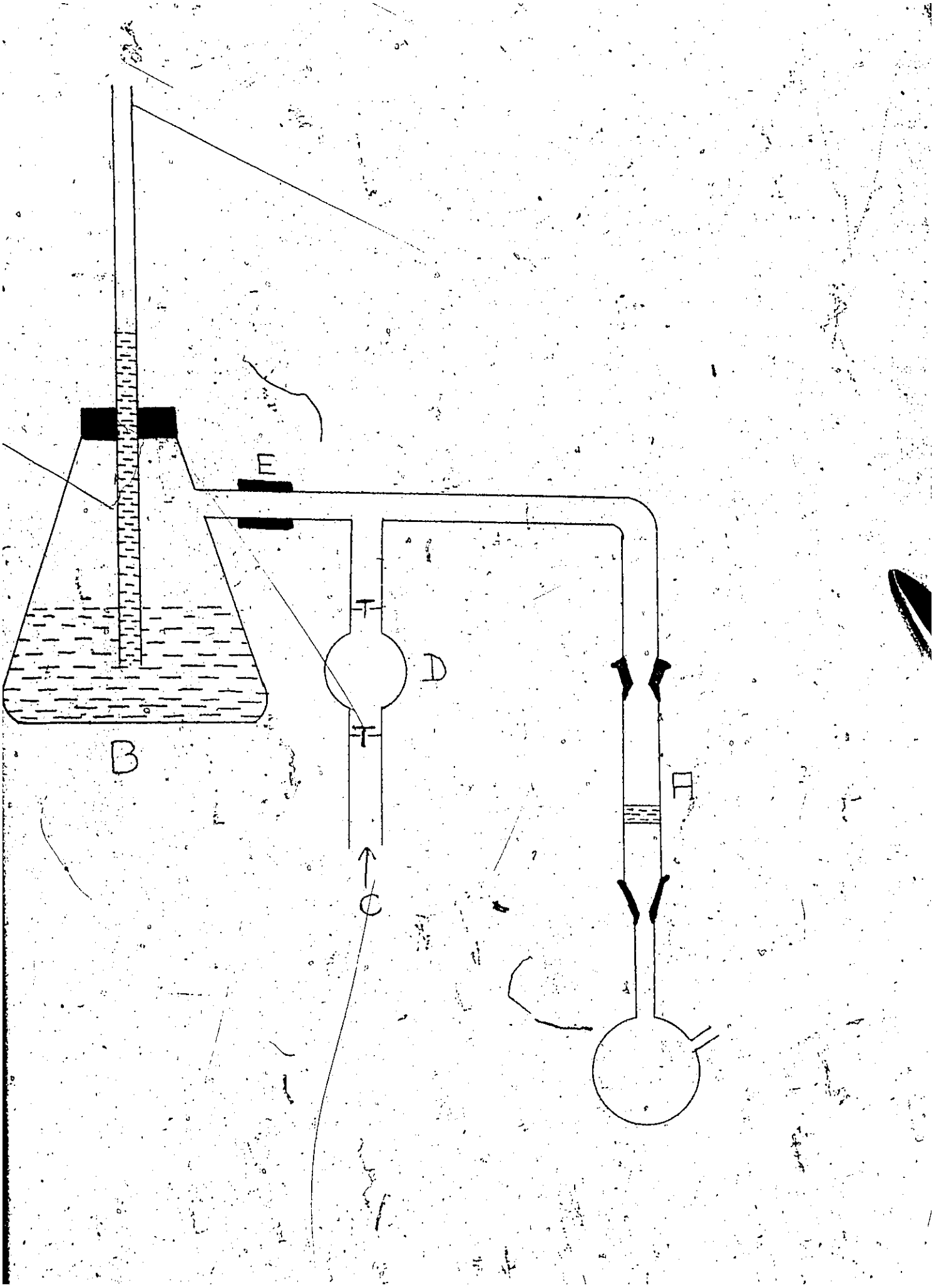
E
D
B
A
C

The wet product was dried over phosphorous oxide in an atmosphere of HCl.

Analytical Results

Calc. for Cs_2NbCl_6: Nb, 16.3, Cl, 37.2

Found: Nb, 17.0, Cl, 37.1

The preparation of Cs_2NbBr_6 by an aqueous method has not been reported.

In these aqueous preparations there is considerable danger of hydrolysis of the product if the acid concentration is not kept high. Hydrolysis may be more likely in hydrobromic acid than in hydrochloric acid because HBr is less soluble in water on a molar basis.

To prevent hydrolysis the apparatus shown in Fig. 8 was used. The reaction vessel was flushed with dry argon Distilled hydrobromic acid was poured through the opening A. Hydrogen bromide gas was then bubbled through the solution, which was kept cool by an ice-bath, via inlet B . After saturation of the acid, an intimately ground mixture of CsBr and $NbBr_4$ in the ratio 3:1 was poured through A with the aid of the funnel. Openings A and C were then stoppered. Hydrogen bromide gas was allowed to bubble through until reaction was complete. Inlet B was then stoppered and the

Fig. 8: Apparatus for preparation of Cs_2NbBr_6 in aqueous medium

A = inlet for starting materials

B = HBr inlet

C = inlet for HBr for drying the product. This opening was later used for taking the product out of the vessel.

D = magnetic stirring bar

E = ice bath

F = fritted disc

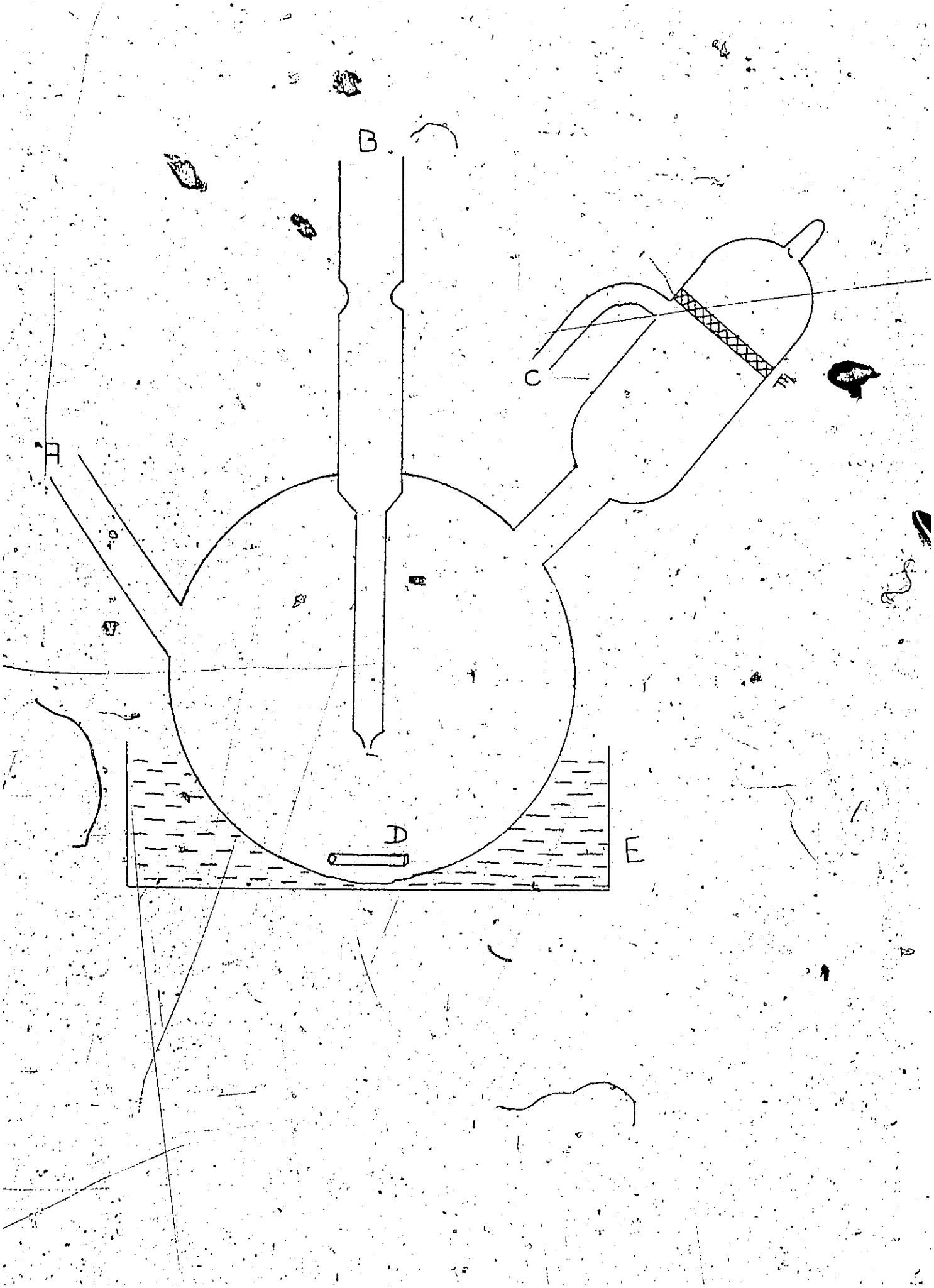
B
C
A
D
E

product poured into the filtering section of the apparatus by inclining the vessel appropriately. The filtration was slow requiring 24 hours. When filtration was complete the precipitate was washed with saturated hydrobromic acid. The product was then dried by passing HBr gas through C. The final drying was done over P_2O_5 in an atmosphere of HBr. An impure product was obtained and no further attempt was made to repeat the preparation.

(iv) Attempted preparation of K_2NbCl_6 in aqueous medium

Morozov and co-workers (45) were unable to obtain a precipitate in HCl solution when solutions containing KCl and $NbCl_4$ were saturated and mixed. We attempted the preparation by sealing a solution of KCl and $NbCl_4$ (containing excess KCl crystals) in cold saturated hydrochloric acid. The tube was then shaken for a week in a mechanical agitator. A brown solution was obtained but there was no sign of precipitate.

(v) Growth of single crystals of K_2NbCl_6

The growth of a single crystal was carried out by the step freeze method. The main feature of this technique is that there is a furnace with a flat temperature profile and a steep temperature gradient at the end of the furnace maintained by water cooled baffles. The hot temperature zone was controlled by an "Ether Transistral" proportionate controller.

An evacuated quartz amouple ≈ 6 c.m. long and having a 7 m.m. inside diameter and containing stoichiometric quantities of KCl and $NbCl_4$ was placed in a "mullite" carrying tube. The temperature of the hotter furnace was gradually raised to 900°C and held there for 3 hours. The carrier tube was mounted on small wheeled dollies on tracks at either end of the furnace. A gear assembly allowed the movement of the tube at a rate of 2 cm per day.

After preparation of the sample, it was examined in the dry box.

$(PyH)_2NbCl_6$

Anhydrous pyridinium chloride was synthesized by bubbling dry hydrogen chloride gas through an ether solution of spectrograde pyridine. The product was distilled in an inert atmosphere and dried *in vacuo* at 40°.

The preparation of $(PyH)_2NbCl_6$ was accomplished by the reaction of excess molten pyridinium chloride with $NbCl_4$ at about 150° in evacuated, sealed pyrex bulb. A red solution was obtained. The reaction was allowed to proceed for 3 hours. The product was ground in a dry box and the excess pyridinium chloride sublimed away at 100° in a sealed

evacuated tube. The sublimation required 10-14 days. Higher temperatures are not desirable as they may lead to decomposition of the product. After sublimation a brown product was obtained.

Analytical Results

Calc. for $C_{10}H_{12}NbCl_6$: C, 25.79; H, 2.6; N, 6.0, Cl, 45.7; Nb, 20.0

Found for C, 25.80; H, 3.1; N, 6.30; Cl, 44.8; Nb, 21.6

The low Cl to Nb ratio suggests that this compound was not pure. The impurity is likely to be a lower chloride of niobium.

$(PyH)_2TaCl_6$

This compound could not be prepared in the same manner as its niobium analogue. After sublimation of the excess pyridinium chloride, the product obtained showed x-ray patterns of starting materials. Investigation showed that the product was formed but it decomposed readily during the sublimation step.

It was found that excess pyridinium chloride could be removed by washing with carefully dried alcohol. Progress of the washing was followed by testing the filtrate with

blue litmus. A solution of pyridinium chloride in ethanol was acidic to litmus.

No lines could be attributed to starting materials in the diffraction pattern of the new compound and the pattern was identical to that of $(PyH)_2NbCl_6$.

Analytical Results

Calc. for $C_{10}H_{12}TaCl_6$: Cl, 38.3; Ta, 32.7

Found: Cl, 38.6; Ta, 33.3

A_2ZrCl_6

Stoichiometric quantities of ACl and $ZrCl_4$ were heated in a quartz tube. As $ZrCl_4$ develops considerable pressure at the melting point of ACl, the tubes tended to explode. This was overcome by putting the sealed ampoule in a stainless steel bomb along with $ZrCl_4$ to compensate for the pressure inside the quartz tube. The bomb used is shown in Fig. 9.

$NbCl_3$

The niobium-chlorine system has been reported to have a homogeneity region between the limits $NbCl_{2.67}$ and $NbCl_{3.13}$ (72, 81). In preparing a phase corresponding to $NbCl_3$,

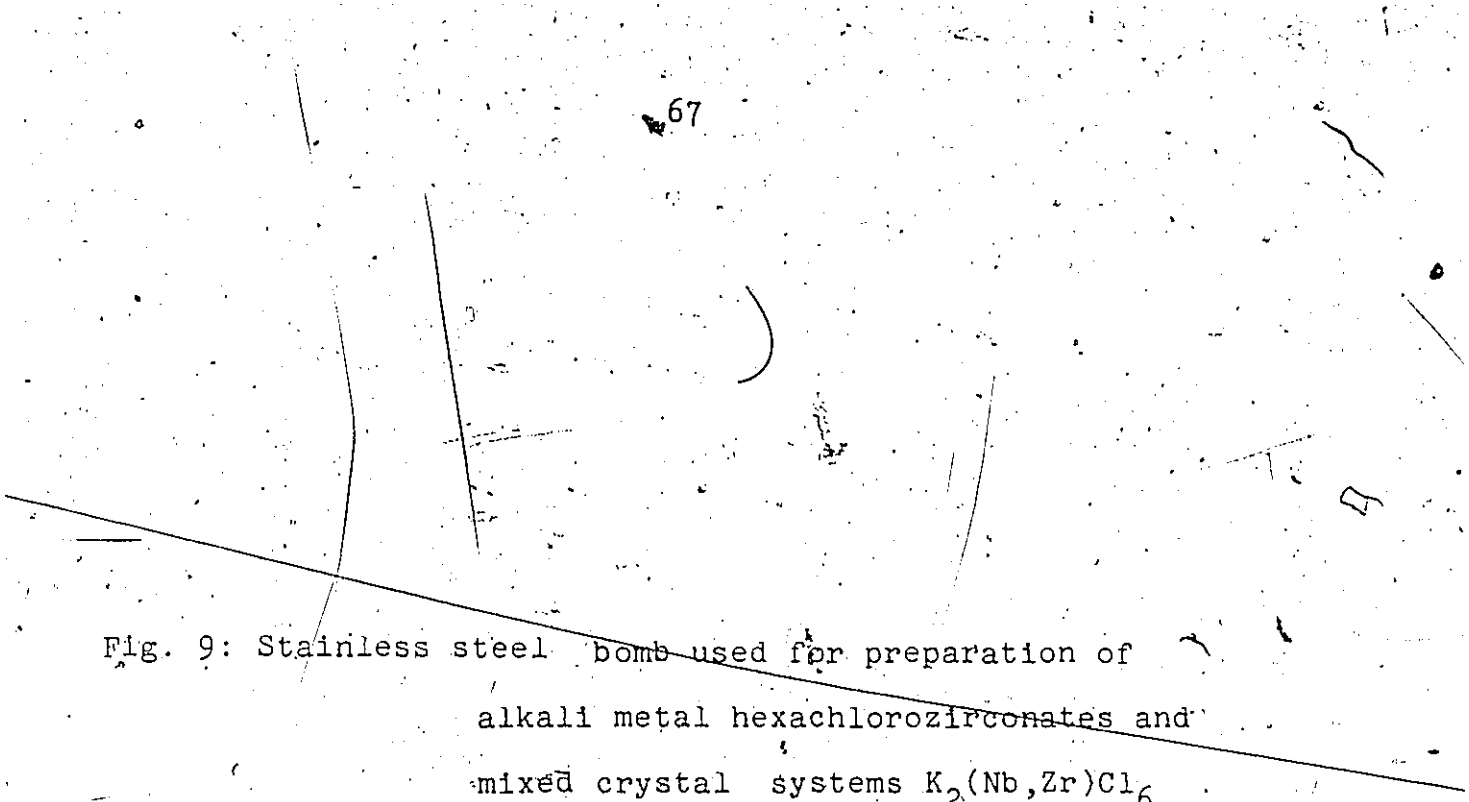

Fig. 9: Stainless steel bomb used for preparation of alkali metal hexachlorozirconates and mixed crystal systems $K_2(Nb,Zr)Cl_6$

A = cap

B = copper gasket

C = quartz reaction vessel

D = $ZrCl_4$ powder

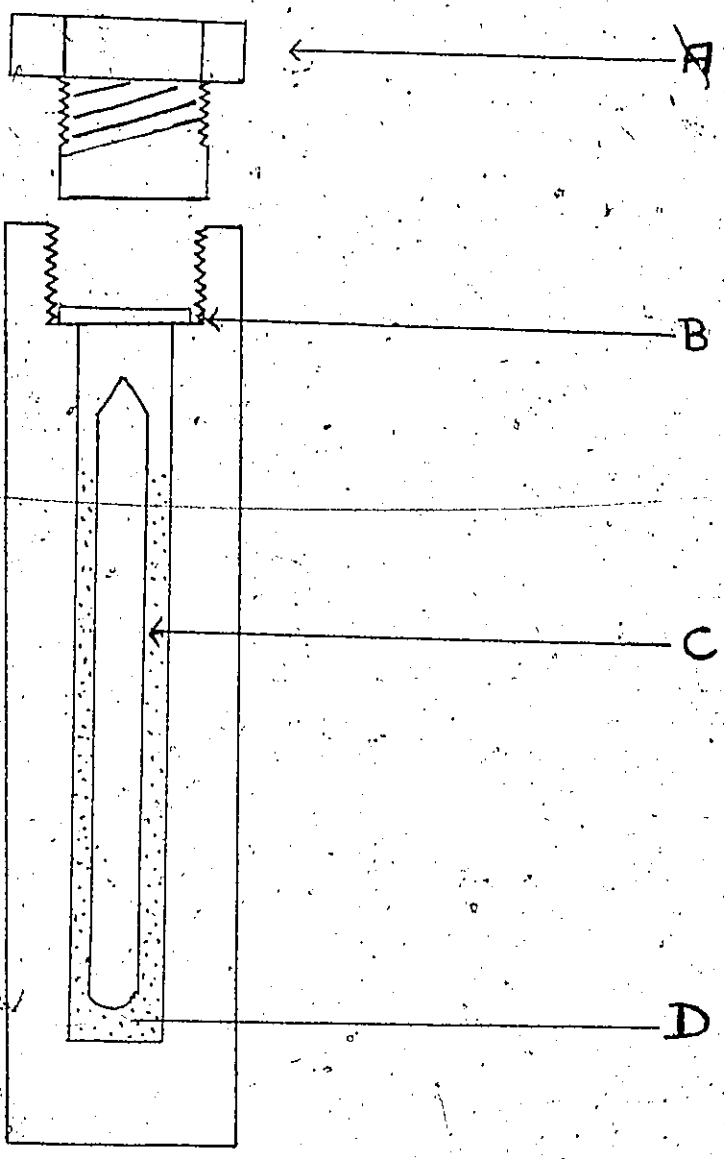
A
B
C
D

we proceeded from a mixture of niobium pentachloride and niobium powder in the proportions necessary for the formation of the trichloride. The temperature was slowly raised over one day to 375°C. The reaction required 10 days during which time the mixture was reground three times. This procedure was similar to the one described by Safonov et al. (58,59) and is a modification of a method used by Schäfer and his co-workers (72).

Analytical Results

Calc. for $NbCl_3$: Nb, 46.6; Cl, 53.4

Found: Nb, 46.1; Cl, 53.8

$NbCl_2$

The most convenient method for the preparation of the dichloride was simply to reduce $NbCl_4$ by niobium powder. Stoichiometric quantities of starting materials were sealed in an evacuated quartz tube and heated at 800°. The mixture was ground three times during the course of the reaction. The reaction went to completion in 5 days. A black solid was obtained.

Analytical Results

Calc. for $NbCl_2$: Nb, 56.7; Cl, 43.3

Found: Nb, 57.1; Cl, 42.6

$NbCl_{2.67}$

The method used was described by Schäfer and Dohmann (72). The preparation involved decomposition of $NbCl_4$. The $NbCl_4$ was heated at 500° and the $NbCl_5$ which was formed was allowed to condense at the extreme end of the reaction tube which was maintained at room temperature. Three days were allowed for the reaction. The product was a green solid.

Analytical Results

Calc. for $NbCl_{2.67}$: Nb, 49.6; Cl, 50.4

Found: Nb, 48.7; Cl, 49.7

"K_2NbCl_5"

Two procedures were used for the preparation.

Stoichiometric quantities of $NbCl_3$ and KCl were heated for 3 hours in a quartz tube to the melting point of the alkal halide as described by Russian workers (57-59). A brown product was obtained. Since there were no lines in the diffraction pattern which could be attributed to either of the starting materials, K_2NbCl_5 was initially assumed to be the product.

$NbCl_3$ is difficult to prepare as it is not stoichiometrically defined. However, $NbCl_{2.67}$ is a well defined compound and easy to prepare. We used this as the

starting material and the complex was prepared by the following reaction:

$$NbCl_{2.67} + 0.16\ NbCl_5 + 2.33\ KCl \longrightarrow 1.16\ "K_2NbCl_5"$$

The reactants were ground together and put into a sealed quartz tube. The temperature was raised slowly over a period of 3 to 4 hours and maintained at 760° for four hours. A brown substance was obtained which had an x-ray pattern which was identical to that of the substance prepared previously.

In both methods of preparation, the product appeared to have recrystallized from a melt.

Analytical Results

Calc. for "K_2NbCl_5": Nb, 26.7; Cl, 50.9

Found: (i) Nb, 27.80; Cl, 50.1

(ii) Nb, 26.51; Cl, 50.7

Thus Cl:Nb (i) 4.72:1

(ii) 5.01:1

"K_2NbCl_4"

Stoichiometric quantities of $NbCl_2$ and KCl were heated to 760° in a quartz tube for 4 hours following the procedure of Safanov (64). The product was essentially brown with a definite greenish tinge. It appeared to have

recrystallized from a melt. The x-ray pattern showed that some reaction had occured.

Preparation of solid solutions $K_2(M,Zr)Cl_6$ (M = Nb,Ta)

The complexes used in forming solid solutions, namely K_2NbCl_6, K_2TaCl_6 and K_2ZrCl_6, are all isomorphous and crystallize with an antiflourite type lattice specifically the K_2PtCl_6 structure.

The values of their lattice constants do not differ appreciably one from another (Table XI).

TABLE XI

Lattice Constants

Complex	Lattice Constants Å	Ref.
K_2ZrCl_6	10.08	82
K_2NbCl_6	9.97	21
K_2TaCl_6	9.96	21

X-ray diffraction patterns for the paramagnetic complexes and the diamagnetic diluent K_2ZrCl_6 displayed only a slight difference in line spacings - so that x-ray patterns could not be used for establishing the homogeniety of the solid solutions. However the lattice constants and the similarity in ionic radii of the metal atoms leave little

doubt that these salts are ideal for forming solid solutions. The solid solutions were prepared by fusing the components. Mixtures of KCl, $NbCl_4$ and $ZrCl_4$ and $TaCl_4$ in appropriate mole ratios to provide the desired concentration, were heated in an evacuated quartz tube contained in the steel bomb referred to earlier. $ZrCl_4$ was used to pressurize the bomb.

4. PHYSICAL MEASUREMENTS

Magnetic Measurements

Susceptibilities were measured by the Gouy method. This consists essentially of suspending a uniform cylindrical sample of the specimen in a non-homogeneous magnetic field and measuring the force exerted on it by a conventional weighing technique. This force is given by

$$f = 1/2 \chi H^2 A \qquad [3]$$

where χ = susceptibility per unit volume

H = field strength

A = area of the cross section

The equation will hold if the susceptibility of the surrounding air is assumed to be negligible. The sample tube is normally evaucated. Moreover, the length of the sample must be sufficiently long (at least 7 cm.) to ensure

that the field strength is essentially zero at the top end of the sample.

If W is the apparent change in the weight of the sample upon application of the magnetic field, then,

$$f = g.\Delta W = 1/2\,\chi H^2 A \qquad [4]$$

where g = acceleration due to gravity.

This can be rearranged to give

$$\chi = \frac{2.\ g.\Delta W}{H^2 A} \qquad [5]$$

where χ is volume susceptibility. Gram susceptibility is then given by,

$$\chi = \frac{2.\ l.\ g\ \Delta W}{H^2 M} \qquad [6]$$

For each sample, measurements were carried out from room temperature to -180°C. For lower temperatures a copper jacket surrounding the sample was cooled by a flow of nitrogen from a liquid nitrogen boiler. Various temperatures in the range 90° - 300° K could be obtained by varying the rate of flow of nitrogen. The temperatures were measured by a Thermoelectric Minimite bridge using a calibrated copper-constantan thermocouple the operating junction of which was fused on the inside of the jacket at

about the middle of the sample.

When the susceptibility was found to be dependent on the magnetic field strength, an attempt was made to correct for this by plotting susceptibility against reciprocal field strength and extrapolating to infinite field. Only a few samples were contaminated with ferromagnetic impurity and these not seriously. Part of the apparatus is shown schematically in Fig. 10.

Electron Spin Resonance Spectra

The measurements were carried out by Dr. A. Manoogian of the Department of Physics, University of Ottawa.

A Hilger and Watts commercial spectrometer operating at the order of 9.4 GhZ microwave frequency was used to record the esr spectra. All the resonance work was done at 4.2° K. The powdered samples were contained in a 2 mm diameter evacuated Vycor tube.

The spectrometer employing 100 Khz resolution was used to detect the esr spectra. An eight inch Newport magnet was used in the measurements. The magnetic field positions of esr lines were measured using the N.M.R. of protons in H_2O.

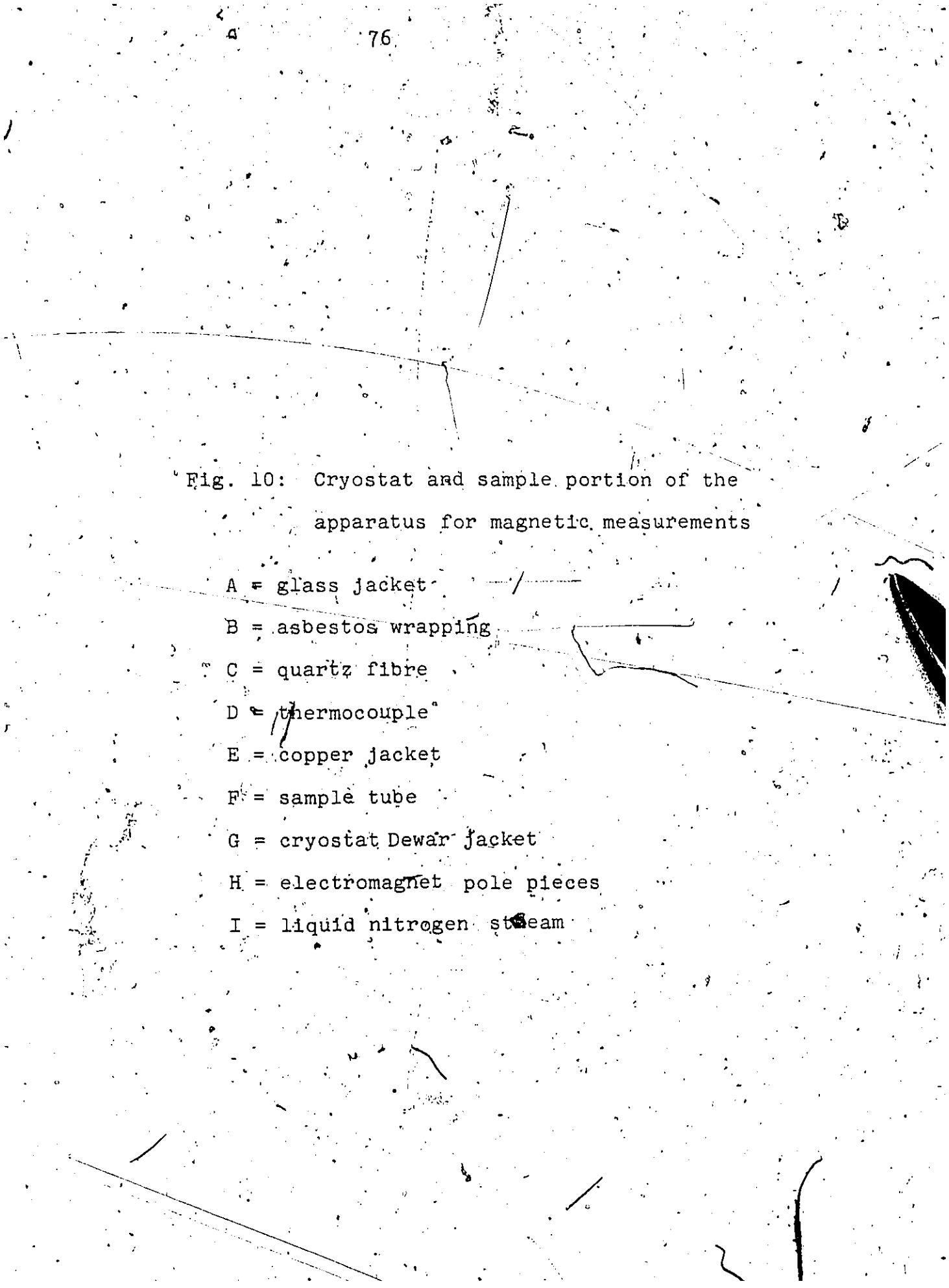

Fig. 10: Cryostat and sample portion of the apparatus for magnetic measurements

A = glass jacket

B = asbestos wrapping

C = quartz fibre

D = thermocouple

E = copper jacket

F = sample tube

G = cryostat Dewar jacket

H = electromagnet pole pieces

I = liquid nitrogen stream

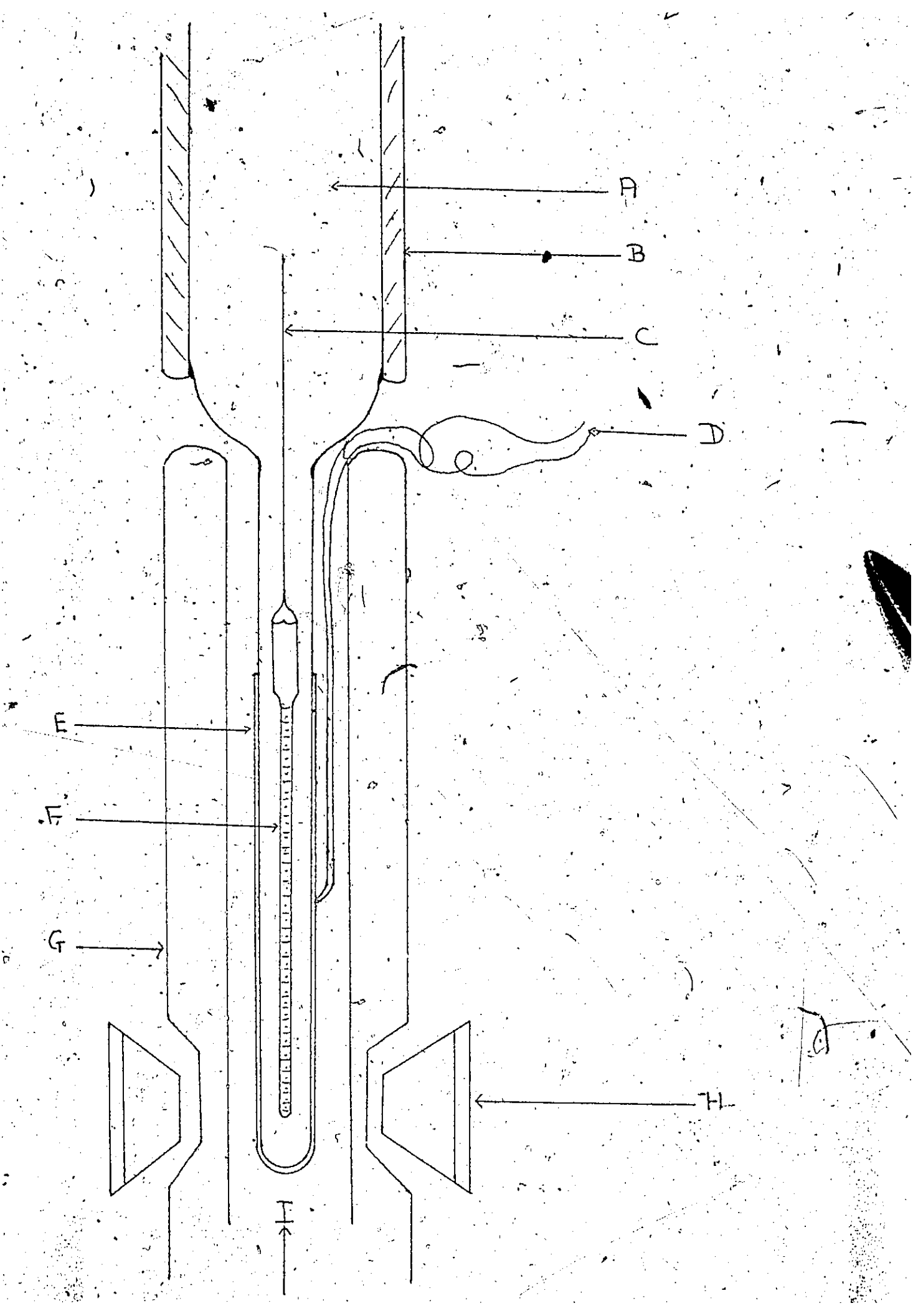
A
B
C
D
E
F
G
H
H

To obtain esr absorptions, the microwave frequency was kept constant and the magnetic field was swept in magnitude. Resonance occurred when the condition

$$h\nu = g\beta H \qquad [7]$$

where h = Planck's constant

ν = frequency of the radiation

g = spectroscopic or Landé splitting factor

β = Bohr Magneton

was satisfied.

Diffuse Reflectance Spectra

The diffuse reflectance spectra of the solid complexes were measured from 250 mμ to 1200 mμ on a Beckman DU spectrometer equipped with a Beckman 2580 reflectance attachment.

The samples were uniformly ground and if required diluted with appropriately matched alkali halide.

The stainless steel cell used is shown in Fig. 11. The samples were contained in a depression and protected from the atmosphere by a quartz disk resting on a neoprene O-ring. The reflectance spectra were measured in reference to finely ground magnesium carbonate or matched alkali halide if samples were diluted.

Infrared Spectra

Infrared spectra were recorded on a Beckman IR-20 spectrophotometer which was flushed with nitrogen for four

Fig. 11: Cell used for measurement of diffuse reflectance spectra

A = cell cover

B = quartz window

C = sample well

D = Neoprene O-ring

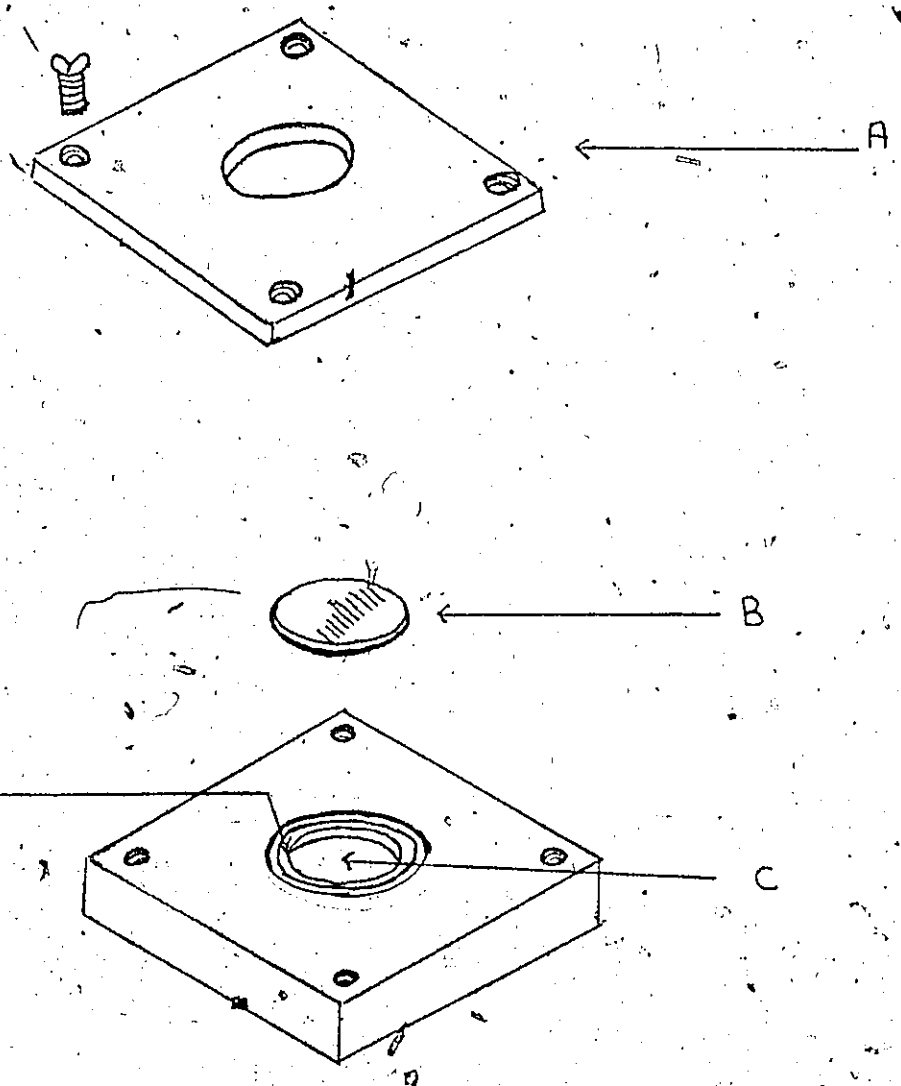
A
B
D
C

hours prior to use and during the course of running the spectrum.

Infrared spectra at high wave numbers were recorded by grinding the sample with Nujol and the resulting mull was pressed between two NaCl plates inside the dry box. Nujol used in recording the spectra was dried over sodium wire. A spectrum of Nujol was run in the region where water peaks are observed. With a prolonged drying period, it was possible to eliminate the water bands in the spectrum of Nujol.

Pellets and CsI plates were used for infrared spectra at long wavelengths. Sample preparations were carried out in a dry box. The powdered complexes were contained in a capsule which was mounted on a mechanical agitator. The sample was violently agitated for one minute to ensure a homogeneous mixture. The powder was then loaded into a pellet die. The pressing to a transparent disc was done by a hydraulic press under a continuous flow of nitrogen. The pellet was taken back into the dry box and both sides of it covered by Nujol to prevent hydrolysis. The pellets were scanned immediately upon removal from the dry box. The samples were also run as Nujol mulls between CsI plates. No difference in spectral features were found,

for a given sample, by these two methods.

Raman Spectra

The exciting lines 4880Å and 5144Å of a Radiation model 52 argon-ion laser were used. The power used was of the order of one watt.

The spectra were obtained with a Jarrell-Ash model 25-102 one meter double mononchromater using a cooled ITT FW-120 photomultiplier tube and photon counting electronics.

To avoid thermal decomposition of the sample, a Kiefer-Bernstein type of cell was employed (83). The main features of this rotating disc cell device for absorbing crystal powder are given in Figures 12a and 12b.

The sample was placed in a groove in the stainless steel sample holder and pressed by means of a tool press. To prevent hydrolysis or oxidation during measurement, an optical quartz disc was mounted and glued at all edges to prevent contact with the atmosphere. An O-ring was also used to keep the quartz disc from falling off during rotation. The sample holder was attached to a motor driver with variable speeds. The optical arrangement is shown in Fig. 12b.

Unfortunately we obtained a high background due to scatter from the quartz disc and were unable to observe any

Fig. 12(a) and 12(b): Rotating disc cell devised for obtaining Raman spectra

A = press

B = press tool

C = annular powder sample

D = sample holder

E = optical glass

F = O-ring

G = pressed powdered sample

H = focussed laser beam

I = scattered light to spectrometer

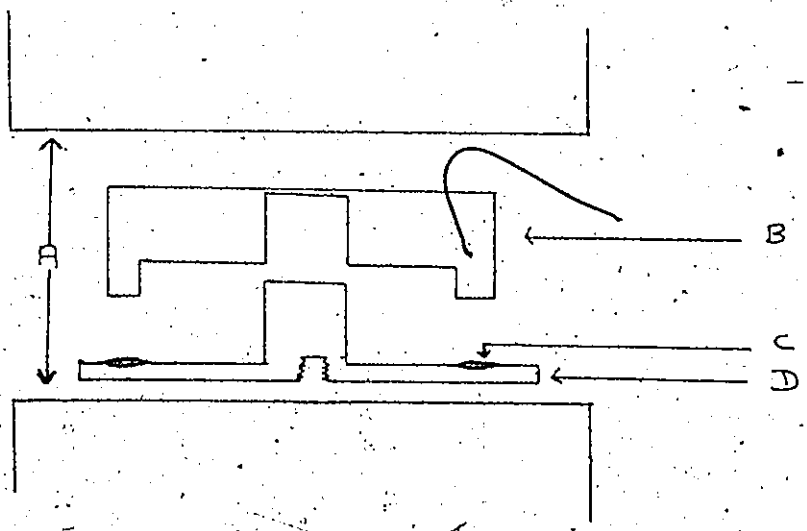

(a).

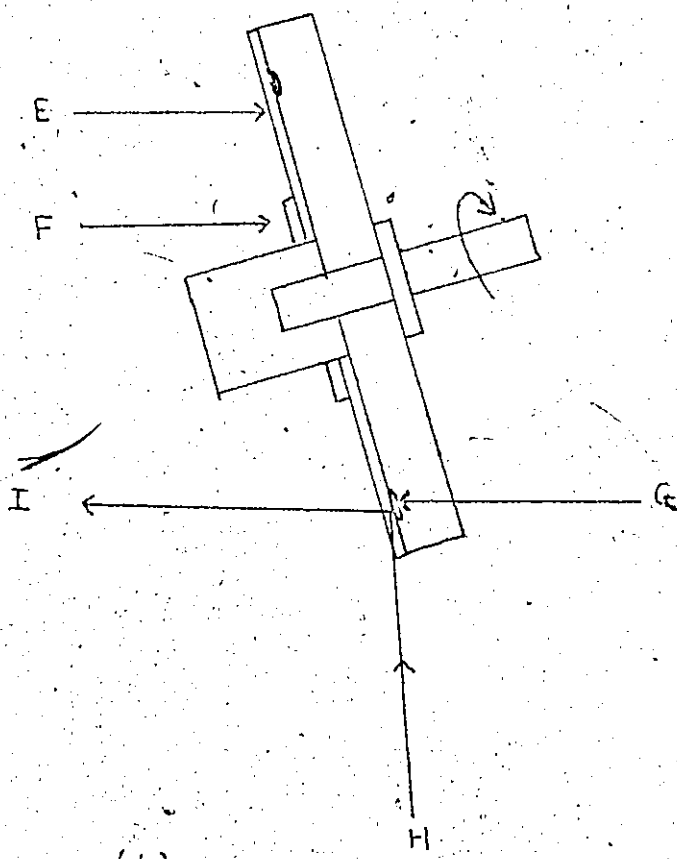

(b)

lines due to the sample.

X Ray Diffraction

X-ray diffraction patterns were obtained by the Debye-Scherrer method using Ni filtered CuK_α radiation and a camera with a diameter of 114.7 mm. Potassium chloride served as an internal standard.

Samples were ground to a fine powder and packed well in 0.3 mm capillaries of Lindemann glass. The whole operation was carried out in the dry box. The capillaries were sealed immediately after removing from the dry box. The x-ray exposure time varied from 5 to 8 hours depending on the sample.

The d-spacings were calculated from the formula

$$n\lambda = 2d \sin\theta \qquad [8]$$

where the wavelength $\lambda = 1.5418\text{Å}$

The relative intensities of the lines were estimated visually.

Microscope Studies

Crystals were mounted on a glass slide which had been dried in a desiccator. The crystals were bathed in Nujol and a cover slip put over the crystals. The crystals were observed with a petrographic microscope under a low

power (40x) in plane polarized light.

The crystals were photographed by a Leitz Aristophot apparatus. The photography was done under orthoscopic illumination. No filters were used for this purpose. Photography was done by Mr. E. Hearns of the Department of Geology, University of Ottawa.

Decomposition pressures of $NbBr_4$

The Apparatus: The decomposition pressures of $NbBr_4$ were measured by dew point technique. The design of the apparatus was a slight modification of that used by Schäfer (34) for measurement of the decomposition of $NbCl_4$. The apparatus is shown in Fig. 13.

The dew point apparatus A was constructed of Pyrex glass, 20 mm in diameter and 100 mm long. It contained the sample at the bottom. A cold finger B, for observing the $NbBr_5$ condensate extended about 20-25 mm into the upper part of the vessel. The cold finger contained a clear constant boiling liquid. The liquid was heated by means of a coil heater which was made by wrapping nichrome resistance wire on a quartz rod. Power was supplied to this heater from a variable autotransformer. A fine gauge calibrated chromel-alumel thermocouple and potentiometer were used for

Fig. 13: Dew point apparatus and assembly for measurement of decomposition pressures of $NbBr_4$ (not to scale)

A = reaction vessel

B = cold finger

C = condenser

D = vapour mantle

E = boiling liquid

F = furnace

G = copper block

H = furnace control thermocouple

I = measuring thermocouple

J = condenser to prevent escape of vapour from the mantle

K = cold finger thermocouple

L = cold finger heater

M = thermometer

N = MgO packing

O = opening for thermocuples

P = connection to manostat

Q = sample

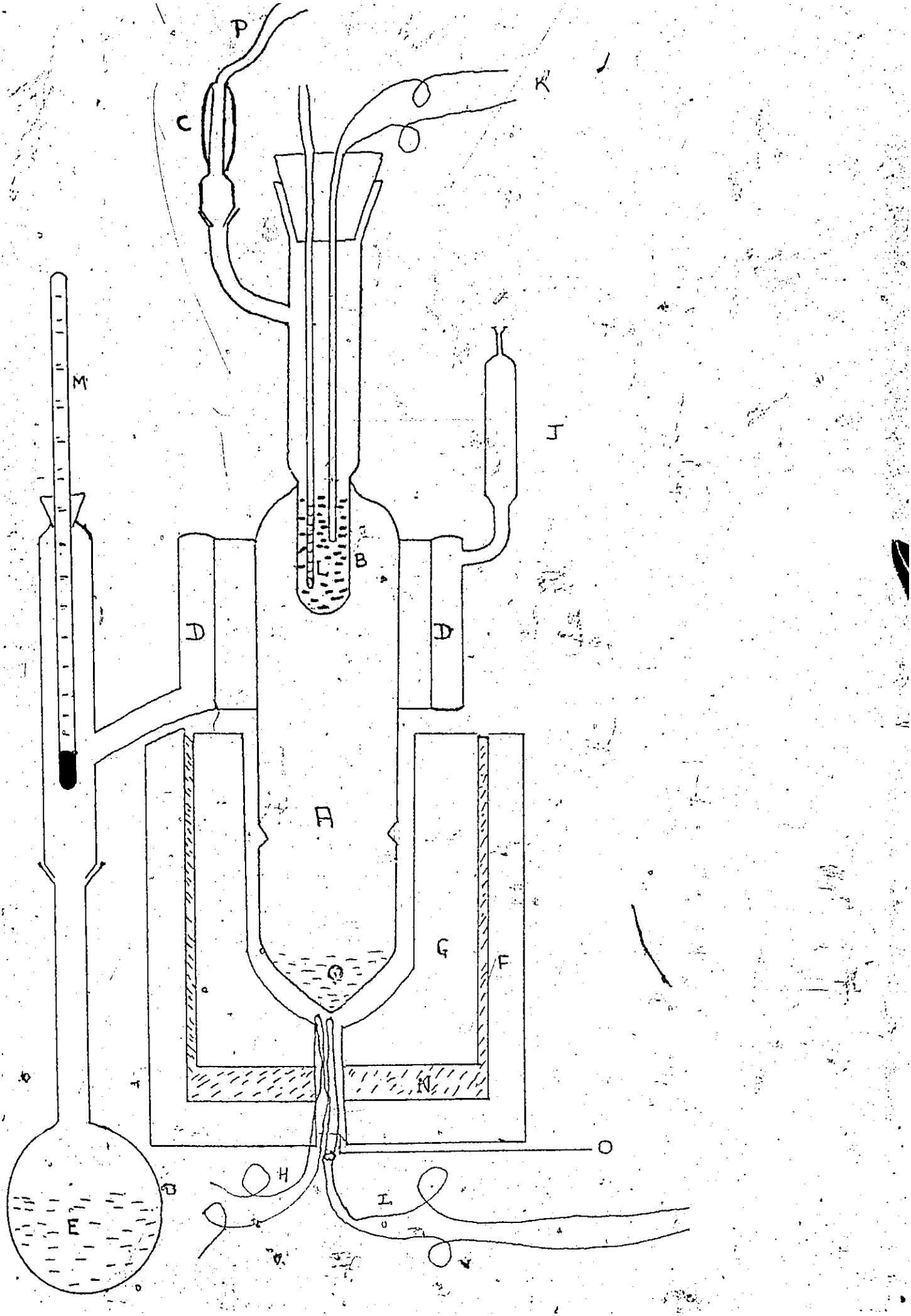
P
C
K
M
J
B
D
D
A
G
F
Q
N
O
H
I
E

temperature measurements. The reference junction was maintained at 0°C. The thermocouple was contained in a glass jacket to prevent attack by the hot liquid. The temperature of the liquid in the cold finger was adjusted by means of a Gilmont-Othmer type (84) manostat which controlled the pressure of the vapour. To prevent loss of liquid during measurement, condenser C was included between the cold finger and the manostat.

A vapour mantle D surrounded the upper part of the reaction vessel and its temperature was kept well above the dew point temperature so that condensate only appeared on the cold finger and not on the inner surface of the reaction vessel. The vapour was supplied by a boiler E which was surrounded by a heating mantle. To ensure a free flow of vapour to the vapour mantle, the boiler and the attached parts were well insulated by asbestos tape. Condenser J with a $CaCl_2$ tube prevented escape of vapour to the atmosphere.

Two liquids, nitrobenzene (b.p. 210°) and benzophenone (b.p. 306°) were used as boiling liquids. For the vapour bath, benzophenone was found to be the more suitable.

The heating system consisted of a large diameter furnace F made by winding nichrome ribbon on a ceramic tube

12 inches in length. It was closed at one end except for a 4 mm opening O. Placed inside of this furnace was a tightly fitted copper block G, 50 mm in diameter and containing a 22 mm diameter opening for the reaction vessel. The copper block had a 4 mm opening at the bottom for thermocouples: One (H) for the control of the temperature and the other (I) for measuring the furnace temperature by means of a potentiometer. These were led through to the reaction vessel in fine ceramic tubing. The heavy copper block was kept at the upper part of the furnace by magnesia packing which minimized heat loss from the bottom.

The temperature of the furnace was controlled by a Melab proportional controller with platinum resistance thermometer.

Measurement: The sample was transferred to the reaction vessel in a transferring apparatus. It was then thoroughly outgassed (10^{-5} torr) and sealed. The temperature of the solid sample was adjusted to a predetermined temperature. The fluctuations in the temperature were recorded by taking temperature readings every 10 minutes for the first hour and every 5 minutes for the next half-hour and thereafter

every minute for 15 minutes until absolutely steady temperature readings were obtained. With the proportionate controller it was possible to maintain the temperature of the solid sample to $\pm 0.2°C$. The temperature of the vapour mantle was kept 20° higher than the dew point temperature.

The measurements were begun several hours after the required furnace temperature was reached. To effect a measurement, the temperature in the cold finger was lowered from a point about 20° above the dew point until condensate appeared on the upper part of the cold finger. A slight raising of temperature caused the condensate to disappear.

Initially the temperature was approached from above by lowering the temperature in steps of 5°, followed by 2° steps and finally in steps of 0.5°. This was repeated several times to get consistent readings.

The observation of the condensate at the cold finger was done with the aid of adequate lighting and a magnifying lens. Much care was taken to distinguish between liquid and crystalline condensate. A crystalline condensate of $NbBr_5$ was red-orange and its whisker like growth on the cold finger was easily recognized. Appearance of liquid condensate, which was very deep orange, was somewhat more difficult to observe.

At high furnace temperatures, fine needles of $NbBr_4$ deposited on the cold finger but this deposit caused little interference in the observation of the dew point. Moreover it was an easy matter to sublime the $NbBr_4$ crystals back to the bottom part of the reaction vessel by placing the vessel in a temperature gradient.

The unavoidable presence of $NbOBr_3$ in small amounts, caused problems in the initial stages of the measurements. Its appearance on the cold finger was similar to that of $NbBr_5$ crystals. However with little experience it was possible to differentiate between the shiny red-orange crystals of $NbBr_5$ and the dull yellow-brown crystals of $NbOBr_3$. It should be mentioned that $NbOBr_3$, may dissolve in liquid $NbBr_5$. Schäfer and Pietruck (85) have shown that in the case of the chloride, the solubility is rather small and it did not markedly affect the saturation pressure of $NbCl_5$ (34). We expect that the bromide system is similar in this respect.

The static method employed here for measuring the vapour pressure is superior to the dynamic method because the former method allows the equilibrium to be established over a period of time while the dynamic method requires the equilibrium to be established instantaneously. Schäfer

and Dohmann (92) have shown that in the case of $NbCl_4$ decomposition, equilibrium was established only slowly. We would expect that the bromide system would show essentially the same behaviour.

To ensure that equilibrium was established we proceeded in the following way. The block furnace was heated to a predetermined temperature. Readings were carried out for several days and the dew point remained unchanged. Then the temperature of the furnace was altered by ±3° and the dew point redetermined. A corresponding change of a few degrees in dew point was observed. Return to the original furnace temperature gave the original dew point.

The measurements were performed on the second sample from a different preparation to check the validity of the data obtained.

Vapour pressure of $NbBr_4$

The type of reaction vessel (30) used is shown in Fig. 14. It consisted of a Pyrex glass chamber with a thin glass rod carrying a strip of metal.

The true vapour pressure of $NbBr_4$ can only be measured in an atmosphere of $NbBr_5$ which prevents the

Fig. 14: Pyrex reaction vessel for measuring true vapour pressures of $NbBr_4$.

A = $NbBr_5$

B = niobium metal strip

C = glass rod for holding the metal in centre of the reaction vessel

D = seal-off point

E = connection to vacuum line

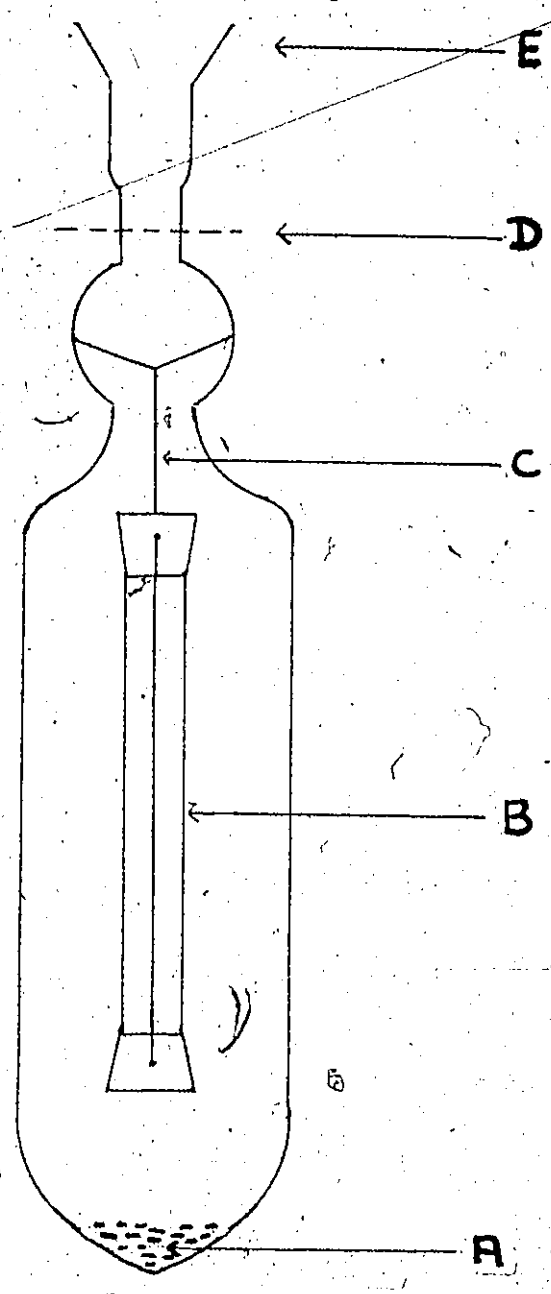
E
D
C
B
A

disproportionation of the tetrabromide. The experimental technique thus demands a procedure in which the vapour pressure of $NbBr_4$ in equilibrium with $NbBr_5$, is determined. To establish this particular equilibrium, $NbBr_5$ and Nb metal are allowed to react in a sealed vessel of the type described above. If the vessel is suddenly quenched, the constituents of the gaseous phase i.e. $NbBr_4$ and $NbBr_5$ will deposit on the glass wall because it is the first to cool. The crystals on the glass wall are analysed and the vapour pressure determined from the ideal gas relationship.

Owing to considerable experimental difficulties this experiment was discontinued. In particular, deposition of $NbBr_4$ was not wholly confined to the glass walls. A considerable quantity of $NbBr_4$ deposited on the glass rod. This was attributed to the latent heat of fusion of liquid salts (used for high temperature baths) solidifying on the outer walls of the reaction vessel during quenching and this heated the glass wall to a higher temperature than the glass rod itself.

Calorimetry -

Construction of calorimeter

(i) Thermostat: The thermostat consisted of a glass jar which was insulated with vermiculite.

This thermobath temperature was controlled by a mercury contact thermoregulator. The temperature was controlled at 25.0°±0.1°C. The thermostat heater was controlled by an electronic relay, 115 V and 50-60 cyc. supplied by Precision Scientific Co., Chicago. The cooling coils were directly connected to the tap water. The thermostat was positioned by a jacking system.

(ii) Calorimeter: An all-glass calorimeter similar to that used by Greenwood and Perkins (86) was constructed but some improvements were incorporated. Fig.15a shows the construction of the calorimeter.

The calorimeter head was a 60/65 male joint. It carried the following attachments: wells of thin glass, A and B, for containing the calibration heater and the thermistor; a stirrer C with a ball joint arrangement: a 7/25 female joint F, to admit dry argon while G is a 7/25 male joint which serves as an outlet for argon; connection H for a vacuum line; mercury sealed sample and getter holders D and E - this arrangement is shown in Fig.15b.

The calorimeter was placed in the thermostat and secured in position by means of a clamp.

The temperature sensing element: The temperature changes were detected by means of a Sargent-Welch model thermistor immersed

Fig. 15a: Diagram showing the calorimeter and its cross section through X-Y.

A = well for calibration heater

B = well for thermistor

C = stirrer

D = sample bulb

E = getter bulb

F = argon inlet

G = argon outlet

H = connection to vacuum line

I = ball-joint arrangement for the stirrer

J_1, J_2 = spring holders to keep the calorimeter head and body together

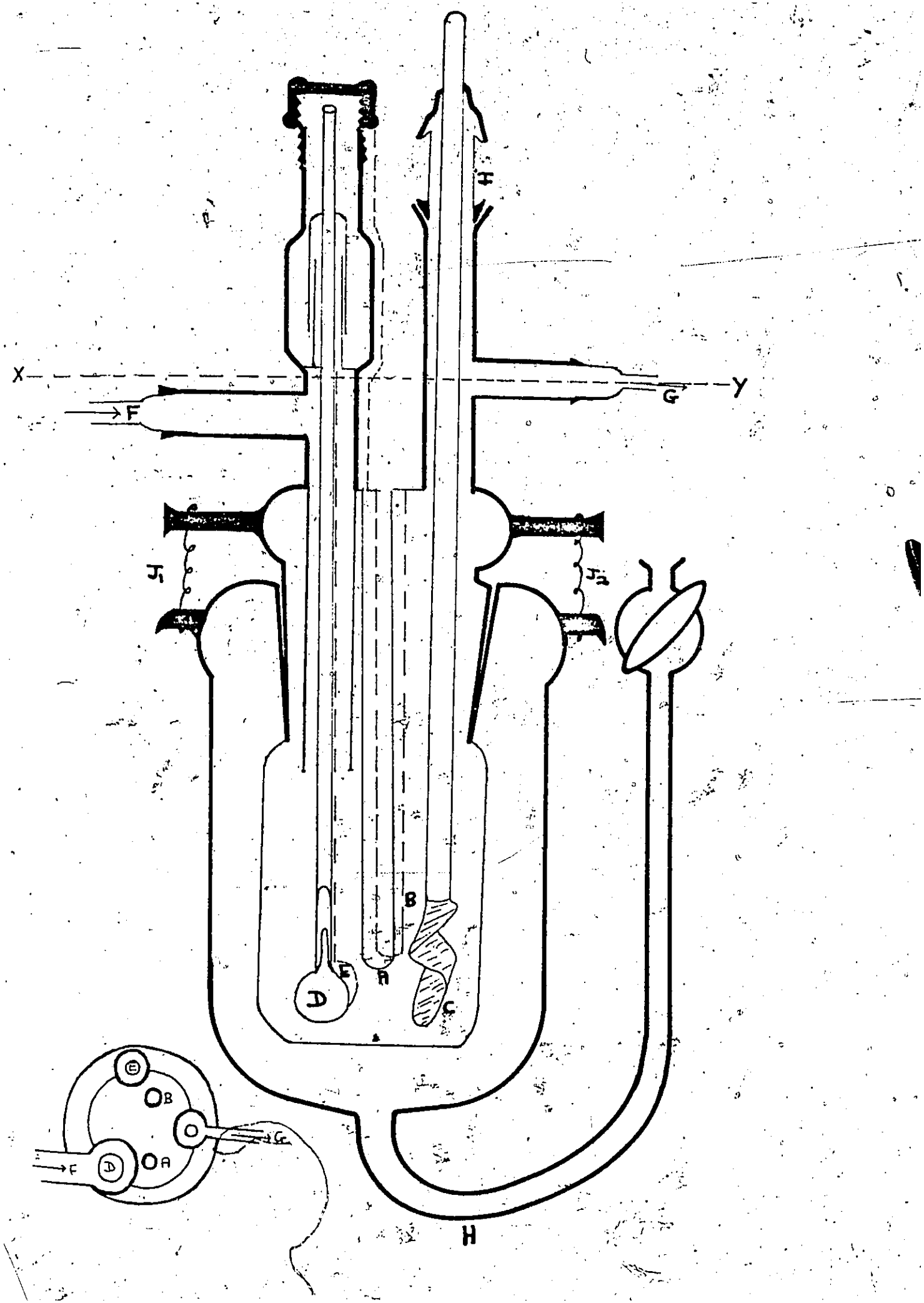
H
X
Y
G
F
J1
J2
B
A
E
D
C
H
E
OB
O
Oc
D
OA
F

Fig. 15b: Enlarged view of sample or getter holder with mercury seal.

A = screw cap for thrusting sample or getter holder against floor of calorimeter in order to break bulb E.

B = mercury seal

C = sample or getter holder

D = bulb adapter with a teflon sleeve

E = sample (getter) bulb

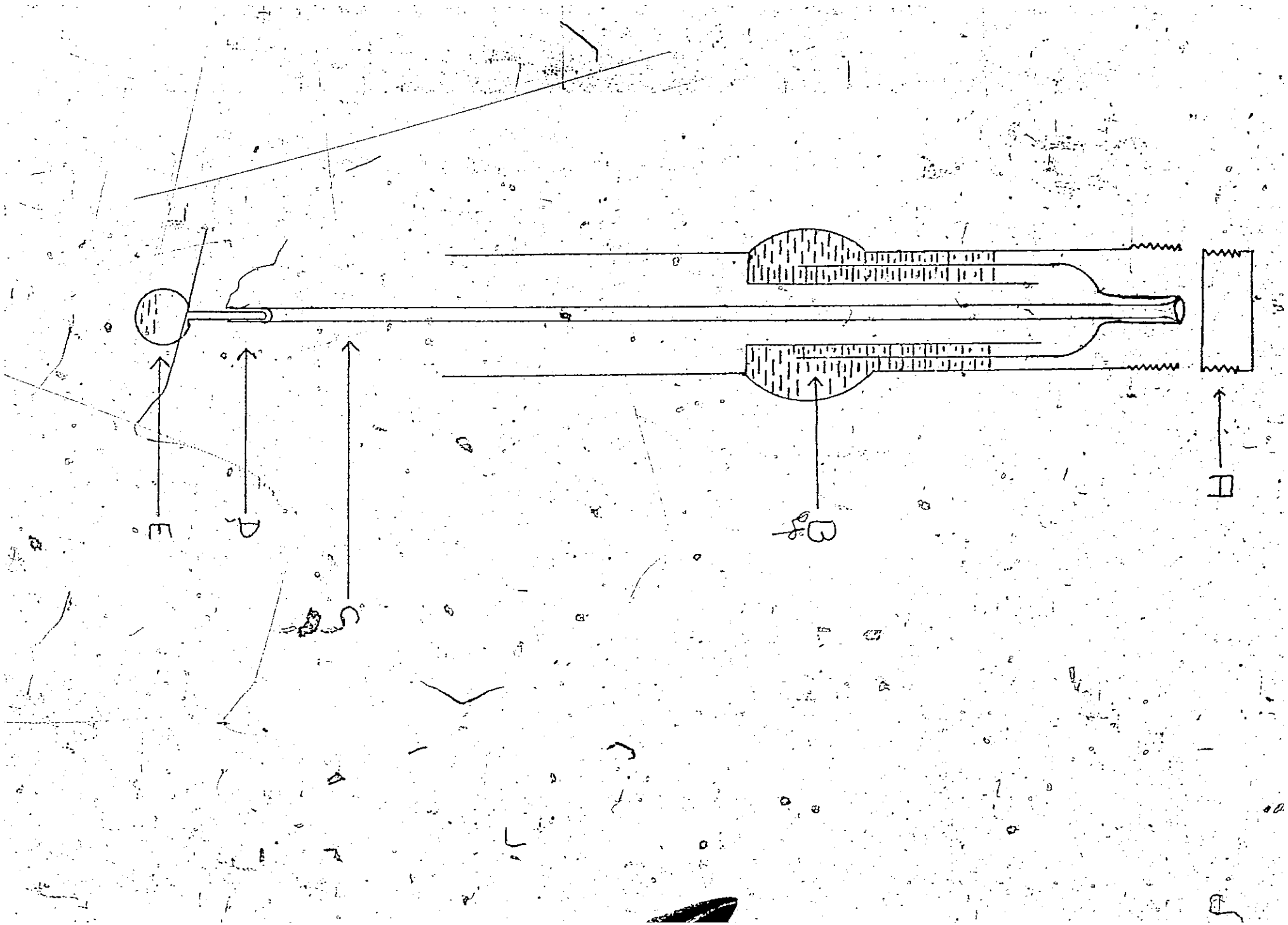

in silicone oil. This was connected through a Sargent-Welch model S-81601 thermistor bridge to a 10 m.v. recorder which was used as a null instrument.

The calibration heater: The calibration heater coil, made from No. 30 constantan wire and having a total resistance of about 5 ohms was standardized with a resistance thermometer bridge, type J-1003, supplied by M. Tinsley Co. Limited. Current was taken from three 2 volt wet cells connected in parallel. In order to achieve a steady current, it was passed through a dummy heater of 5 ohms resistance for at least one hour before a measurement. The current drawn was about 0.4 amps. The duration of the electrical heating was timed by means of an electric timer (reading to 0.1 second) which was synchronized with the heater by a three pole double throw switch as shown in Fig. 16.

The current was measured by means of a potentiometer, supplied by Derritron Electronics Limited, connected across five one ohm stndard resistors connected in parallel to give a resistance of 0.2 ohm.

Calorimetric liquid: The calorimetric liquid was 6.20N HCl This was prepared in bulk from concentrated 12N acid. The solution was stored in a large glass container fitted with a

Fig. 16: Synchronization circuit of calibration heater and the timer used for calorimetric measurements

A = 6 volt lead storage cells

B = 110 volt supply

C = timer

D = calibration heater

E = dummy heater

F = standard 1 ohm resistors

G = potentiometer

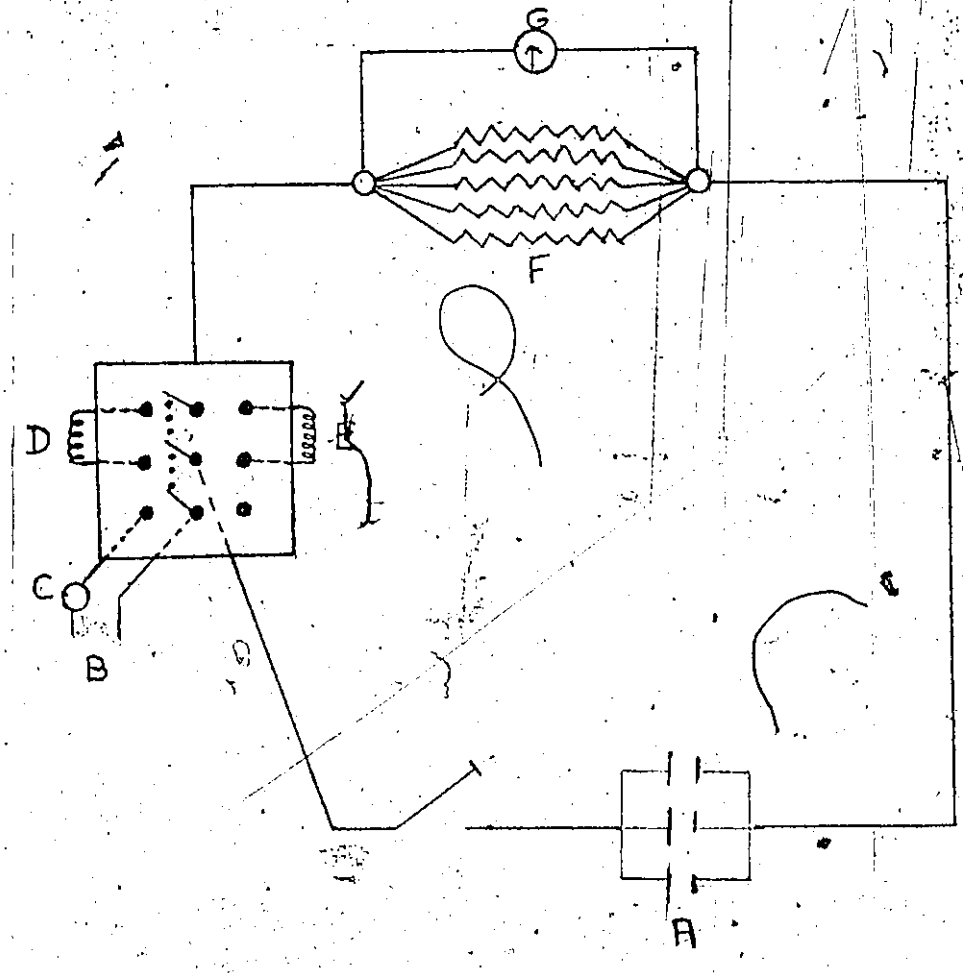
G
F
D
C
B
A

dispensing burette. The strength of the acid was determined by titration from time to time and found to be quite constant.

Measurement: Thin-walled sample bulbs were filled with the finely ground samples. While being sealed under nitrogen the bulb was kept cool with a wet filter paper to avoid decomposition of the sample. A glass rod was sealed on to the stem of the bulb to act as a holder. The sample bulb was then attached to the bulb holder by means of a Teflon sleeve. The getter bulb was filled with $NbCl_4$ in a dry box and attached to the getter holder.

About 180-200 ml. of the calorimetric liquid were introduced into the calorimeter. The joints were greased and the calorimeter assembled. The head of the calorimeter was insulated by a polystyrene cover plate and glass wool wrapping. The whole arrangement is shown in Fig. 17.

When the calorimeter liquid and the bath had reached approximately the same temperature, the calorimeter jacket was evacuated, the heating circuit was closed in the dummy position. Argon was passed for one hour through the calorimeter and then the getter bulb broken in order to consume any dissolved oxygen in the calorimeter liquid.

Fig. 17: A schematic diagram showing the calorimeter assembly.

A = The calorimeter (the various parts that constituted the calorimeter have been shown in Fig. 15a)

B = thermostat sitrrer and motor

C = the calorimeter stirrer motor

D = cooling water

E = thermostat heater

F = thermoregulator

G = thermometer

H = jacks

I = water level in thermobath

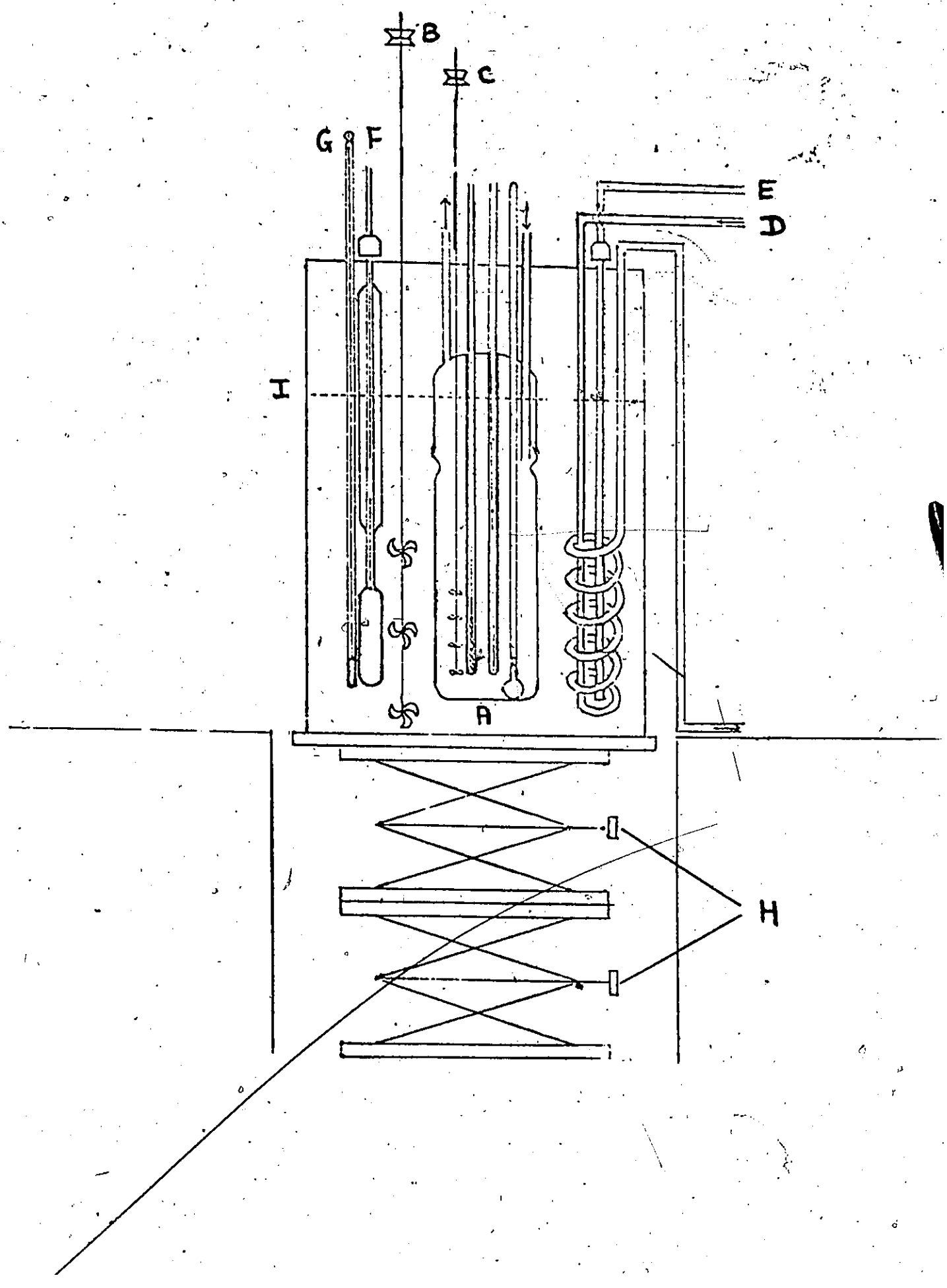
B
C
G
F
E
D
I
A
H

For purposes of evaluating the heat changes in the calorimeter, a correction was made for the exchange of heat between the calorimeter and its surroundings during the process. For this purpose, the course of the temperature changes was divided into three periods. The first period was observed for 8-10 minutes prior to the reaction or calibration. During the reaction or calibration heating and for some time afterwards the temperature of the inner vessel changes. The third period began when the rate of cooling of the calorimeter followed Newton's Law. A schematic diagram below shows the three periods typically observed for exothermic reactions (Fig. 18).

When the calorimeter had reached a steady state after the getter was broken, the heat capacity of the calorimeter was determined. The temperature of the calorimeter was followed for about 8-10 minutes. The heater switch was turned to the calorimeter position and the current measured every minute for the duration of the heating. The heating time varied from 250 to 350 seconds. The heater switch was turned back to the dummy position when the heating was stopped and the calorimeter temperature recorded every minute until the temperature change was constant over a fairly long

Fig. 18: A typical temperature-time curve for the purposes of evaluating heat changes in a calorimeter

Curve A-B = initial period

Curve B-C = reaction period

Curve C-D = cooling period

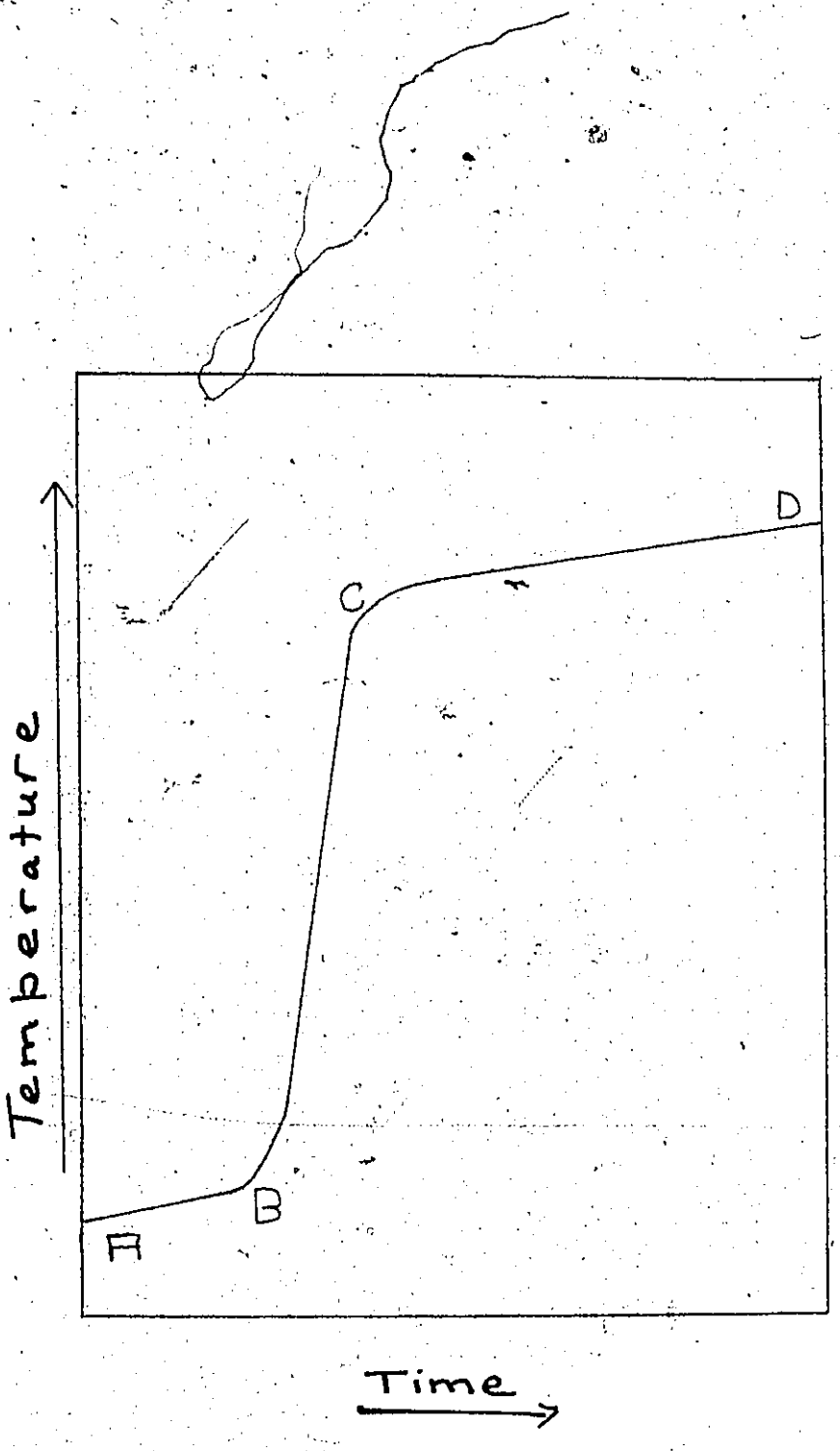
Temperature
A
B
C
D
Time

period of time (20-30 minutes). The sample bulb was then broken. Dissolution was complete in 2 to 4 minutes in most cases. Initially the temperature was recorded every thirty seconds for the first 8-10 munutes and every minute thereafter until the rate of temperature change was constant. Following the reaction, a second calibration was carried out in the usual manner.

It was essential that the dissolution was rapid following the breaking of the sample bulb. If not, graphical methods of evaluating the heat changes proved unreliable. To achieve this, the calorimetric liquid was stirred rapidly. Secondly the sample bulbs were crushed well so that the swirling liquid could take the entire sample rapidly into solution. If the sample bulbs were not broken well, there was a tendency of the remaining part of the bulb to trap the sample by resting at the bottom of the calorimeter allowing the solution to reach it only with difficulty. This problem was eliminated by raising the sample holder from the bottom of the calorimeter after breaking the bulbs, thus preventing trappping of the sample by the unbroken part of the bulb at the bottom of the calorimeter.

Evaluation of Data

Heat capacity of the calorimeter: The energy q in calories supplied by calibration heater was determined using the

equation:

$$q = \frac{I^2Rt}{4.184} \text{ cal} \qquad [9]$$

where R is the resistance of the coil in ohms, I the current in amperes and t the time in seconds. When I varied slightly, which was seldom, I^2R values were plotted against t, and q was then the area under the curve. The heat capacity C of the calorimeter for the fore and after period was then determined by using the equation

$$C = \frac{q}{T} \text{ cal degree}^{-1} \qquad [10]$$

where C is the heat capacity, q the energy in calories and T the temperature change. The two measurements generally agreed within 2% of each other. The average of the two was taken as the heat capacity of the calorimeter.

The reaction temperature

The heat changes were determined graphically. A vertical line was drawn through the curve at the point corresponding to half the determined total time. The temperature-time curves in the preperiod and after-period were extrapolated to intersect this vertical line. The difference of the two intersecting points was then taken to be the temperature change.

A more precise method of evaluation has been described by Kubaschewski et al. (87). This method was used where dissolution was too slow to permit heat evaluation by the graphical method as in the case of iodides and in checking the accuracy of the calorimeter by dissolving KCl in water.

Heats of solution: The molar heats of solution ΔH_s were calculated by use of the equation

$$\Delta H_s = C \times T \times \frac{m.w}{w} \text{ cal/mole} \qquad [11]$$

where m.w is the molecular weight of the sample. w is the weight of the sample. C and T have been defined earlier. Since the concentration used were very low, the values obtained were very nearly equal to the differential heats of solution at infinite dilution.

Chapter 4

Results and Discussion

1. Magnetic Studies

Introduction

In our general attempt to characterize better the A_2MX_6 complexes, we found it necessary to repeat certain of the magnetic studies reported by Torp (21). As pointed out earlier, the susceptibilities of these systems showed anomalous dependence on temperature.

The purity of the niobium metal used by Torp was not stated, while the tantalum used was 99.9% pure. On the other hand, we possessed metals of a high degree of purity (99.95%). In order to establish whether our pure materials would give preparations whose properties would be free of the above-mentioned anomalies, we undertook initially to re-examine the magnetic properties of these A_2NbX_6 complexes.

As will be shown later, these magnetic studies assumed a paramount importance in characterization of A_2MX_6 preparations and for this reason, a fairly detailed account of magnetic theory will be given in the next section.

General aspects of magnetism

Before discussing the experimental results, a brief account of the pertinent aspects of magnetic theory will be given.

In the Langevin (88) theory of magnetism each molecule is considered to be a small permanent magnet which tends to be oriented in the direction of an applied magnetic field. This tendency is opposed by the disorienting effect of thermal energy. Consideration of these two factors, leads

to the expression:

$$\chi_m = \frac{N\mu^2}{3kT} \qquad [12]$$

where χ_m = molar susceptibility

N = Avogadro's number

k = Boltzmann constant

μ = permanent magnetic moment

T = absolute temperature.

Langevin's theory of paramagnetism was improved by Van Vleck (89). His expression was similar to Langevin's but it contained an additional term:

$$\chi_m = \frac{N\mu^2}{3kT} + N\alpha \qquad [13]$$

where α contains the diamagnetic part as well as a small temperature independent paramagnetic contribution (T.I.P.).

According to Langevin's formula, the paramagnetic susceptibility varies inversely with absolute temperature. This generalization is known as the Curie Law and was discovered before Langevin derived his expression. The magnetic moment of such a compound is obtained from the slope of a plot of χ_m against 1/T by application of equation [13].

In order for the Curie Law to hold, μ must, of course, be independent of temperature.

However, the magnetic susceptibility of a great many substances deviates from the requirements of the Curie Law in a way which may be described by the Curie-Weiss law:

$$\chi_m = \frac{C}{(T-\theta)} \qquad [14]$$

where C = Curie constant

θ = Weiss constant

The origin of the Weiss constant frequently is to be found in the exchange forces between ions. Under these circumstances, the moment may be calculated by use of Equation [14]. Experimentally θ may be determined from the intercept of a plot of $1/\chi_m$ against absolute temperature if such a plot is linear. If the origin of θ cannot be ascribed to exchange forces then no particular significance can be attached to the Weiss constant.

The term $N\alpha$ in equation [13] is frequently used to express only the diamagnetic contribution. In such cases, the slope of a plot of χ_m against 1/T does not give the true moment. The slope is then said to give an "effective" moment, μ_{eff}.

The effective magnetic moment (μ_{eff}) can be calculated at a particular temperature by application of the equation:

$$\chi_m = \frac{N\beta^2\mu^2_{eff}}{3\,kT} + N\alpha \qquad [15]$$

or

$$\mu_{eff} = 2.828\sqrt{\chi_m (corr)T} \qquad [16]$$

where $\chi_m(corr) = \chi_m' - N\alpha$

The second term, $N\alpha$, in Van Vleck's formula needs further consideration. As this term can make considerable contribution to the total susceptibility and in many cases, is the cause of departure from ideal Curie Law behaviour, its origin and significance is worth noting. In a completely general way the energy of a particular level, i, of an ion in a magnetic field of strength H may be expressed as:

$$E_i = E_i(0) + E_i(1)\, H + E_i(2)\, H^2 + \ldots \qquad [17]$$

where $E_i(0)$ is the energy of level i in the absence of the external magnetic field, $E_i(1)$ is the coefficient of the first order Zeeman effect and $E_i(2)$ is the coefficient of the second order Zeeman effect. (The perturbation of the energy levels of an ion by the magnetic field is known as the Zeeman effect.) The second order Zeeman effect may be visualized as a distortion of the electron distribution of the ground state by the magnetic field H. This is achieved by mixing into the ground state some of the character of a higher state by an

amount proportional to H^2. This is in contrast to the first order effect which leaves the centre of gravity of the state unchanged. This effect is illustrated in Fig. 19.

Fig. 19: Splitting of levels under H

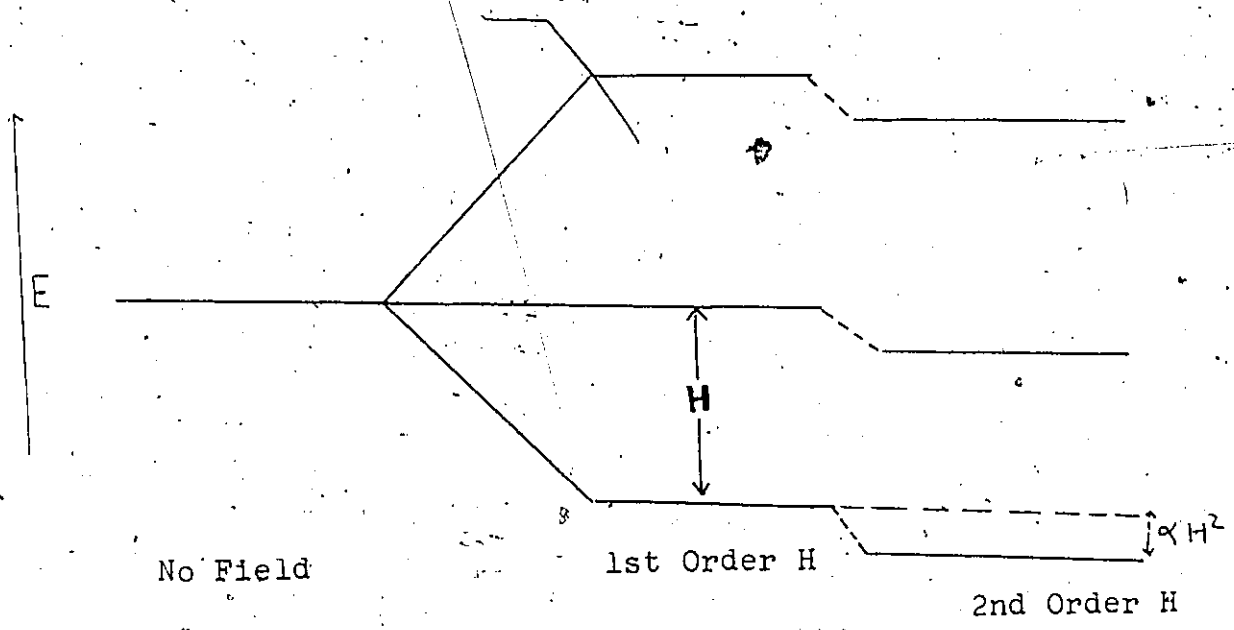

The second order Zeeman effect contribution is distinct from the mixing in of a higher level due to spin orbit coupling, which makes a constant contribution to the moment. The former leads to departure from the Curie or Curie-Weiss law, the latter does not. The separation between

interacting levels is of great importance, since not only is the magnitude of the effect dependent on it but, if it is comparable to kT, the higher level will actually be populated and a temperature dependent susceptibility will arise. When the separation of the interacting levels is much greater than kT, thermal population of the upper level does not occur and the contribution is independent of temperature. It is therefore frequently known as temperature independent paramagnetism (T.I P.) or Van Vleck paramagnetism. This situation is found in transition metal ions where the interacting levels have been split by the ligand field. Because this splitting is comparatively large, the contribution is rather small and is usually only observable at higher temperatures where the normal Curie paramagnetism is relatively small.

Owing to covalency, the molecular orbitals in which the unpaired electrons are to be found are composed only partly of metal orbitals; ligand orbitals can be an important constituent. This has the effect of reducing the orbital angular momentum and any contribution to the magnetic moment from this momentum. The spin-orbit coupling is also reduced. A delocalization factor k which is combined with the angular momentum operator has been introduced in order to take account

of the effect. This factor may be taken to be the fraction of time which the d-electron spends on the metal. A value of k=1 represents the extreme ionic case and k is reduced as the covalency increases. This factor was first introduced by Stevens (90) to explain the hyperfine splitting of the e.s.r. spectrum of K_2IrCl_6. However, Stevens did not specifically describe the effect in this way. The effect of reducing k is to reduce the orbital contribution and this causes the moment to approach the spin only value. Experimentally it is observed that in regular octahedral complexes, the orbital reduction factor usually will not be less than about 0.7 although for tetrahedral complexes, it may be as low as 0.5. The theoretical reasons for this have been outlined recently (91).

Ligand field components of symmetry lower than cubic lift the orbital degeneracy of T terms. Such components markedly affect the magnetic properties of T terms because they alter the arrangement of energy levels amongst which thermal distribution occurs. If the lower symmetry component causes a splitting, which in the absence of spin-orbit coupling

would be of energy less than about the spin-orbit coupling constant λ, then the effect on the magnetic moment is small. As the splitting by the low symmetry ligand field component becomes larger than the spin-orbit coupling constant, the magnetic moment tends towards the spin only value, and the temperature dependence tends to decrease.

Magnetic theory for Octahedral d^1 systems

Some particular aspects of magnetic theory relevant to a d^1 system should be mentioned. Energy levels for a t_{2g}^1 configuration under the influence of a strong octahedral field and spin orbit coupling are represented diagrammatically in Fig. 20.

Because T ground states retain some orbital angular momentum they give rise to an orbital contribution to the magnetic moment. However spin-orbit coupling removes some of their degeneracy and a quantitative estimation of the orbital contribution is possible only if the actual magnitudes of the splittings are known.

As seen in Fig. 20, the $^2T_{2g}$ state gives under the influence of spin-orbit coupling a ground state Γ_8 (t_{2g})

Fig. 20: Energy levels of d^1 system in an octahedral environment.

(A) Field-free ion term energy

(B) Levels in a strong octahedral field

(C) Strong octahedral field + weak spin-orbit coupling

(D) Strong octahedral field + medium spin-orbit coupling

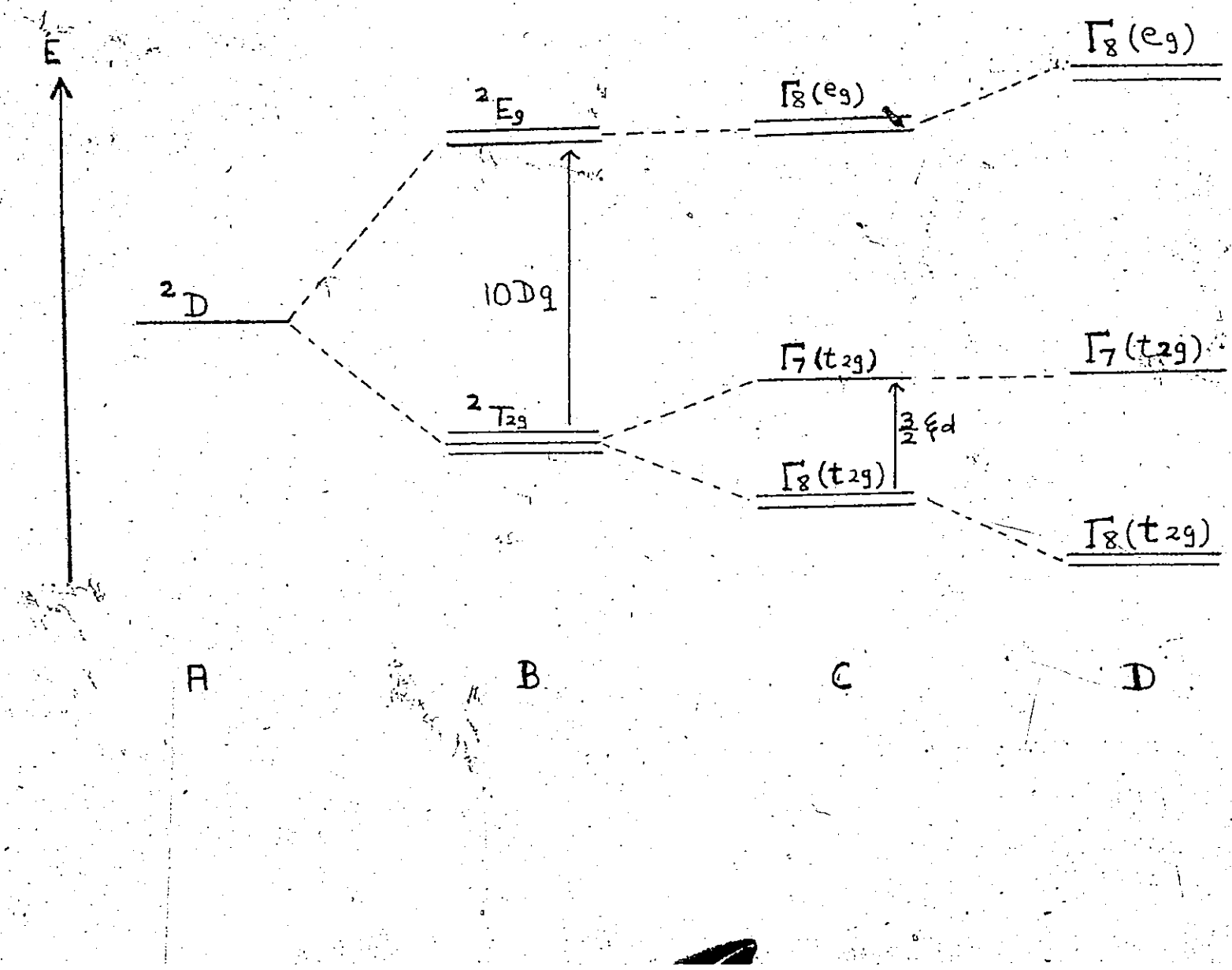
E
^2D
^2E_g
$^2T_{2g}$
10Dq
$\Gamma_8(e_g)$
$\Gamma_7(t_{2g})$
$\Gamma_8(t_{2g})$
$\frac{3}{2}\xi d$
$\Gamma_8(e_g)$
$\Gamma_7(t_{2g})$
$\Gamma_8(t_{2g})$
A
B
C
D

and at still higher energy $\Gamma_8 (e_g)$. To a first order the ground state $\Gamma_8 (t_{2g})$ is non-magnetic since the matrix elements for the magnetic operator:

$$< \Psi_8 (t_{2g}) \mid l_z + 2S_z \mid \Psi_8 (t_{2g}) >$$

are zero. There is a second order Zeeman contribution because the non-diagonal matrix elements

$$< \Psi_8 (t_{2g}) \mid l_z + 2S_z \mid \Psi_7 (t_{2g}) >$$

are non-zero. To this particular temperature independent contribution to the susceptibility, Kotani (92) added the first order terms arising from thermal excitation to the $\Gamma_7 (t_{2g})$ state and derived an expression for variation of μ_{eff} with spin-orbit coupling and temperature:

$$\mu^2_{eff} = \frac{8 + (3x-8)e^{\frac{-3x}{2}}}{x\,(2 + e^{\frac{-3x}{2}})} \qquad [18]$$

where $x = \frac{\xi}{kT}$ (ξ is the one-electron spin-orbit coupling constant)

In deriving this formula Kotani assumed a perfect cubic field and no magnetic interaction between neighbouring ions.

When the energy difference between the $\Gamma_7 (t_{2g})$ and the $\Gamma_8(t_{2g})$ state is not large with respect to kT (this

energy difference being $\frac{3\xi}{2}$), the $\Gamma_7(t_{2g})$ state may become populated and the magnetic behaviour tends to become more "normal" with μ_{eff} independent of temperature.

Liehr (93) argued that when $\xi >> kT$ i.e. for 5d elements, the excitation to the $\Gamma_7(t_{2g})$ state is much less important than mixing of the $\Gamma_8(e_g)$ wave function into the ground state $\Gamma_8(t_{2g})$ via spin-orbit coupling. Such intermixing makes the ground state diagonal matrix elements non-zero and a temperature dependent contribution to the susceptibility is produced. The susceptibility of heavy d^1 ions always shows some, but not substantial, temperature dependence.

While Kotani neglected the intermixing of wave functions entirely, Liehr applied the resulting corrections only to the diagonal matrix elements. The resulting expressions of Kotani and Liehr were considered useful in calculations dealing with first row and third row transition elements respectively (94, 95). Westland (96) has corrected the off-diagonal matrix elements to take account of orbital mixing between $\Gamma_8(e_g)$ and $\Gamma_8(t_{2g})$ and the calculations showed that there is a curvature in the χ_m versus $\frac{1}{T}$ plot only when kT is of the order of the spin-orbit coupling parameter. This may be the case with first row transition elements but is hardly

expected for Nb(IV) for which the free ion value of ξ is about 750 cm^{-1} (97). (kT is 209 cm^{-1} at room temperature.)

The spin-orbit coupling constant is smaller in complexes than in the free ions and the reduction may be quite considerable (98, 99, 100). Even if ξ for Nb(IV) is lowered in the complex, the value is expected to be large relative to kT at room temperature.

Experimental plots of χ_m against $1/T$ for A_2NbX_6 complexes

All the complexes studied in this thesis were found to be paramagnetic. Plots of χ_m, corrected for diamagnetism, versus 1/T are given in Figures 21 to 25. Susceptibilities obtained by Torp (21) are given for comparison in certain cases. The data were somewhat influenced by the conditions of preparation. Quenching or slow cooling of samples gave different results. In spite of very pure starting materials the susceptibilities of A_2NbCl_6 were essentially similar to those reported by Torp when his preparative procedures were followed.

This is not easily explained as particle size, conditions of packing and other experimental variables appeared to be fairly uniform from one measurement to another. One may suspect, however, that such a variation in properties arose through some chemical peculiarity, i.e., some alteration in crystal composition.

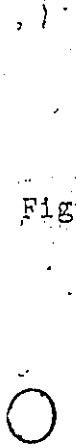

Fig. 21: Variation of corrected magnetic susceptibilities with reciprocal absolute temperature of some A_2NbCl_6 complexes prepared at high temperatures.

○ K_2NbCl_6: sample cooled rapidly

⊗ K_2NbCl_6: powdered single crystals

△ K_2NbCl_6: This sample was prepared by heating $NbCl_4$+2KCl with 5 milligrams of $NbCl_5$ and cooled slowly

⊠ Rb_2NbCl_6: sample cooled rapidly

□ Cs_2NbCl_6: sample cooled rapidly

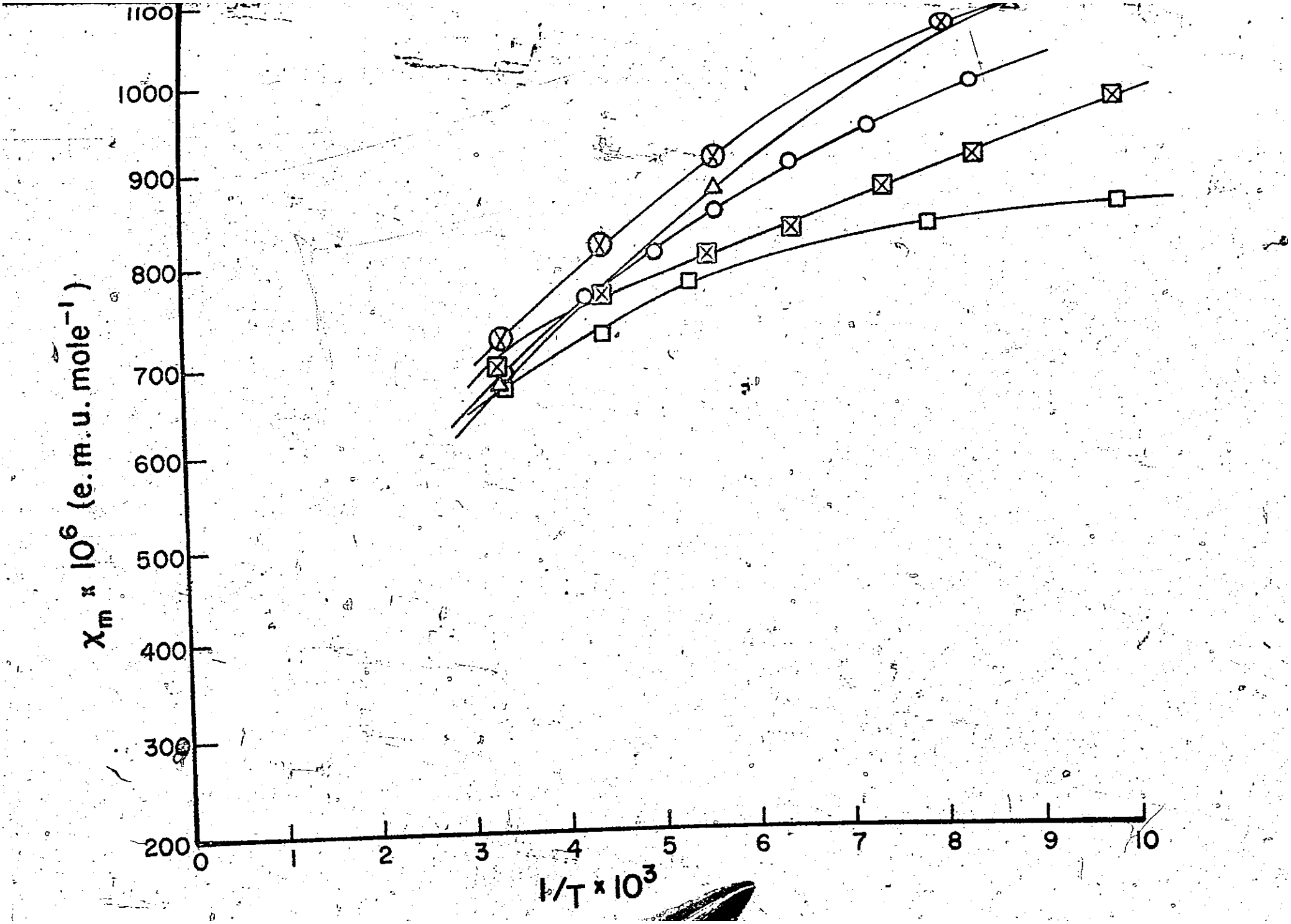
1100
1000
900
800
700
600
500
400
300
200
$\chi_m \times 10^6$ (e.m.u. mole^{-1})
0
1
2
3
4
5
6
7
8
9
10
$1/T \times 10^3$

Fig. 22. Variation of corrected magnetic susceptibilities with reciprocal absolute temperature of some A_2NbCl_6 complexes prepared at low temperatures.

● Cs_2NbCl_6 (300°)

○ Rb_2NbCl_6 (300°C)

△ K_2NbCl_6 (300°C)

□ Cs_2NbCl_6 (275°C)

■ Cs_2NbCl_6 (Aqueous)

The numbers in parenthesis indicate the temperature or method of preparation.

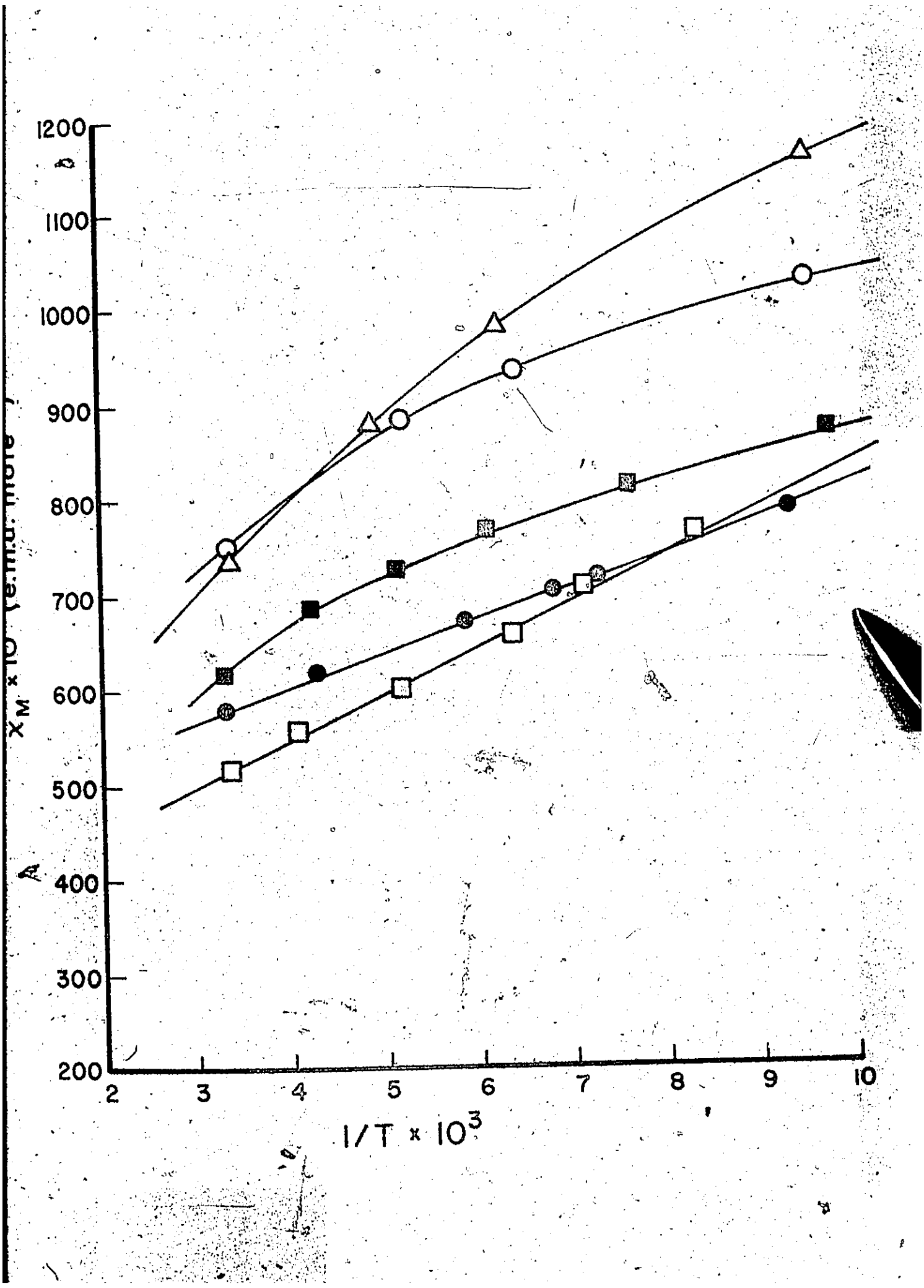
1200
1100
1000
900
800
700
600
500
400
300
200
2
3
4
5
6
7
8
9
10
1/T x 10³

Fig. 23: Variation of corrected magnetic susceptibilities with reciprocal absolute temperature of Na_2NbCl_6 (▲) and $(PyH)_2NbCl_6$ (○).

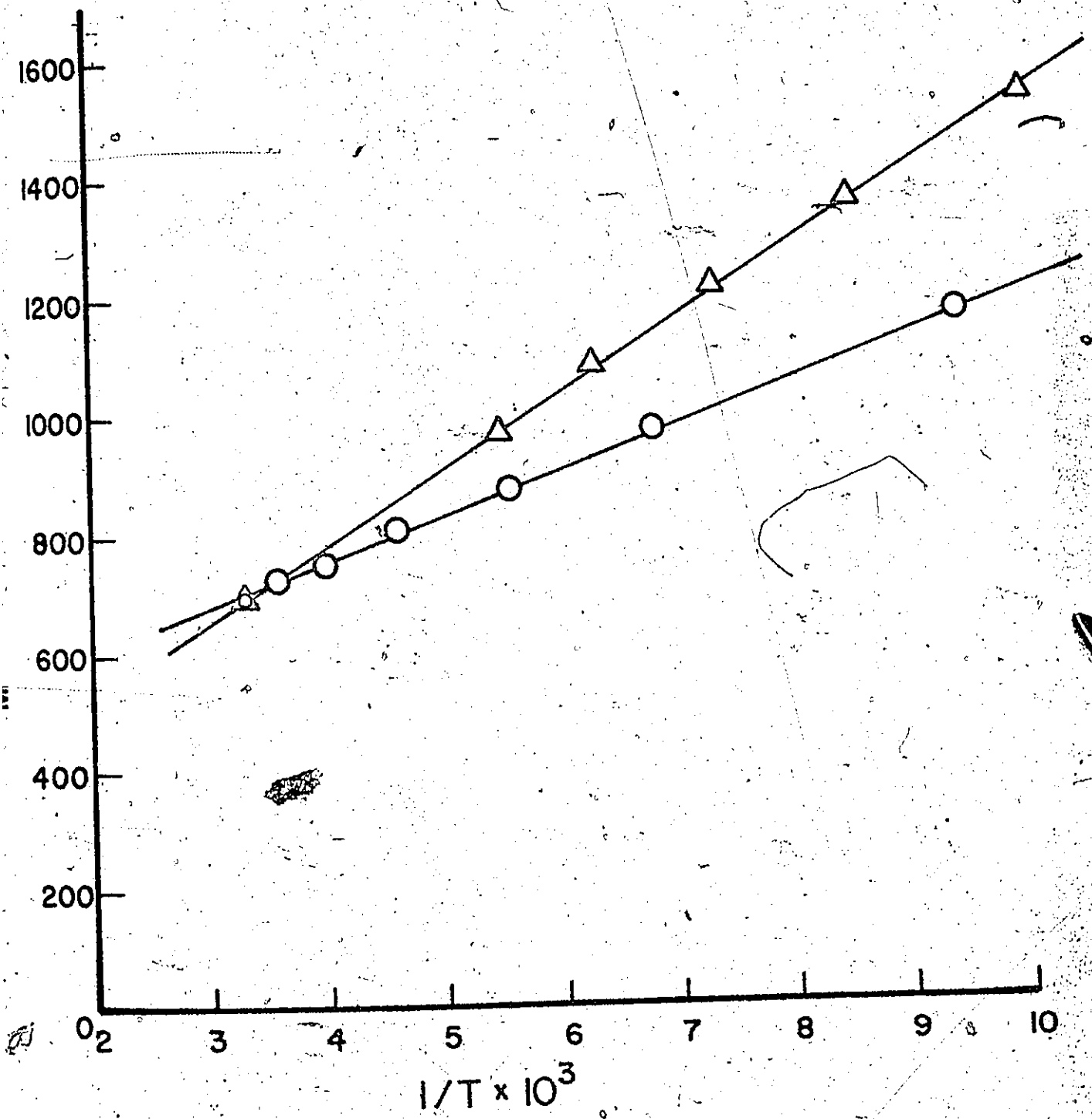
1600
1400
1200
1000
800
600
400
200
0
2
3
4
5
6
7
8
9
10
1/T x 10^3

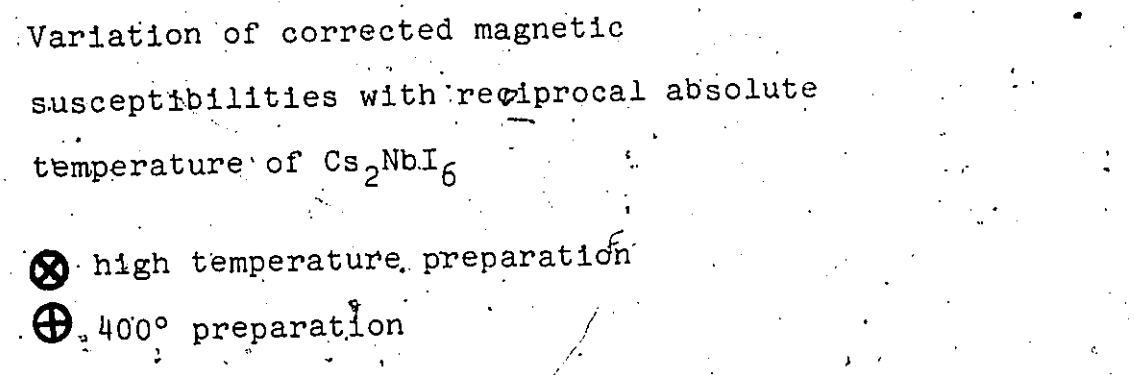

Fig. 24: Variation of corrected magnetic susceptibilities with reciprocal absolute temperature of Cs_2NbI_6

⊗ high temperature preparation

⊕ 400° preparation

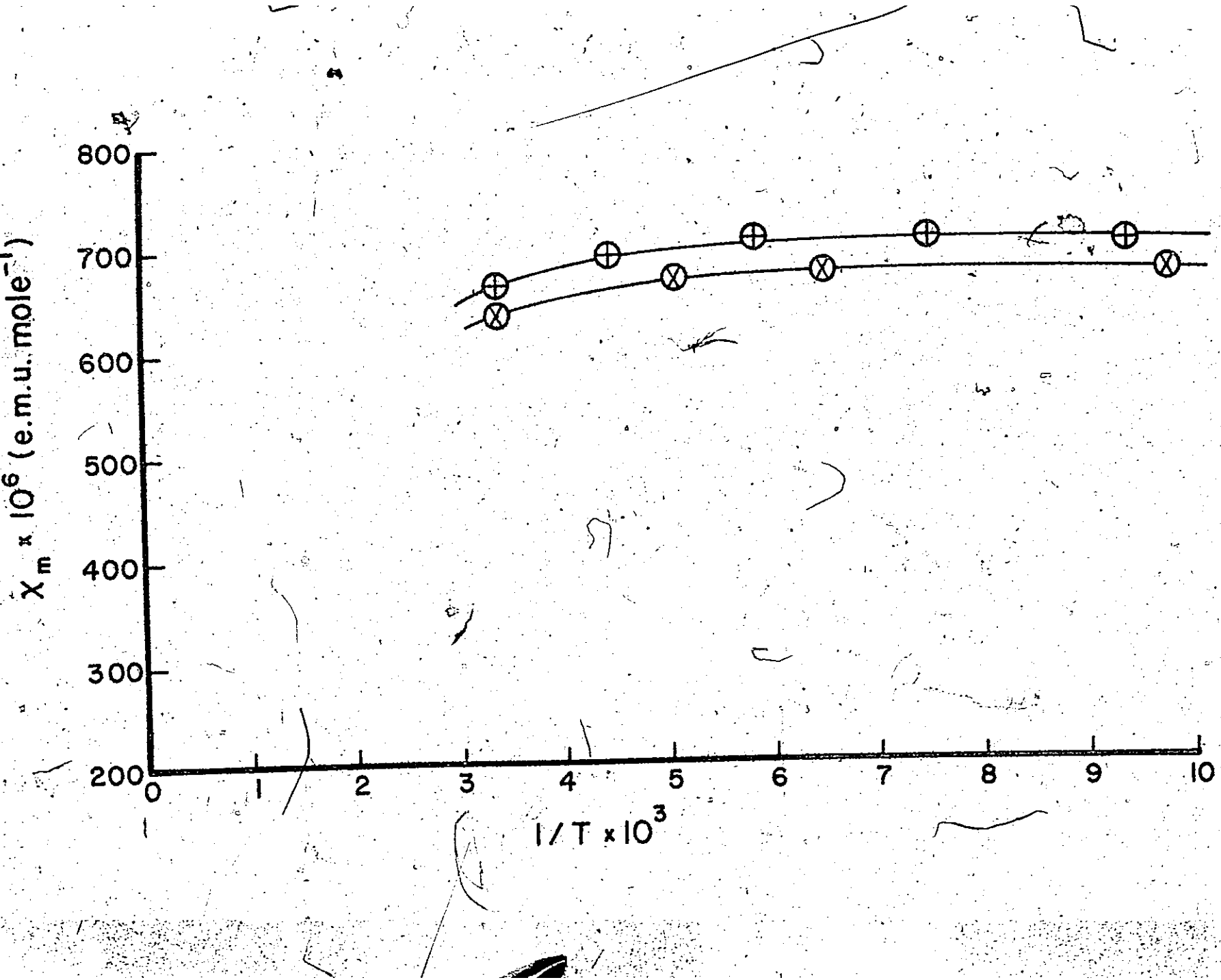
800
700
600
500
400
300
200
0
1
2
3
4
5
6
7
8
9
10
$\chi_m \times 10^6$ (e.m.u. mole^{-1})
$1/T \times 10^3$

Fig. 25: Magnetic data reported by Torp (ref. 21). Values of susceptibilities are apparently uncorrected for diamagnetism..

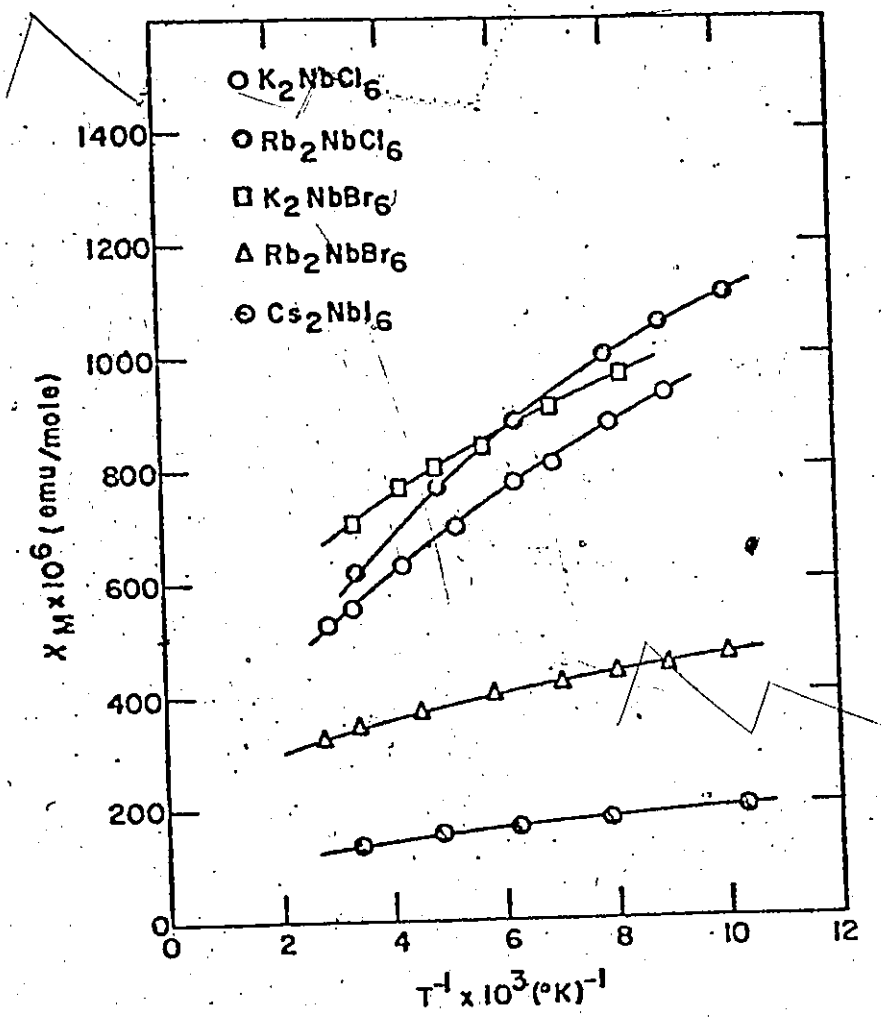
O K_2NbCl_6
O Rb_2NbCl_6
□ K_2NbBr_6
Δ Rb_2NbBr_6
Θ Cs_2NbI_6
$\chi_M \times 10^6$ (emu/mole)
$T^{-1} \times 10^3 (°K)^{-1}$
0
200
400
600
800
1000
1200
1400
2
4
6
8
10
12

Attempt at selection of magnetic parameters for $NbCl_6^{2-}$ ions

Both Torp (21) and Benzinger (29) found that there was only a rough correlation between experimental data and theoretical curves obtained by the use of the Kotani formula (92) - in other words, the theory did not satisfactorily account for the observed magnetic properties. Theoretical calculations of χ_m were carried out by us using choices of the various parameters in Westland's (96) expression which were considered reasonable for K_2NbCl_6. It was found that there was considerable latitude in the choice of Dq in fitting the experimental data. This parameter was assigned the value 2100 cm^{-1} as this value appears to be suitable for quadrivalent ions of the second transition period. Even if, as it appears from the electronic spectrum, the value is as high as 2500 cm^{-1}, there is little effect upon the accuracy of the curve-fitting process. In Fig. 26 a plot calculated using values of 425 cm^{-1} and 0.44 for ζ and k respectively, is shown fitted to the experimental points. Both of these parameters are remarkably low and are most probably unrealistic. It is to be noted that the value of ζ for the free ion has been given as 750 cm^{-1} (97), and as pointed out earlier, k should not normally be less than 0.7. Distortion of the complex might account in some cases for such behaviour

(91, 100) but the x-ray diffraction pattern of K_2NbCl_6 indicates a cubic symmetry. Jahn-Teller distortion of the d^1 system is very slight. As the curve fitting was considered to be unsatisfactory, further examination of the system was undertaken.

Calculated values of the true moments (which arise from the first order Zeeman terms) for a d^1 system have been obtained by the use of Westland's expression (96). The values were found to be dependent on k but they were almost independent of ξ. It was evident that for any reasonable choice of k and ξ, the true moment will not exceed the value of 0.53 B.M. for a regular octahedral complex.

Experimental values of the apparent true moments were obtained from the Curie-Weiss law. Values of the Weiss constant θ, obtained by plotting $1/\chi_m$ against T, were -230 for K_2NbCl_6 (powdered single crystal), -340 for Rb_2NbCl_6 (high temperature preparation) and -430 for Cs_2NbCl_6 (high temperature preparation). Since the T.I.P. contribution cannot in general be neglected for the heavier transition elements, these values are only approximate.

Starting from these approximate values, it was a simple matter to refine θ by a process of curve fitting which

Fig. 26: Variation of corrected magnetic susceptibilities with reciprocal absolute temperature:

A: pure K_2NbCl_6, line calculated for $\xi = 425\ cm^{-1}$, $Dq = 2110\ cm^{-1}$ and $k = 0.44$.

B: $K_2(Nb,Zr)Cl_6$, 36.7 mole % K_2NbCl_6

C: $K_2(Nb,Zr)Cl_6$, 5.67 mole % K_2NbCl_6

D: $[(C_2H_5)_4N]_2NbCl_6$ (ref. 28)

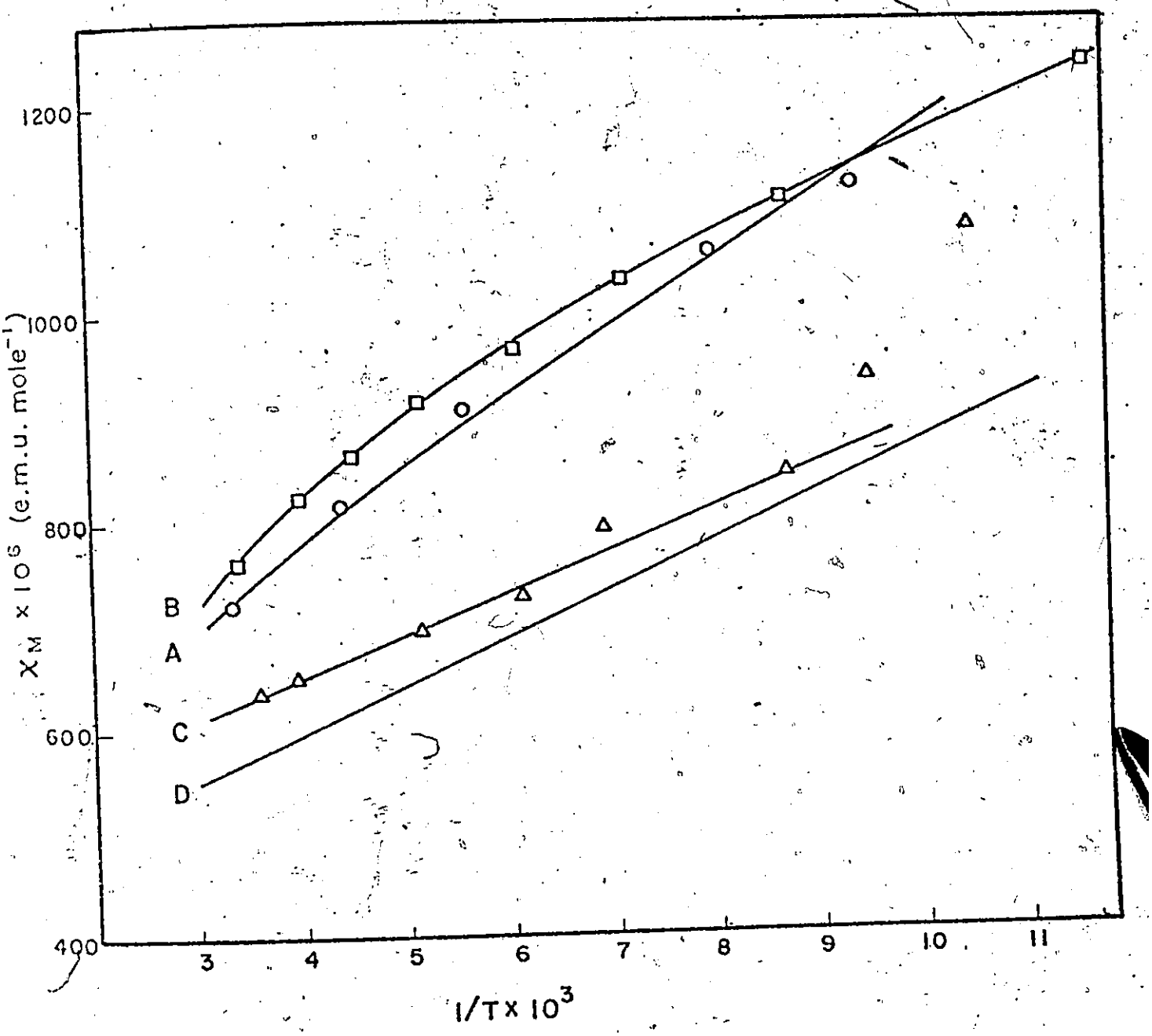
1200
1000
800
600
400
$\chi_M \times 10^6$ (e.m.u. mole^{-1})
B
A
C
D
3
4
5
6
7
8
9
10
11
$1/T \times 10^3$

afforded straight plots of χ_m against $1/(T-\theta)$. The values of θ obtained by this procedure were as follows: -170 (K_2NbCl_6), -270 (Rb_2NbCl_6) and -450 (Cs_2NbCl_6).

The apparent true moments were obtained from the slopes of the plots of χ_m against $1/(T-\theta)$ and the values were found to be: 1.5 B.M. (K_2NbCl_6), 1.6 B.M. (Rb_2NbCl_6) and 1.8 B.M. (Cs_2NbCl_6). Clearly the values obtained for these preparations are much greater than the upper limit, 0.53 B.M., given by theory for Nb(IV).

At first sight the magnetic evidence suggested that the stoichiometry of the systems was quite different from the nominal overall composition, A_2NbCl_6. However the fact that they possessed the K_2PtCl_6 type structure leads one to conclude that although they consisted largely of $NbCl_6^{2-}$ anions, they really were mixtures containing one or more additional paramagnetic species. Comparatively small quantities of substances which are more strongly paramagnetic than Nb(IV) ions could greatly enhance the apparent true moments while showing spuriously large values of θ. For example moderate quantities of species containing two unpaired electrons and having modest values of θ (say -50) would, upon admixture

with a Nb(IV) compound, show magnetic behaviour such as that observed.

It was evident from the spectrographic analysis provided by Fansteel Metals Corporation that the unusual magnetic behaviour cannot be ascribed to the presence of foreign metals in the starting materials. The total impurity content consisting of metals which form paramagnetic ions was less than 0.03%. If these metals were present, carrying on the average two unpaired electrons, and having an average atomic weight of 100, this would contribute 4×10^{-6} e.m.u. $mole^{-1}$ to the susceptibility value at room temperature. This is clearly a negligible susceptibility in a total of 700×10^{-6} e.m.u. $mole^{-1}$.

The effect of ferromagnetic impurity was only slight in every case and was eliminated by extrapolating susceptibility to infinite field strength. We may conclude that all of the observed paramagnetism was due to niobium ions.

One obvious possible species of niobium impurity is the oxyhalide. This could very possibly contain the bonding -Nb-O-Nb- and with such a structure magnetic exchange is almost certain to arise. The sample of K_2NbCl_6, the magnetic properties of which are given by the points shown as open circles in Fig. 21, exhibited no infrared absorption in the region 600 cm^{-1} to 4000 cm^{-1}.

Metal-oxygen stretching modes have been reported to occur at 950±100 (21,29). On the other hand, there was weak absorption at 915 cm^{-1} in the case of Cs_2NbCl_6 crystallized from aqueous solution (see experimental section, Page 57), thus revealing a slight degree of hydrolysis. We conclude that there was a negligible quantity of oxychloride in this preparation.

It is very improbable that there was any other compound of Nb(IV) present in appreciable quantities because the impurity levels of C, Si, N, etc. in the starting materials were very low and despite considerable preparative work in this area there are no known halo complexes of Nb(IV) other than those containing NbX_6^{2-} ion. Impurities could be introduced through etching of the quartz reaction vessel. Close examination of the reaction vessels after reaction revealed no sign of any etching by the reactants. Thus, we are left with the possibility of a lower valent ion or ions of niobium causing the abnormal magnetic behaviour. (Of course, having no d electrons, Nb(V) would not contribute to the moment.) The suggestion is a plausible one in view of the fact that NbX_4 decomposes easily upon heating to NbX_5 and a lower valent species according to the following equation (72,81).*

$$4NbX_4 \longrightarrow NbX_3 + 2NbX_5$$

*The lower valent product does not necessarily have the exact stoichiometry shown above. The lower valent species may range in composition from $NbX_{2.67}$ to $NbX_{3.1}$.

Upon initial examination, preparations of A_2NbX_6 normally did not appear to contain additional phases as mechanical mixtures. As this point is an important one, rather close examination by variety of techniques was carried out and this will be discussed in appropriate sections that are to follow.

Admittedly, certain preparations were found to contain minor quantities of $A_4Nb_6Cl_{18}$ (61-63). In our system the cluster would presumably form according to equation:

$$16K_2NbCl_6 \rightleftharpoons K_4Nb_6Cl_{18} + 10KNbCl_6 + 18KCl$$
$$\Downarrow$$
$$10KCl + 10NbCl_5$$

The presence of this cluster compound was revealed by dissolving the A_2NbX_6 in 6 to 12 normal hydrochloric acid which left the cluster compound undissolved. Fortunately, the formation of this compound was hindered under certain conditions. We suspect that the cooling procedure - whether rapid or slow - may be the determining factor. The exact conditions under which this compound failed to appear were however not established as improved methods of preparation were sought and readily found. The susceptibility of this compound has been reported (61) to be temperature independent so that in any event its presence cannot account for the anomalous magnetic properties observed.

A minute trace of insoluble substance invariably remained (its quantity was less than 0.5%) after continuous leaching of A_2NbCl_6 systems with f2N hydrochloric acid and water. An x-ray pattern showed that it was NbO. The oxygen is probably derived from $NbOCl_3$ in the starting pentachloride.

It was apparent that in order to investigate Nb(IV) systems it was essential to find a means of suppressing the decomposition described above. Various experimental approaches were investigated.

(a). Attempted application of Le Chatelier's principle.

It was hoped that the addition of a few milligrams of $NbCl_5$ to the reaction mixture would reverse the equilibrium shown in the equation above. Contrary to what was hoped, the magnetic behaviour, indicated by triangles in Fig. 21, was less satisfactory than ever. With hindsight one may rationalize this finding by assuming that the free KCl shown in the equation was effectively complexed as $KNbCl_6$. Free KCl would be necessary for the reverse of the disproportionation reaction to occur.

(b) Preparation at low temperatures.

Failure of the preceding experiment suggested that it is perhaps necessary to avoid decomposition altogether by operating at sufficiently low temperature. There is an inherent difficulty here if one wishes to proceed by direct

synthesis from crystalline starting materials. Solid state reactions normally proceed with appreciable velocity only at elevated temperatures. A compromise was struck by heating mixtures of $NbCl_4$ and ACl for extended periods at about 300°C with intermittent regrinding.

In most cases the magnetic properties of these complexes were again disappointing. The data are given in Fig. 22. The data for the potassium and rubidium complexes were essentially similar to those of high temperature preparations.

However the data for the caesium complex were different. In this instance, samples prepared at 300° and cooled slowly over 3 days gave much lower susceptibilities. The 275° preparation, cooled more rapidly over a period of 6 hours, gave slightly different results from the 300° preparation. However both these low temperature preparations gave plots of χ_m against 1/T that were linear. The plot for the 275° preparation had a greater slope. The linear plot for χ_m against 1/T for the caesium complex is what is expected for a d^1 system.

The electronic spectrum discussed later showed that there was still a foreign phase in this preparation. However we believe that fitting the experimental results to theory provides an estimate of the moment which is correct to within 10 percent.

The plot in Fig. 22 corresponds to the parameter values $\xi = 530$, $k = 0.59$ and $Dq = 2500\ cm^{-1}$. Moreover the experimental true moment was found to be 0.54 B.M. The following set of parameters: $\xi = 550$, $k = 0.6$ and $Dq = 2100$ in the theory for d^1 systems gives 0.50 B.M. as the value of the true moment. The magnitudes of the k and ξ parameters for this preparation are much more reasonable than those described previously. This suggests that the samples prepared at these temperatures were relatively free of the magnetically anomalous material. The result of the preceding experiment leads to a very important conclusion, viz. the susceptibilities of pure A_2NbX_6 systems must be either about equal to or less than that of Cs_2NbCl_6 prepared at $\sim 300°C$.

(c) Precipitation from concentrated hydrochloric acid.

It would appear that the best method of preparation would entail the lowest possible temperatures. Russian workers have prepared Cs_2NbCl_6 by crystallizing from concentrated hydrochloric acid at room temperature. We succeeded in repeating this preparation of the caesium salt but failed, as they did, to obtain the potassium salt. The magnetic properties of the caesium salt are shown as black squares in Fig. 22. The plot is similar to that of the salt prepared at 650°C but with slightly less curvature. It was apparent that the magnetic behaviour of aqueous preparations seemed to be subject to the same influences as high temperature preparations. Reasons for such behaviour will be given later.

(d) Dilution studies.

As a further attempt to suppress decomposition, dilution experiments were carried out. It was assumed that by diluting the A_2NbX_6 in a diamagnetic host such as A_2ZrCl_6 many niobium atoms would have no immediate niobium neighbour. A low valent niobium ion would be more stabilized by having a Nb(V) neighbour close by in the melt than it would be if surrounded only by $ZrCl_6^{2-}$ ions. This low-high valent stabilization should be diminished upon increasing dilution.

Because of their very different structures the cluster and ACl should be relatively insoluble in K_2ZrCl_6 - thus the activities of these components will be unity. From the equation

$$16\ K_2NbCl_6 \rightleftharpoons K_4Nb_6Cl_{18} + 18\ KCl + 10\ KNbCl_6$$

we may write

$$K_{eq} = \frac{a_{K_4Nb_6Cl_{18}} \cdot a^{18}_{KCl}\ [KNbCl_6]^{10}}{[K_2NbCl_6]^{16}}$$

or

$$K_{eq} = \frac{[KNbCl_6]^{10}}{[K_2NbCl_6]^{16}}$$

(where 'a' refers to activities of the compounds).

Let the concentration of K_2NbCl_6 upon dilution be changed to $\chi[K_2NbCl_6]_{init}$ where $0 < \chi << 1$ and $[K_2NbCl_6]_{init}$ is the initial concentration of K_2NbCl_6.

Then we may write

$$K_{eq} = \frac{\chi^{16}\,[KNbCl_6]^{10}_{init}}{\chi^{16}[K_2NbCl_6]^{16}_{init}}$$

Hence the concentration of $KNbCl_6$ which satisfies the mass law action for the dilute system is $\chi^{16/10}[KNCl_6]_{init}$.

Since the power of χ is greater than unity, the concentration of $KNbCl_6$ decreases more rapidly as χ approaches zero than does the concentration of K_2NbCl_6. It follows that dilution should suppress the disproportionation process.

The dilution experiments were performed by Dr. W. Rank. Samples of $K_2(Nb,Zr)Cl_6$ which were 36.7 and 5.67 mole percent in K_2NbCl_6 were investigated. The gram susceptibilities of the K_2NbCl_6 was determined from the observed susceptibilities by use of the equation:

$$\chi_{obs.} = w_1\chi_{K_2NbCl_6} + w_2\chi_{K_2ZrCl_6} \qquad [19]$$

where w_1 and w_2 are the weight fractions of K_2NbCl_6 and K_2ZrCl_6 respectively. The mole susceptibilities were obtained by subtracting the atomic contributions tabulated by Selwood (101). The results are given by line B and C in Fig. 26. Westland and Bhiwandker (22,23) have shown that there is little effect on the magnetic moment until the paramagnetic ion is diluted to less than ~20%.

There was a drop in susceptibility upon dilution to 5.67 mole percent (line C of fig. 26) and the curvature which is still seen in the plot for the 36.7 mole percent sample seems to have been eliminated. However the data in this latter case are not precise enough to permit a definite appraisal of the degree of curvature.

The straight line C in Fig. 26 has been calculated theoretically using the values $\xi = 480\ cm^{-1}$ and $k = 0.56$. The points at the extreme right hand end have not been considered when obtaining the best straight line because the susceptibility data for K_2ZrCl_6 became field dependent below about 115°K and the points were therefore considered to be unreliable.

It is to be supposed that at infinite dilution the susceptibilities of $NbCl_6^{2-}$ would be lower still. This would mean that ξ is equal to or greater than $480\ cm^{-1}$ which is a reasonable value. The value of 0.56 for k is small for an octahedral value. However, it has been reported (102) that for the $[Ti(H_2O)_6]^{3+}$ ion, which is a d^1 system the k value has been estimated to be ~ 0.6. Nyholm (102) has pointed out that the sometimes small values that k can assume in octahedral complexes still pose a difficult problem.

The sudden drop in susceptibility upon dilution is noteworthy. However it is not surprising when the relative order of susceptibility of K, Rb and Cs complexes of Nb(IV) is recalled (Figures 21 and 22). We found that susceptibilities of Cs_2NbCl_6, a compound which is magnetically more dilute,

are much lower than those of the more concentrated K_2NbCl_6. Hence the drop in susceptibilities on dilution of the A_2NbCl_6 system indeed appears to be real.

One finds that there is a similarity in the magnetic susceptibility data for three systems: Cs_2NbCl_6 prepared at 300°C, $[(Et_4N)]_2NbCl_6$ and the most dilute $K_2(Nb,Zr)Cl_6$ solution. It is precisely in these systems that we expect the Nb(IV) ion to be most stabilized. The $[Et_4N)]_2NbCl_6$ and Cs_2NbCl_6 were both somewhat impure since they showed a band which is presumably due to presence of the cluster ion $Nb_6Cl_{18}^{4-}$.

Stabilization of (III)-(V) or (II)-(V),(V) clusters would be greater for those salts with smaller anion-anion distances. Thus the sodium salt should exhibit such stabilization to a maximum. Among the alkali salts, Cs_2NbX_6 could be expected to contain the highest proportion of Nb(IV) atoms. Salts containing large organic cations should be more homogeneous still.

Other experimental methods were sought to investigate the effect of dilution. These investigations included a crystallographic examination of the mixed crystal systems and electron spin resonance studies. The former gave no meaningful results and the latter will be discussed in a later section.

Purification by growth of single crystals

In order to provide a method leading reproducibly to a product free from inclusion of foreign phases, fairly large single crystals (up to 2 mm. in breadth) were grown by slow cooling of a melt containing KCl and $NbCl_4$. (See experimental section, page 63). The ingot so produced when fractured gave fragments having cubic cleavage. The colour of a cleavage face was virtually black but the material when powdered was of the usual deep violet colour. The X-ray pattern was identical to that of other samples of K_2NbCl_6. The sample was totally soluble in 6N hydrochloric acid as expected and even did not reveal the usual traces of NbO. This verified our expectation that the tendency of the material to incorporate foreign phases is reduced many fold when large crystals are grown slowly.

Somewhat surprisingly, the magnetic behaviour showed the anomalous characteristics of the majority of the preparations. Susceptibilities are plotted in Fig. 21, experimental points being shown as crossed circles. This result supported by additional techniques of examination described in later sections led us to conclude that the low valent states of niobium which are responsible for the anomalously high magnetic susceptibilities are dissolved in the K_2NbCl_6 phase. In order for the stoichiometry to be satisfied an equivalent quantity of Nb(V) must also be dissolved in the crystal. In the A_2NbX_6 systems one may conceive of Nb(II), Nb(III) and Nb(V) ions present in

appropriate ratios in addition to the host ion (Nb(IV). The present experiments do not provide a basis for deciding which of the lower valent ions is present.

We may now rationalize the magnetic behaviour as follows. There is (a) the expected contribution of $NbCl_6^{2-}$ groups which would contribute a susceptibility linear in 1/T and (b) a contribution from lower valent species such as Nb(II) or Nb(III) which would be relatively large even for small concentrations of the ions. The low valent ion may enter into ferrimagnetic interaction with Nb(IV) or antiferromagnetic interaction with itself producing a contribution to the susceptibility which is non-linear in 1/T. At the left hand intercept of the plot, i.e. where 1/T = 0, the only contribution will be the T.I.P. of the Nb(IV) species. The plot would proceed to the right with greater slope than that of a line representing the contribution of Nb(IV) only, but owing to the interactions the slope would progressively decrease. Such is the shape of the experimental plots.

If we assume that the plot for the Cs_2NbCl_6 preparation at 300° is a fair representation of the susceptibility of Nb(IV), we may estimate that the concentration of Nb(II) in other preparations does not exceed 5 mole percent and if the low valent ion is Nb(III), the concentration may be of the order of 15 mole percent.

Miscellaneous magnetic results

(a) Susceptibilities of non-cubic Nb(IV) complexes

The data for the pyridinium and sodium hexachloroniobates(IV) are shown in Figure 23. The plot of χ_m against

1/T was linear for both of these complexes which suggests that they are relatively normal systems in respect of their magnetic components. The x-ray diffraction patterns show that both compounds have a crystal symmetry which is lower than octahedral. The linear plot for Na_2NbCl_6 could be explained if the system does not possess a non zero Weiss constant θ. This may arise if (i) the products of disproportionation in the sodium-containing system are quite different. (Note that $Na_4Nb_6Cl_{18}$ does not seem to exist) or (ii) there are lower valent niobium atoms dissolved in the preparation but the Neél point is above room temperature. This incidently is more likely for a lattice with a smaller cation.

From the previous discussions it appears that either isomorphous dilution or the presence of large cations in the lattice provides a stabilizing effect for Nb(IV)-ion. This seems to be the reason for the linear plot observed for the pyridinium salt.

(b) Susceptibilities of iodo salts

Susceptibilities of iodo complexes prepared at low and higher temperatures were identical within experimental error and they were somewhat lower than those for chlorocomplexes. (Fig. 24)

The behaviour of iodo salts shows that there is a significant difference in the parameters: 10 Dq and k. The data suggest that k is much nearer to unity for iodo than for chloro analogues.

(c) Susceptibilities of tantalum complexes

Plots of χ_m versus 1/T for K_2TaCl_6 and $(PyH)_2TaCl_6$ were linear as may be seen from Fig. 27. As expected the susceptibility values are markedly lower than those for salts of the A_2NbCl_6 type.

The energy level scheme for a $5d^1$ ion is approximated by (d) in Fig. 20. Since ξ for the third row transition elements is of the same order of magnitude as 10Dq, only the lowest energy level is occupied. Paramagnetism arises in this case in two ways, namely: (1) a temperature independent contribution from the second order Zeeman effect between the ground state and the Γ_7 (t_{2g}) state and (2) mixing of the two Γ_8 states through spin-orbit coupling which gives rise to a temperature dependent contribution.

The T.I.P. contribution for K_2TaCl_6 was obtained from the intercept of the plot in Fig. 27 and was found to be 185×10^{-6} e.m.u./mole. This is less than the value found for niobium salts which is in accord with the higher value for the spin-orbit coupling constant.

Owing to the smallness of the paramagnetic component in K_2TaCl_6, dilute solid solutions of the composition $K_2(Ta,Zr)Cl_6$ gave no meaningful results. In view of this difficulty, an e.s.r. spectrum of a sample of K_2ZrCl_6 doped with K_2TaCl_6 was measured and the results of this experiment will be discussed later.

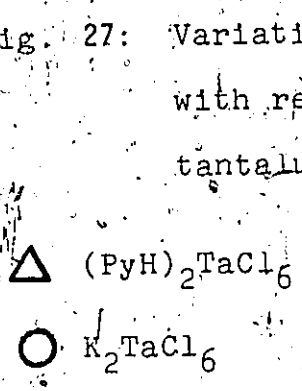

Fig. 27: Variation of corrected magnetic susceptibilities with reciprocal absolute temperature of tantalum complexes.

△ $(PyH)_2TaCl_6$

○ K_2TaCl_6

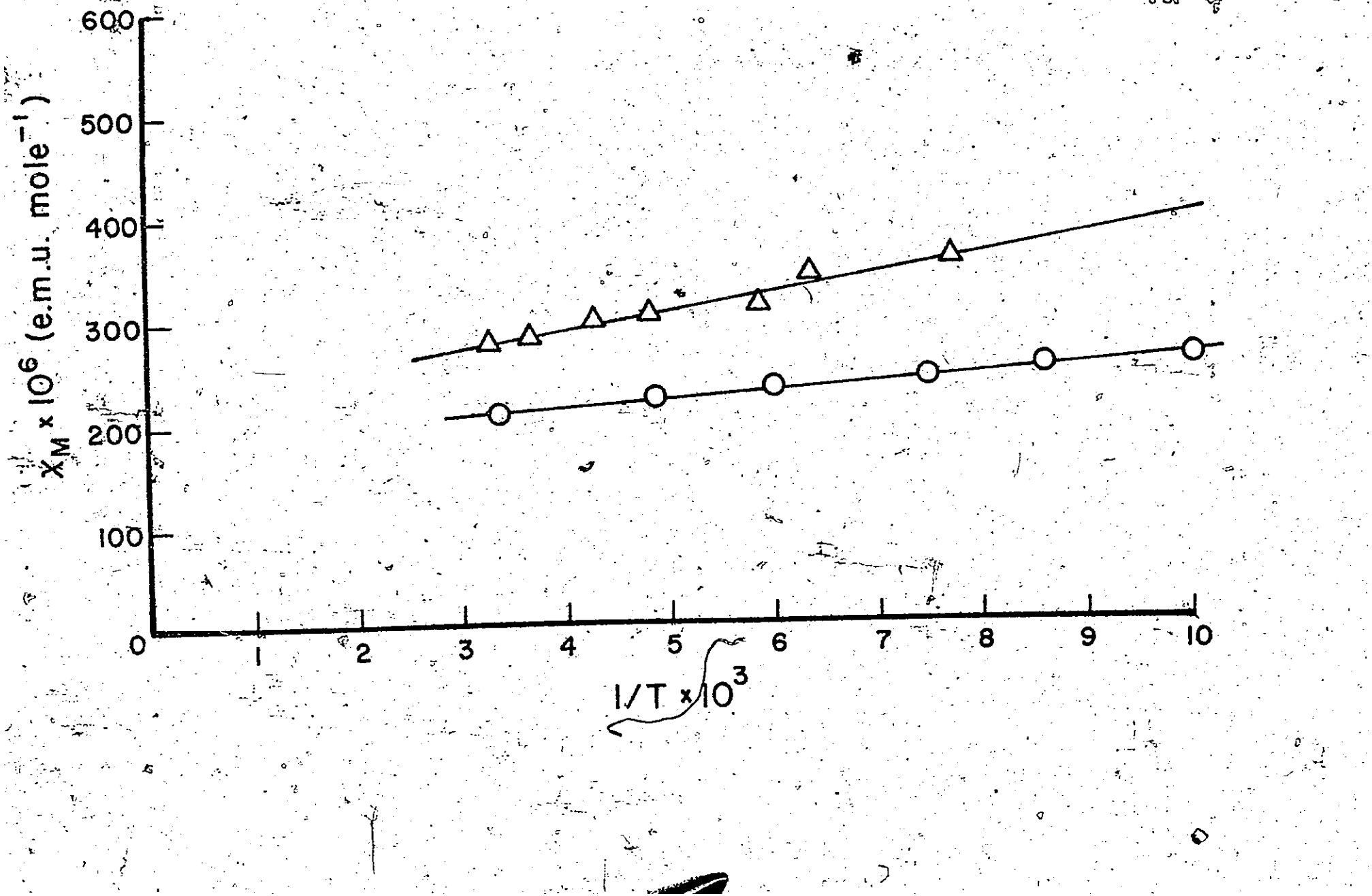
600
500
400
300
200
100
0
$\chi_M \times 10^6$ (e.m.u. mole^{-1})
1
2
3
4
5
6
7
8
9
10
1/T x10^3

Like its niobium analogue, $(PyH)_2TaCl_6$ has a crystal symmetry which is lower than octahedral. This may explain the higher susceptibilities observed for this complex.

Susceptibility data

Tables XII to XIX give the numerical magnetic data for the various complexes studied in this thesis. The diamagnetic corrections were taken from Selwood (101) and the corrected susceptibility is referred to as χ_m corr.

Electron Spin Resonance Studies (e.s.r.)

Principles of e.s.r.

The electron has associated with its spin a magnetic moment μ_e given by

$$\mu_e = -g\beta S \text{ (erg gauss}^{-1}\text{)} \qquad [20]$$

where β is called the Bohr magneton, S is the spin quantum number of the electron and g is the gyromagnetic ratio with a value of 2.0023.

The orientation of the spin vector is normally of no consequence, but in the presence of an external magnetic field alignment of the spin occurs. A low energy state arises when the electron moment is aligned with the field and a higher energy state when the moment is aligned against the field.

The difference in energy between the two states is proportional to the applied field H_o.

In quantum mechanical terms, the two spin states are quantized and the component M_s of the electron spin vector in the field direction can only take one set of discrete

TABLE XII

K_2NbCl_6 (Sample (1)

$\chi_m \times 10^6$ (e.m.u. mole^{-1})	$\chi_m^{corr} \times 10^6$ (e.m.u. mole)	Temp (°K)	μ_{eff} (B.M.)
480	674	298	1.27
555	749	233	1.18
608	802	201	1.14
650	844	179	1.10
693	887	157	1.06
736	930	139	1.02
789	983	121	0.976

K_2NbCl_6 (Single Crystal)

522	716	298	1.31
620	814	227	1.22
714	908	180	1.14
863	1057	125	1.03
925	1119	107	0.979

K_2NbCl_6 (Sample 3)

472	666	300	1.26
679	873	179	1.12
890	1084	114	0.995

K_2NbCl_6 (300° preparation)

533	727	296	1.31
679	873	205	1.20
783	977	161	1.12
967	1161	105	0.988

$\chi_{diamag.} = -194 \times 10^{-6}$ e.m.u. mole^{-1}

TABLE XIII

Rb_2NbCl_6 (High temperature prepration)

$\chi_m \times 10^6$ (e.m.u. mole^{-1})	$\chi_{corr} \times 10^6$ (e.m.u. mole^{-1})	Temp. (°K)	μ_{eff} (B.M.)
475	683	299	1.28
513	723	259	1.22
555	763	225	1.17
596	804	181	1.07
624	832	156	1.02
664	872	136	0.97
700	908	120	0.93
759	967	102	0.89

Rb_2NbCl_6 (300° preparation)

535	743	298	1.33
669	877	193	1.16
719	927	156	1.08
819	1027	105	0.929

$\chi_{diamag.} = -208 \times 10^{-6}$ e.m.u. mole^{-1}

TABLE XIV

Cs_2NbCl_6 (High temperature preparation)

$\chi_m \times 10^6$ (e.m.u. mole^{-1})	$\chi_m^{corr} \times 10^6$ (e.m.u. mole^{-1})	Temp. (°K)	μ_{eff} (B.M.)
434	664	299	1.26
416	646	300	1.25
493	723	225	1.14
549	779	188	1.08
603	833	128	0.92
625	855	102	0.84

Cs_2NbCl_6 (Aqueous preparation)

385	615	301	1.22
451	681	237	1.14
493	723	195	1.06
519	749	164	0.99
561	791	132	0.91
641	871	102	0.84

Cs_2NbCl_6 (300° preparation)

342	572	300	1.17
386	616	234	1.07
438	668	171	0.96
475	705	147	0.91
485	715	138	0.89
557	787	107	0.82

$\chi_{T.I.P} \sim 450 \times 10^{-6}$ e.m.u. mole^{-1}

True Moment = 0.54 B.M.

TABLE XIV

Cs_2NbCl_6 (275° preparation) Cont'd

281	511	296	1.10
323	553	242	1.04
365	595	194	0.961
425	655	157	0.908
476	706	140	0.890
535	765	120	0.857

χ T.I.P. $\sim 340 \times 10^{-6}$ e.m.u. mole^{-1}

True Moment ~ 0.63 B.M.

χ diamag. $= -230$ e.m.u. mole^{-1}

TABLE XV

Na_2NbCl_6

$\chi_m \times 10^6$ (e.m.u. mole^{-1})	$\chi_m^{corr} \times 10^6$ (e.m.u. mole^{-1})	Temp. (°K)	μ_{eff} (B.M.)
520	698	299	1.29
679	857	226	1.25
791	969	182	1.19
910	1088	159	1.18
1038	1216	136	1.15
1207	1385	118	1.14
1370	1548	100	1.11

$\chi_{diam.} = -178 \times 10^{-6}$ e.m.u. mole^{-1}.

TABLE XVI

$(PyH)_2NbCl_6$

$\chi_m \times 10^6$ (e.m.u. mole^{-1})	$\chi_m^{corr} \times 10^6$ (e.m.u. mole^{-1})	Temp. (°K)	μ_{eff} (B.M.)
425	691	299	1.29
454	720	273	1.25
482	748	249	1.22
540	806	216	1.18
610	876	179	1.12
708	974	147	1.07
908	1174	106	1.00

$\chi_{diamag.} = -266 \times 10^{-6}$ e.m.u. mole^{-1}

$\chi_{T.I.P.} = 440 \times 10^{-6}$ e.m.u. mole^{-1}

True Moment = 0.80 B.M.

TABLE XVII

Cs_2NbI_6 (High temperature preparation)

$\chi_m \times 10^6$ (c.g.s. m.u. mole^{-1})	$\chi_m^{corr} \times 10^6$ (e. m.u. mole^{-1})	Temp. (^oK)	μ_{eff} (B.M.)
251	637	298	1.23
286	672	198	1.03
292	678	155	0.92
288	674	103	0.75

Cs_2NbI_6 (400^o preparation)

276	662	299	1.26
317	703	229	1.14
302	688	173	0.976
317	703	135	0.872
305	691	108	0.773

$\chi_{diamag.} = -386 \times 10^{-6}$ e.m.u. mole^{-1}

TABLE XVIII

K_2TaCl_6

$\chi_m \times 10^6$ (e.m.u. mole^{-1})	$\chi_m^{corr} \times 10^6$ (e.m.u. mole^{-1})	Temp. (°K)	μ_{eff} (B.M.)
7.98	209	297	0.71
14.77	216	252	0.66
21.76	223	205	0.61
32.40	233	167	0.56
40.59	242	134	0.51
52.39	253	117	0.49
59.00	260	100	0.46

$\chi_{diam} = -201 \times 10^{-6}$ e.m.u. mole^{-1}

$\chi_{T.I.P.} = 185 \times 10^{-6}$ e.m.u. mole^{-1}

True Moment = 0.24 B.M.

TABLE XIX

$(PyH)_2TaCl_6$

$\chi_m \times 10^6$ (e.m.u. mole^{-1})	$\chi_m^{corr} \times 10^6$ (e.m.u. mole^{-1})	Temp. (°K)	μ_{eff} (B.M.)
13.0	283	272	0.79
30.2	300	235	0.75
35.0	305	208	0.71
43.3	313	177	0.67
73.7	344	158	0.66
86.4	356	131	0.61

$\chi_{diam} = -270 \times 10^{-6}$ e.m.u. mole^{-1}

$\chi_{T.I.P.} = 216 \times 10^{-6}$ e.m.u. mole^{-1}

True Moment = 0.38 BM.

values which are, $M_s = +\frac{1}{2}$ or $-\frac{1}{2}$. Electrons in the lower state $M_s = -1/2$, can now be excited by electromagnetic radiation to the upper state, $M_s = +1/2$ as shown in Fig. 28, and for a given applied field Ho (gauss), the energy ΔE (ergs) required for the transition will be:

$$\Delta E = h\nu = g\beta H_o \text{ (ergs)} \qquad [21]$$

where ν is the frequency of the applied radiation. Since ΔE is very small, the most convenient radiation frequencies occur in the microwave region of the electromagnetic spectrum. The constant g assumes values other than 2.0023 when the unpaired electron is no longer free, i.e. when it occurs in complexes.

An e.s.r. spectrometer thus measures the energy required to reverse the spin of an electron while it is in an external magnetic field.

In all the foregoing theories of magnetism, it has been assumed that the individual paramagnetic ions in a compound act independently of each other. In most coordination compounds the shell of ligands surrounding the metal ion is sufficient to ensure this. However, the situation often arises where the individual magnetic dipoles do influence each other leading to "co-operative" or "exchange" phenomena. This may be simply because the distance between the paramagnetic ions is small, or because the intervening atoms are

capable of transmitting the magnetic interaction. If the orbital magnetic moments of the ions are neglected, the interaction between dipoles (S_i and S_k) may be described by

$$E = 2J\, S_i S_k \qquad [22]$$

where J is the "exchange" coupling constant. If J is positive, the lowest state is that with the spins aligned in the same direction and if negative, the lowest state is that with spins opposed. The former case leads to ferromagnestism. The latter causes a lowering of χ and μ_{eff} and when the interaction is direct and large with respect to kT, it is identical to covalent bonding. However, if the interaction is indirect, that is, if it occurs via intervening atoms, it is then known as "superexchange".

Spin superexchange is detected in the e.s.r. experiment because this technique is extremely sensitive to this particular effect. Griffiths *et al.* (103) investigated the paramagnetic resonance of adjacent iridium ions ($IrCl_6^{2-}$) in chloroplatinate crystals and determined the exchange interactions between them. More recently Westland (25) investigated the magnetic properties of hexachlororhodate(IV) ion by this method. In this work (25), although susceptibility measurements failed to reveal any superexchange in the lattice, e.s.r. spectra gave some evidence for such coupling.

Mixed crystal systems of $K_2(M,Zr)Cl_6$ (M = Nb,Ta) containing between 1-2% of Nb or Ta, were studied as described

Fig. 28: The energy levels of an electron under an external magnetic field. An energy transition induced by electromagnetic radiation is also shown.

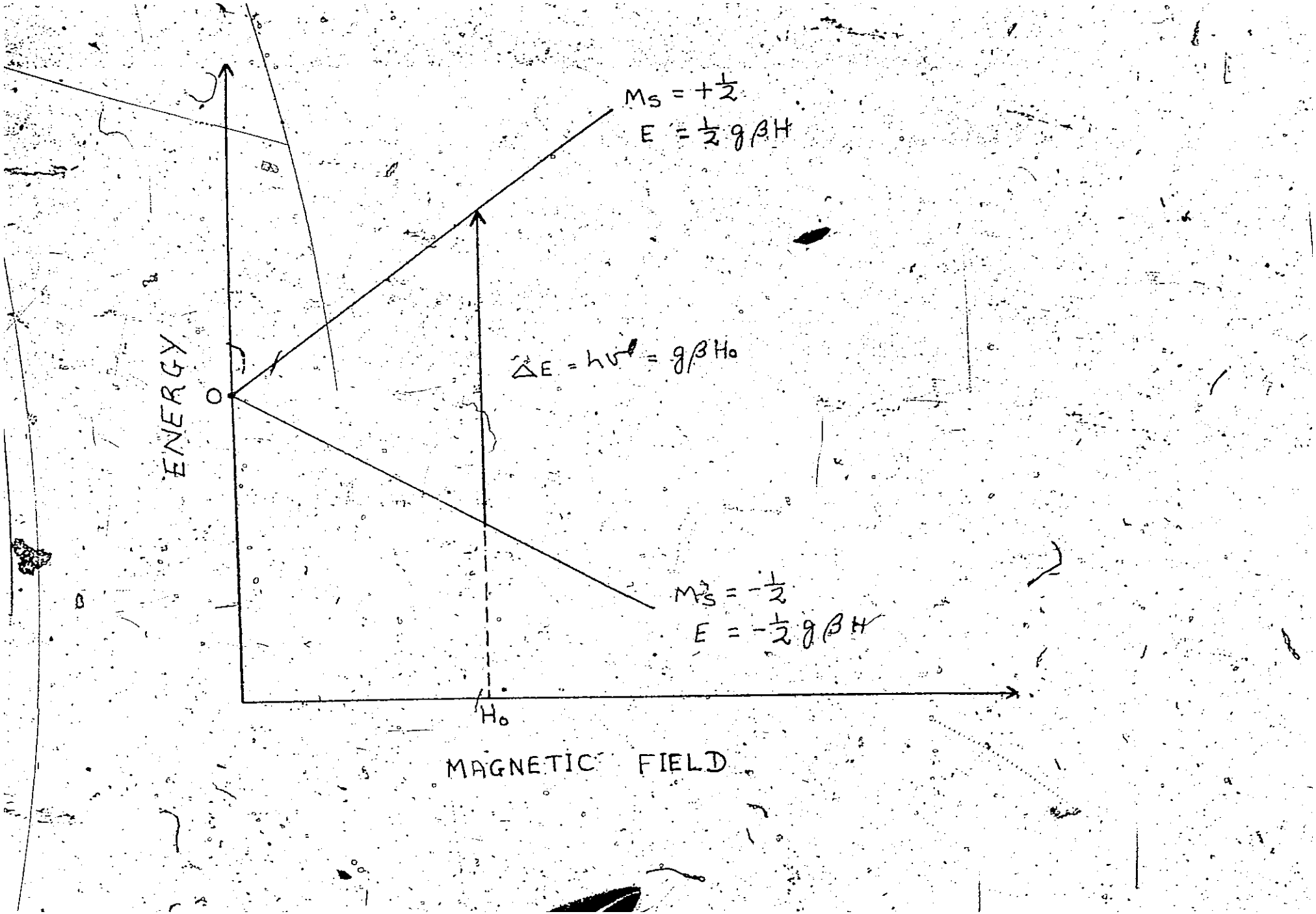
$M_S = +\frac{1}{2}$
$E = \frac{1}{2} g\beta H$
$\Delta E = h\nu = g\beta H_0$
$M_S = -\frac{1}{2}$
$E = -\frac{1}{2} g\beta H$
ENERGY
O
H_0
MAGNETIC FIELD

in the experimental section.

$K_2(Nb,Zr)Cl_6$

An e.s.r. spectrum of a sample of K_2ZrCl_6 doped with K_2NbCl_6 gave only a weak signal with g = 2.120. As the ground state of an octahedral d^1 complex is not split by a magnetic field, there should be no absorption to a first approximation. Absorption through second order intermixing of the upper $^2T_2$ (e_g) state (Fig. 20) should provide a small g value but this would likely be beyond the range of our spectrometer.

It is to be expected that at high dilution practically all of the $[NbCl_6^{2-}]$ groups will be entirely surrounded by $ZrCl_6^{2-}$ groups. A few $[NbCl_6^{2-}]$ groups however will have another $[NbCl_6^{2-}]$ as a nearest anion neighbour. A cluster of two $NbCl_6^{2-}$ groups will constitute a two electron system if exchange or superexchange is in operation. In such a case a spin triplet state arises as well as a singlet state. Transitions between these states may be detected by e.s.r. and the g value would be 2.0.

Thus the g value obtained in this experiment could be due to the presence of an impurity.

$K_2(Ta,Zr)Cl_6$

Magnetic susceptibility measurements on very dilute solid solutions of composition $K_2(Ta,Zr)Cl_6$ could lead to substantial errors as the paramagnetic component in these

systems is very small. However the sensitivity of an e.s.r. experiment overcomes this problem. The spectrum we obtained was weak with g = 1.94. As in the case of Nb, a cluster of two $TaCl_6^{2-}$ groups will give rise to a singlet and a triplet spin states. Transition between these states may be detected by e.s.r. and the g value would be 2.0. Thus the g value obtained in this experiment could also be due to an impurity.

2. Detailed Search for Impurities

The magnetic studies described in the previous section indicated that in the course of preparation of alkali hexahaloniobates from $NbCl_4$, the Nb(IV) undergoes a certain amount of disproportionation. The partial insolubility of some preparations indicated that contaminating phases may be produced. However, certain preparations appeared to be essentially or entirely free of insoluble phases. The preparation of a single crystal of K_2NbCl_6 having anomalous magnetic properties led to the tentative conclusion that products of disproportionation may be soluble in the $K_2Nb^{IV}Cl_6$ host lattice. Since this supposition is novel, a close examination of A_2NbCl_6 phases was carried out making use of a variety of techniques.

It was particularly necessary to establish whether or not complexes of niobium in lower oxidation states may have escaped detection. In addition to the insoluble cluster compounds referred to earlier, search of the literature revealed the compounds "A_2NbCl_5" and "A_2NbCl_4" (57-59,64). The x-ray diffraction patterns given in the literature for these compounds were

hardly accurate enough for the purposes of identifying them if present as impurities in A_2NbCl_6 preparations.

The results of x-ray diffraction studies are reported in the next pages.

X-Ray Diffraction Studies

The x-ray powder photographs were obtained as described in the experimental section.

The d-spacings of the powder patterns of A_2NbX_6 and K_2TaCl_6 complexes obtained by us were compared with those recorded in the literature (21,45). In all cases, the results were identical within experimental error. Even upon close examination there were no lines which could not be indexed on the basis of the space group of the principal phase. The x-ray data for other complexes containing NbX_6 groups, namely, $(PyH)_2NbCl_6$ and Na_2NbCl_6 are recorded in Tables XX and XXI. Since $(PyH)^+$ is a planar cation, it forces the symmetry of the crystals to be lower than cubic and indeed the powder patterns of pyridinium complexes could not be indexed on the basis of a cubic unit cell. The crystal symmetry of Na_2NbCl_6 is also distorted from cubic.

The x-ray data for preparations having the composition "K_2NbCl_4" and "K_2NbCl_5" are recorded in Tables XXII and XXIII. These complexes gave rather weak patterns. Very few lines could be indexed precisely to give any indication of the symmetry. However it is interesting to compare d-spacings of "K_2NbCl_5" with

"K_2NbCl_4" and K_2NbCl_6 which are given in the tables below. With the exception of one line, namely, d = 2.61 Å in the pattern of "K_2NbCl_5", all of the values may be found in one or the other of the patterns of "K_2NbCl_4" and K_2NbCl_6.

Table XX*

X-Ray Diffraction Data for $(PyH)_2NbCl_6$

Sin^2	d(Å)	Relative Intensity
0.010036	7.70	50
0.012492	6.90	65
0.014938	6.31	60
0.020941	5.33	100
0.024081	4.97	50
0.028152	4.60	40
0.035103	4.12	70
0.056331	3.25	10
0.063462	3.06	60
0.081970	2.69	55
0.104252	2.39	5
0.125377	2.18	5
0.133782	2.11	5
0.147253	2.01	5
0.180080	1.82	60
0.249647	1.54	5

Table XX * Continued

$\sin^2\theta$	d(Å)	Relative Intensity
0 298158	1.41	60
0.357572	1.29	40

*In Tables XX to XXIV, relative intensities have been estimated visually relative to a value of 100 for the strongest line in a given x-ray photograph.

Table XXI

X-Ray Diffraction Data for Na_2NbCl_6

$\sin^2\theta$	d(Å)	Relative Intensity
0.011559	7.17	10
0.015910	6.11	10
0.018896	5.61	100
0.021559	5.25	15
0.026173	4.77	70
0.043185	3.71	20
0.049944	3.44	20
0.067840	2.96	55
0.071571	2.88	55
0.075233	2.81	65
0.087556	2.61	30
0.103728	2.39	30
0.125402	2.18	20
0.132505	2.12	20
0.152526	1.97	50
0.166772	1.89	40
0.217748	1.65	30
0 229559	1.61	30

Table XXII

X-Ray Diffraction Data for "K_2NbCl_4"

$Sin^2\ \theta$	d(Å)	Relative Intensity
0.008191	8.52	100
0.009313	7.99	90
0.011055	7.33	100
0.016549	5.99	50
0.021869	5.21	20
0.032604	4.27	14
0.045663	3.61	10
0.083862	2.66	40
0.106608	2.36	60
0.179610	1.82	40
0.201584	1.72	30

Table XXIII

X-Ray Diffraction Data for "K_2NbCl_5"

$Sin^2\ \theta$	d(Å)	Relative Intensity
0.017232	5.87	100
0.022438	5.15	20
0.046451	3.58	30
0.065980	3.00	10
0.072405	2.87	70
0.082590	2.68	10
0.086976	2.61	10
0.095008	2.50	80
0.144050	2.03	30
0.192469	1.76	20

Table XXIV

X-Ray Diffraction Data for K_2NbCl_6

$Sin^2\ \theta$	d(Å)	Relative Intensity
0.01791	5.74	100
0.02380	4.99	20
0.04781	3.52	80
0.06592	3.00	80
0.07162	2.87	100
0.09541	2.46	70
0.11362	2.30	20
0.11957	2.23	20
0.14374	2.01	20
0.16130	1.92	10
0.19121	1.76	60
0.20964	1.68	10
0.21600	1.65	10
0.25668	1.51	10
0.26357	1.50	8
0.28711	1.43	20
0.30303	1.40	10
0.33557	1.33	10

X-ray diffraction photographs show that "K_2NbCl_5" contains K_2NbCl_6. The stoichiometry obviously requires that one or more additional substances with overall composition K_2NbCl_4 be present. The most likely set of substances is KCl, Nb and $K_4Nb_6Cl_{18}$. Since KCl was used as an internal standard, its presence was not verified. None of the lines in the diffraction pattern of "K_2NbCl_5" could be attributed to Nb. Presumably it would be formed in a very finely

divided state. The weaker lines (5.21, 3.61, 2.66 and 1.72 Å) in the diffraction pattern of "K_2NbCl_5" correspond to lines reported for $K_4Nb_6Cl_{18}$ (61) (vide infra) although the intense lines given by this compound were not observed.

As stated earlier, the powder pattern of "K_2NbCl_5" was weak. In addition there was a dark background in the region of small angles which could have effectively masked the lines for $K_4Nb_6Cl_{18}$ with d-spacings of 7.33 Å and greater. The density of the crystals provides further evidence of the mixed nature of the "K_2NbCl_5" preparation. The mean density of an equimolar mixture of "K_2NbCl_4" and K_2NbCl_6 is 2.64 gm cm^{-3} (58,64) while that of "K_2NbCl_5" is 2.64 gm cm^{-3} (58).

The "K_2NbCl_4" preparation is of doubtful authenticity. This may be seen by a comparison of the observed lines for "K_2NbCl_4" with some of the strongest lines reported for $K_4Nb_6Cl_{18}$ (61).

"K_2NbCl_4" *	$K_4Nb_6Cl_{18}$ *
8.52 (100)	8.52 (70)
7.99 (90)	7.88 (100)
7.33 (100)	7.29 (90)
5.99 (50)	5.93 (50)
4.27 (14)	4.28 (20)

This is strong evidence that the preparation "K_2NbCl_4" is in reality $K_4Nb_6Cl_{18}$ containing free KCl and Nb metal, as shown by the following equation:

$$7\ K_2NbCl_4 \longrightarrow K_4Nb_6Cl_{18} + 10KCl + Nb$$

*Numbers in parenthesis refer to relative intensities.

This was verified by triturating a portion of "K_2NbCl_4" in concentrated HCl, whereupon a blue solution and a dark insoluble residue were formed. The residue dissolved sparingly in distilled H_2O to give a brown solution which turned green upon adding HCl. This corresponds to the behaviour described for $K_4Nb_6Cl_{18}$ (62).

Colour of the Complexes

Table XXV presents some of the physical properties of the compounds studied in this thesis.

It was noted that the colour of Cs_2NbCl_6 prepared at low temperature was not as dark as that of the high temperature preparation. Torp (21) has reported that the iodo salts are brown whereas our preparations were black. It is also curious that pyridinium salts of Nb(IV) and Ta(IV) are different in colour.

A striking feature of the alkali metal hexahaloniobates is that they are violet while the pyridinium and tetraethylammonium salts are brown.

We have referred already to the presence in A_2NbX_6 systems of niobium in more than one oxidation state so that there is a parallel here with the colour of iron salts. Compounds of Fe(II) and Fe(III) are not usually dark but the mixed valence systems containing both Fe(II) and Fe(III) are deep blue to black. Similarly Sb(III) and Sb(V) mixed valence systems, e.g. K_2SbCl_6 are dark whereas salts containing antimony

Table XXV

Some Physical Properties of Complexes

Compound	Temp. of Preparation °C	Melting Points (°C)	Colour	Crystal Symmetry
Na_2NbCl_6	780	582*	Blue Black	Unknown
K_2NbCl_6	760	782*	Purple	Cubic
Rb_2NbCl_6	700	802*	"	"
Cs_2NbCl_6	650	822*	"	"
K_2TaCl_6	760	732*	"	"
K_2NbCl_6	300	Sintered solid	"	"
Rb_2NbCl_6	300	"	"	"
Cs_2NbCl_6	300	"	Reddish purple	"
Cs_2NbCl_6	Room Temp. (Aqueous)	"	"	"
$(PyH)_2NbCl_6$	150	≈150	Light brown	Unknown
$(PyH)_2TaCl_6$	150	≈150	Reddish purple	Unknown
Cs_2NbBr_6	640	>650	Green	Cubic
Cs_2NbI_6	621	>620	Black	"
Cs_2NbI_6	400	Sintered solid	Black	"
"K_2NbCl_5"	780	<760	Deep brown	-
"K_2NbCl_4"	800	<760	Brownish green	-

* Reported values

in a single oxidation state are pale in colour. Moreover, the starting materials from which these systems are preparaed are light in colour viz: CsCl, and $SbCl_3$ are colourless while $SbCl_5$ is yellow.

At this stage of the development of mixed valence chemistry, there is only an empirical relationship between colour and constitution of these systems. The dark nature of alkali hexahaloniobates(IV) conforms with other lines of evidence presented in this thesis in suggesting that these are mixed valence compounds. The visual appraisal of the colour of the compounds at least in bulk is most uncertain however so we proceed now to a more minute examination of optical properties.

(a) Microscopic Studies

General

For the purposes of crystallographic microscopy, transparent substances may be divided into two groups: isotropic and anisotropic. In isotropic systems, light travels in all directions with equal velocity and hence an isotropic substance has a single refractive index. In anisotropic substances, the velocity of light varies with crystallographic direction and thus there is a range of refractive indices.

Light-absorbing anisotropic crystals exhibit different colours when light is transmitted along different crystallographic directions. This selective absorption is known as pleochroism. Pleochroism arises when the absorbing ion is in an environment of low symmetry.

Interference colours

Anisotropic systems produce, in most positions, a range of interference colours between the crossed nicols of the polarizing microscope. When two sets of rays emerge on the upper side of the anisotropic crystal, one set has travelled farther than the other. Both travel along a straight line to the analyser and combine to vibrate at right angles. Thus the two rays are resolved in the analyser and emerge vibrating in the same plane. However the initial phase separation due to the crystal is retained. As a result, when the two rays emerge from the analyser, they interfere and colours are observed.

Study of the complexes

The A_2NbCl_6 crystals were opaque when observed with crossed polars confirming that these crystals belong to a cubic system. Under transmitted light we found these crystals to be uniformly red as shown in Fig. 29.

Morozov et al. (18-20) have examined these systems under polarized light. They reported that thin layers of crystalline Cs_2NbCl_6 in transmitted light were ruby red with a weak lilac tinge while crystals of Rb_2NbCl_6 were less ruby and more lilac. In our initial studies, we also observed the lilac tinge. However we found that this was merely due to the varying thickness of the grains and also to the superpositions of grains on each other. Carefully mounted slides showed no

Fig 29: Colour reprint of crystals of K_2NbCl_6 observed under a microscope. This reprint was made from a colour negative and some of the red tint has been lost in the reproduction.

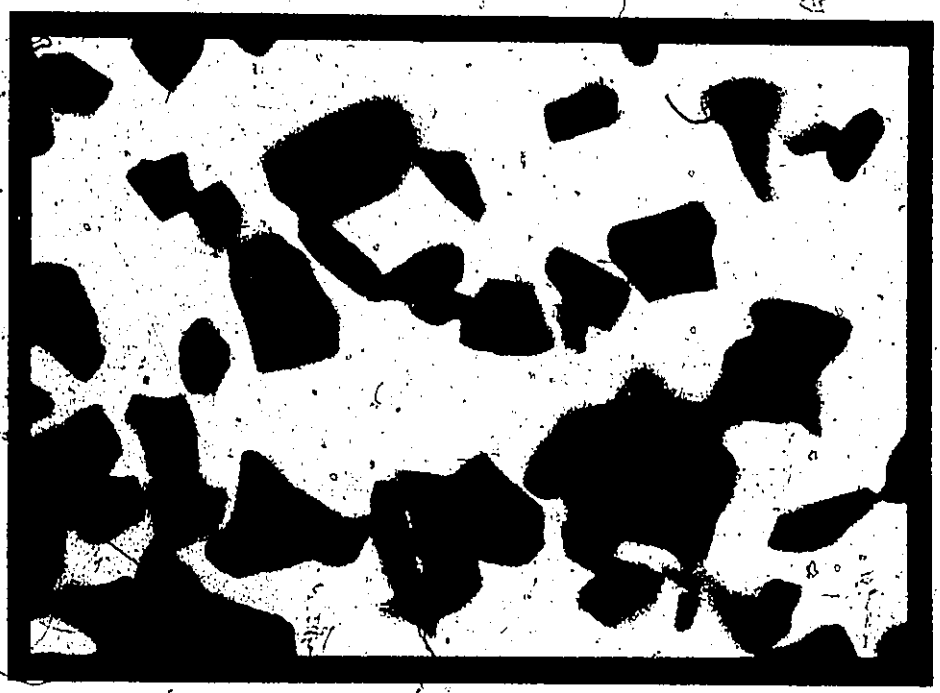

violet tinge but a fairly uniform red. This uniformity in colour suggests that these mixed valence systems form solid solutions, i.e. a single phase, rather than a mixture of compounds containing niobium in different valence states.

Crystals of K_2TaCl_6 were also found to be cubic with a uniform lilac colour confirming the observations of Morozov et al. (18-20).

Safonov (64) and co-workers reported "A_2NbCl_4" crystals to be isotropic and cinnamon red in colour. However, our observations showed that the crystals were anisotropic and the colour varied from orange to red brown in different crystallographic directions. This may have been pleochroism of $K_4Nb_6Cl_{18}$.

The same group of workers (57-59) reported that crystals of "A_2NbCl_5" (A = K, Rb, Cs) were red in colour. The present study showed that there were two types of crystals: orange and red. As expected, under the microscope, these crystals had appearance of $K_4Nb_6Cl_{18}$ and K_2NbCl_6.

(b) Electronic Spectra

Introduction

The UV-visible spectra of the solid complexes were determined by diffuse reflectance spectroscopy. The following discussion presents some pertinent aspects of this technique.

The radiation reflected from a finely ground solid consists of two parts: (i) a regular or specular part which arises from reflection at the upper surfaces of single crystals without transmission through the crystals and (ii) a diffuse part which arises from radiation which, upon penetrating the crystals, loses intensity according to the Lambert law, $\log I_o/I = \epsilon cd$ and re-appears at the surface after multiple scatterings. Perfectly diffused light has equal intensity in all directions.

As these two types of reflections are largely complimentary, the minimization of specular reflectance is one of the essential problems to be overcome in the design of instruments and preparation of samples. Specular reflection is diminished by reducing the particle size.

In a very broad sense, there are several general theories of light scattering. That which concerns us here is the one elucidated by Kubelka and Munk (104). They showed that for a special case of an infinitely thick opaque layer (achieved in practice with a layer thickness of ca. 2 mm) the following

relationship holds:

$$\frac{k}{s} = \frac{(1-R)^2}{2R} = F(R) \qquad [23]$$

where R is diffuse reflectance relative to a nonabsorbing standard, k is the molar absorption coefficient of the material defined by $I = I_o e^{-kd}$ and s is the scattering coefficient, which is practically independent of the wavelength for particles of mean diameter greater than the wavelength of the incident radiation. The function is known as the Kubelka-Munk (KM) function. There are several disadvantages to determining absorption spectra of compounds by reflectance: extensive broadening of the absorption band occurs and this makes exact assignment of the band maxima difficult. It is not possible to obtain extinction coefficients for the bands in diffuse reflectance spectra owing to the fact that s cannot be determined precisely.

However, reflectance measurements permit the resolution of low intensity peaks at long wavelengths. These peaks generally are the Laporte-forbidden d-d transitions with extinction coefficients in the range $10\text{-}10^2$. These peaks may be obscured by Laporte-allowed charge transfer transitions with extinction coefficients of $\sim 10^4$ which normally occur in the ultraviolet region. Our interest lay mainly in the visible region of the spectrum because it is here that

some unexplained features have been reported.

For many purposes it is sufficient in representing an absorption spectrum to plot absorbance against wavelength or frequency. For quantitative work it is necessary to make use of the Kubelka-Munk function rather than absorbance although there always remains some uncertainty about the preparation of the sample i.e. the reproducibility of particle size.

Several theoretical methods have been developed to treat the spectra of inorganic complexes.

Crystal field theory as proposed by Bethe (105) assumes the central metal ion and surrounding ligands to be point charges and the electrostatic interaction between the metals and ligands are considered. The theory states that the five d-orbitals of the transition metals which are degenerate in an isolated gaseous atom, are split into orbitals of different energies by the electrostatic field exerted by the ligands. A partially filled d-shell will then give rise to a variety of energy levels and transitions can occur between these.

The central assumption of crystal field theory, namely that the metal ion and the surrounding ligand atoms interact with one another in a purely electrostatic way and do not mix their orbitals or share electrons, is by no means true. There is always some metal-ligand overlap. The crystal field theory so modified to take account of the existence of orbital overlap is known as ligand field theory. This approach

is essentially a mixture of molecular orbital (M.O.) and crystal field theory. In this method the electrons which are concerned with the σ-bonds supply the greater part of the pertubation potential.

M.O. theory provides a good conceptual picture of how the arrangement of energy levels in a complex is determined by chemical bonding. Much evidence is now available to show that π-bonding must be considered in interpreting the bonding properties of transition metal halide complexes. Owen (106) has studied the magnetic properties of several hexachlorometallates and explains their results in terms of chlorine-metal $d\pi$-$p\pi$ bonding.

The M.O. scheme for d^1 ions with octahedral symmetry has been discussed by various workers (107,108). A schematic diagram is shown in Fig.30 . It is at best semi-empirical. This pictorial representation is sufficient for our purposes for it provides a basis for visualizing the bonding.

In electronic spectra of transition metal complexes there are two general types of transitions observed. In the first class of transitions, the electron moves from a molecular orbital centred mainly on the ligands to one centred mainly on the metal atom or vice versa. In these, the charge distribution is considerably different in the ground state and excited state respectively and so such transitions

Fig. 30: A schematic molecular orbital diagram for octahedral d^1 complexes.

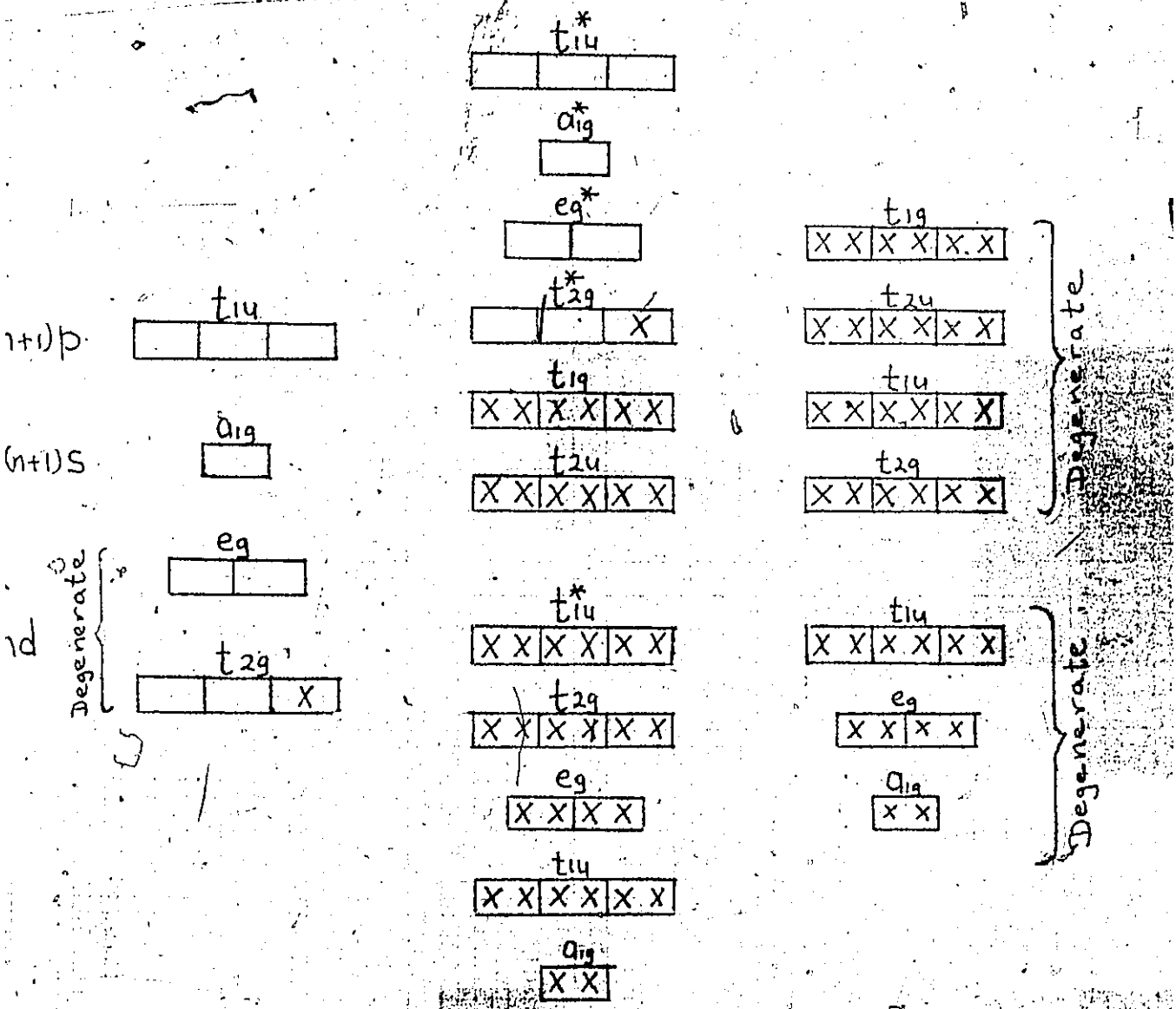
t_{1u}^*
a_{1g}^*
e_g^*
t_{2g}^*
t_{1g}
t_{2u}
t_{1u}
a_{1g}
e_g
t_{2g}
(n+1)p
(n+1)s
nd
Degenerate
Degenerate
Degenerate
Metal Orbitals
Molecular Orbitals
Ligand Orbitals

are said to be of the charge-transfer type. The relative position of the charge-transfer bands depends on the oxidizing power of the metal and the reducing power of the ligands. In this sense the charge-transfer transitions are related to photochemical oxidation-reduction processes. These transitions generally lie in the ultraviolet region.

The second class of transitions involves transfer of an electron between orbitals which have predominantly metal character. These are known as d-d transitions and are usually responsible for the colours associated with transition metal ions since they generally occur in the visible region of the spectrum. As stated earlier, these transitions are weak in comparison with charge-transfer bands. The reason for this is that an electron is promoted from one orbital that is centro-symmetric to another that is also centro-symmetric, and all transitions of this type are forbidden by Laporte's rule. However, such transitions are in fact observed owing to the effects of vibronic interactions and spin-orbit coupling.

A_2MX_6 complexes

The theory leads to the conclusion that the spectra of octahedral d^1 ions will be determined by the nature of a d-d transition between the t_{2g}^* and e_g^* orbitals as seen

from the M.O. diagram. For octahedral d^1 systems there are generally two low intensity peaks in the visible region (109) which arise through a splitting of the excited ^2E_g state. The splitting may be accounted for by the Jahn-Teller theorem. The mean of the two transitions is taken to be the 10Dq value for the complex.

Figures 31 and 32 show typical spectra of chloro complexes of niobium.

It was observed that the diffuse reflectance spectra of A_2NbCl_6 complexes prepared at high temperatures were very similar. The caesium chloro salt prepared by an aqueous method was also similar to the above salts. However this complex prepared at 300°C had prominent bands at ~25 kK and ~10kK which are not clearly distinguishable in the spectra of salts prepared by a different method. The spectrum of Na_2NbCl_6 has more structure than the spectra of the other hexahalo-complexes. It may be concluded that this system is much more complicated than the others. Since $Na_4Nb_6Cl_{18}$ does not appear to form, disproportionation of Na_2NbCl_6 may lead in this case to uncomplexed halide such as Nb_3Cl_{18} or possibly $NbCl_2$. Safanov et al. (64) were unable to find evidence in phase equilibrium studies of compound formation between NaCl and any halide of niobium lower than $NbCl_4$.

Fig. 31: Diffuse reflectance spectra:

(A) powdered single crystals of K_2NbCl_6.

(B) Cs_2NbCl_6 prepared at 300°C.

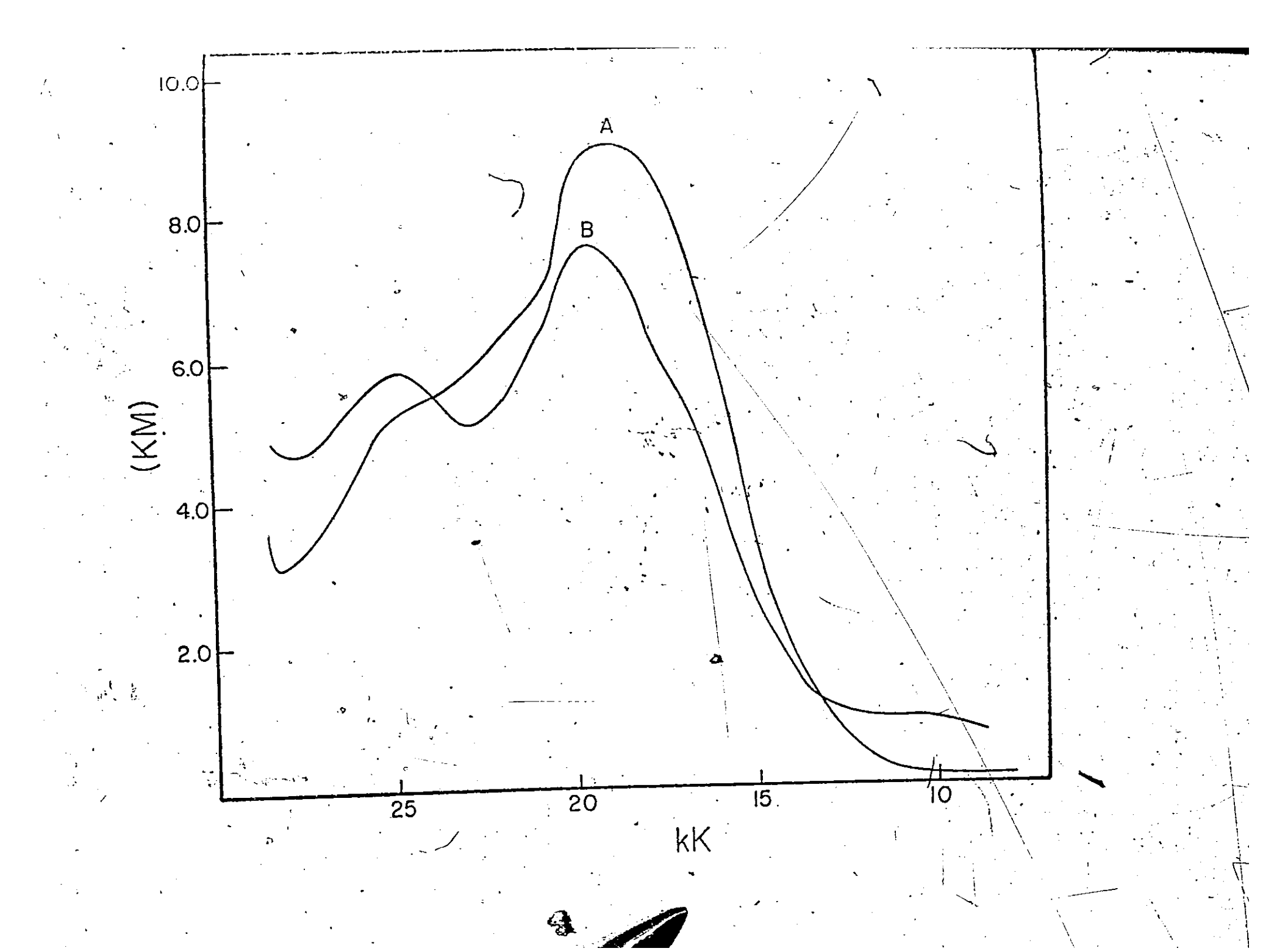
10.0
8.0
6.0
4.0
2.0
(KM)
A
B
25
20
15
10
kK

Fig. 32: Diffuse reflectance spectrum of Na_2NbCl_6

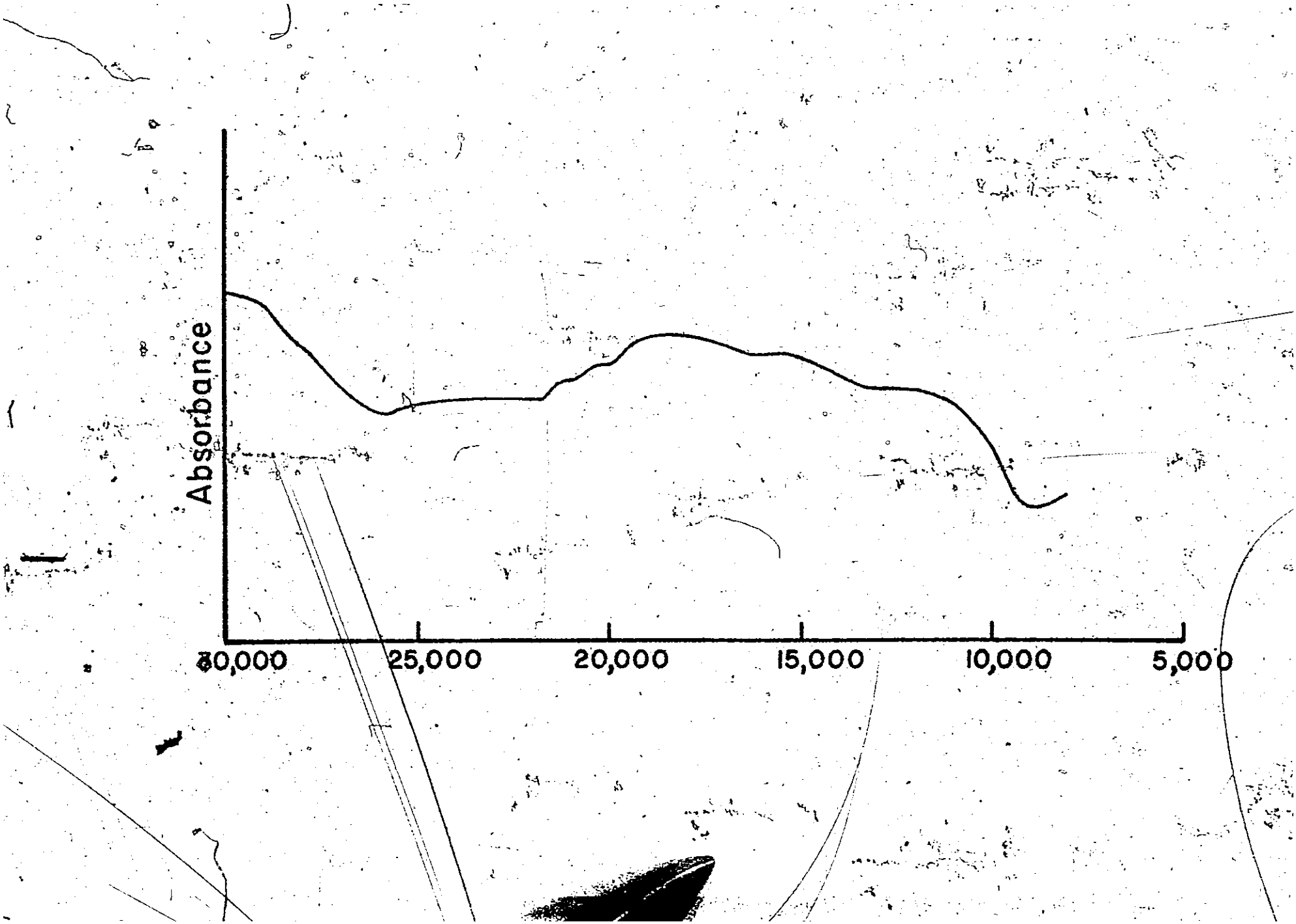
Absorbance
30,000
25,000
20,000
15,000
10,000
5,000

Torp (21) observed two peaks for A_2NbX_6 (A=K, Rb, Cs; X=Cl and Br) which occurred at 18.69 kK and 23.53 kK (shoulder) in the case of the chloro complexes. He also obtained a solution spectrum in molten pyridinium chloride and found it to be in good agreement with the reflectance spectrum of these ions.

Horner et al. (27) have examined the electronic spectra of these salts prepared by a different method (see Experimental section). They also reported two peaks in the visible region but with maxima at 20.4 kK and 25.6 kK (shoulder).

Fowles et al. (28) have reported the solution and solid state spectra of $[(C_2H_5)_4N]_2NbX_6$ (X=Cl or Br) and found them to be similar. Two peaks in the visible region occurred at 16.5 kK and 23.8 kK. The similarity between the solid and solution spectra of this compound led these authors to believe that the spectra were those of the authentic $NbCl_6^{2-}$ anion. An unassigned band at 10.0 kK was also reported. However the spectrum of $[(C_2H_5)_4N]_2NbCl_6$ recorded by Benzinger (29) was somewhat different from that of Fowles. He found one broad band with maximum absorption at 22.5 kK and a shoulder at 20.8 kK, and another broad band of lower intensity at 16.3 kK. The bands at 22.5 kK, and 20.8 kK were assigned to the transition from the $^2T_{2g}$ level to the two components of the ^2E_g level.

There are several points worth noting about the spectra reported by various workers.

(i) There is poor agreement between the positions of the absorption-maxima. This is obvious from Table XXVI. The present work agrees quite closely with Torp's for peaks 3 and 4 in the table, and with Fowles for peaks 2 and 4.

TABLE XXVI

Bands positions recorded by various workers for salts of $NbCl_6^{2-}$ ion

Authors	Ref.	Absorption Maxima (kK)			
		1	2	3	4
This work			16.8*	18-19	23.8*
Torp	(21)			18.69	23.53*
Horner	(27)			20.40	25.60*
Fowles	(28)	10	16*		23.8*
Benzinger	(29)		16.3	20.8*	22.50

*Indicates shoulders

(ii) In most cases there are more than the expected two peaks in the visible region. Fowles et al. (28) failed to identify the origin of the 10 kK band. The cluster compound (62) has a strong bands at ~ 11 kK and ~ 25 kK and a strong shoulder at about 17 kK. There is little doubt that

bands at 10 kK and 17 kK recorded by Fowles for the $NbCl_6^{2-}$ ion are due to the $[Nb_6Cl_{18}]^{4-}$ ion.

It is interesting to note that the spectrum of Cs_2NbCl_6 prepared at 300°C had fairly strong bands at 10 kK and 25 kK which suggests that a considerable quantity of $Cs_4Nb_6Cl_{18}$ was formed at 300°C. Thus the use of lower temperatures failed to achieve the purpose of minimizing the disproportionation of A_2NbCl_6 phase. On the contrary, it would seem that the absence of a melt prevented the dissolution of this compound in the bulk A_2NbCl_6 phase. However, the magnetic data indicate that the A_2NbCl_6 phase was thereby allowed to remain relatively pure.

The $(PyH)_2NbCl_6$ complex studied in this thesis is pale brown like the tetraethylammonium analogue. The reflection spectrum of this compound is given in Fig. 33. It can be seen that the intense band at ~ 19 kK in the spectra of alkali metal hexahaloniobate appears only weakly as a shoulder. Its greatly reduced intensity leads us to suspect that it is not a feature of the spectrum of the $NbCl_6^{2-}$ ion. It appears to be associated with the presence of impurities in the preparations and as it appears strongly in the spectrum of the powdered single crystal, the impurities concerned are probably dissolved in the A_2NbCl_6 phase. We thus come again to the conclusion that Nb(II) or Nb(III) atoms replace certain of the Nb(IV) atoms in the A_2NbCl_6 crystal.

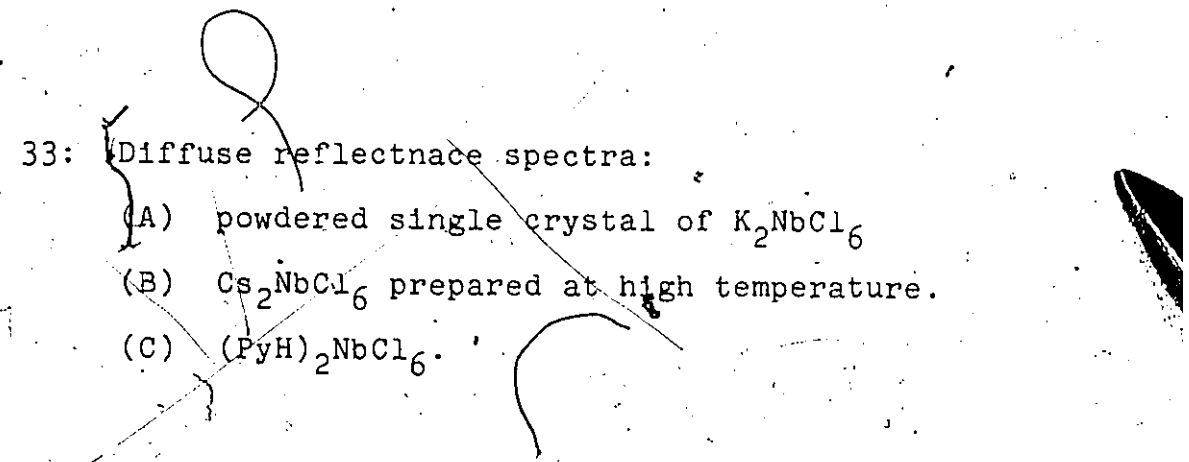

Fig. 33: Diffuse reflectnace spectra:
(A) powdered single crystal of K_2NbCl_6
(B) Cs_2NbCl_6 prepared at high temperature.
(C) $(PyH)_2NbCl_6$.

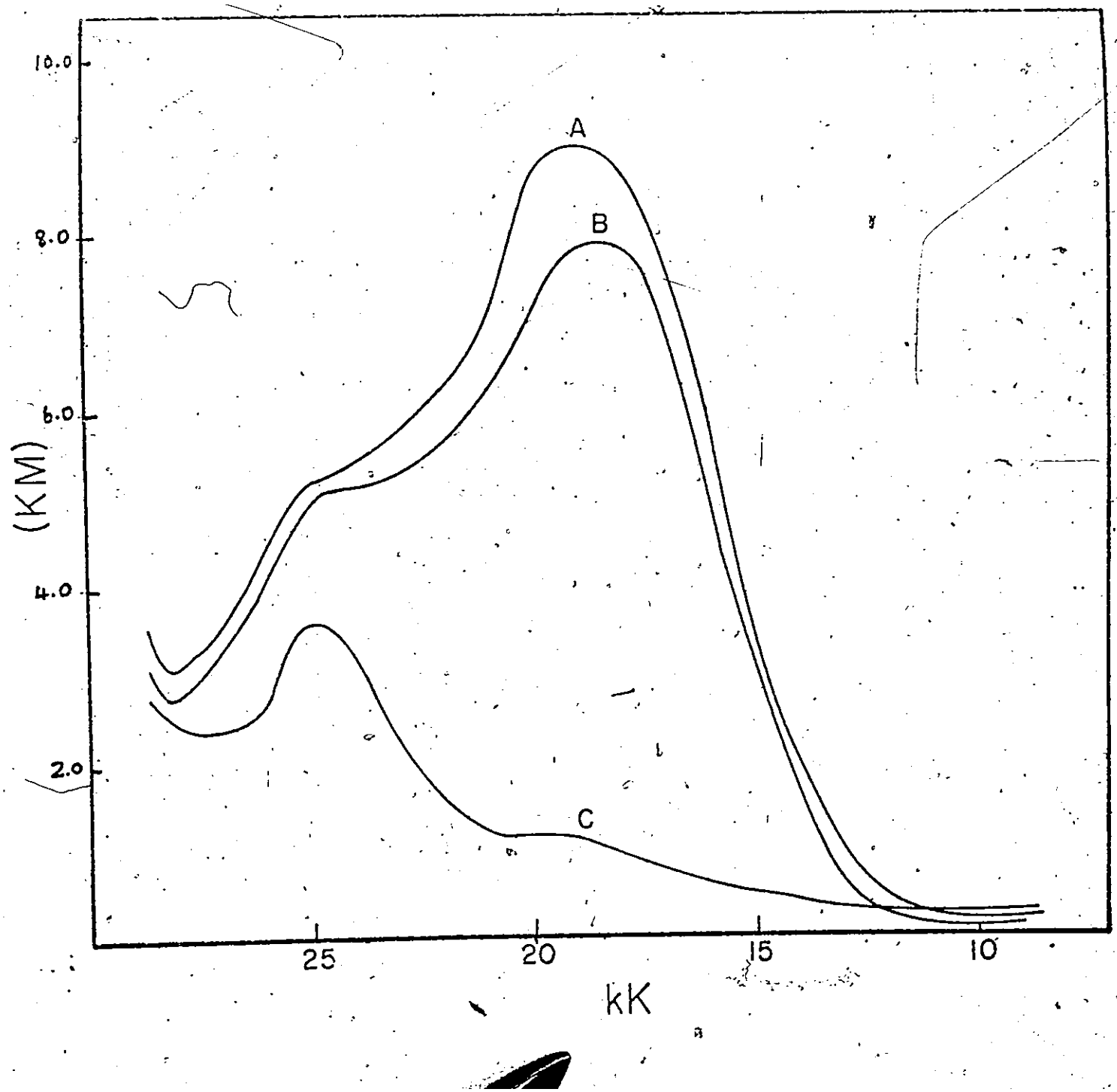
10.0
8.0
6.0
4.0
2.0
(KM)
A
B
C
25
20
15
10
kK

From Fig. 33 it can be seen that there is a progressive decrease in the ratio of the intensity of the "green" and "violet" bands respectively with increasing cation size. Most notable of all is the spectrum of $(Et_4N)_2NbCl_6$ reported by Fowles et al. In this case there is no trace of the lower energy band. Day (110) has noted the decrease in the intensity of bands corresponding to intervalence transition with increasing anion-anion distance in the A_2SbCl_6 systems. If both of the bands in the visible region are to be ascribed to Jahn-Teller split components of the $^2T_{2g}$ to ^2E_g transition, it must be remarked that the splitting energy of about 5000 cm^{-1} is extraordinarily high. Normally, splitting in d^1 systems is 3000 cm^{-1} or less. For instance, $MoCl_5$ has a value of 2700 cm^{-1} for the Jahn-Teller splitting. It seems unlikely that one of the components of the transition should exhibit so much more variable intensity then the other.

Another remarkable feature of this band is its large half-width amounting to some 8 kK, while the other band in $(PyH)_2NbCl_6$, where it is well resolved appears to have a width of about half this value. Intervalence transitions are generally broad owing to the high degree of vibrational distortion in which the product molecules find themselves.

The spectrum of $NbCl_4$ dissolved in saturated hydrochloric acid solution is also suggestive. As may be seen from

figure 34 the "green" band near 19 kK is entirely absent. The only strong feature in the visible region is a band at 22.5 kK which we ascribe to the $T_{2g} \longrightarrow E_g$ transition. There is, curiously, no sign of Jahn-Teller splitting. It may be that the influence of a single d electron on the system of relatively heavy atoms in $NbCl_6^{2-}$ is of minimal importance in influencing the co-ordination geometry.

Spectral examination of the $K_2(Nb,Zr)Cl_6$ crystals provided additional information regarding the band intensities. It can be argued that in the absence of strong interactions between neighbouring anions, the intensity of a given d-d transition should be linearly dependent upon the mole fraction of the ion species. Consequently, a plot of log(KM) against log x, where x is the mole fraction of niobium, should exhibit a slope of 1.0. If an absorption is due to a transition between neighbouring ions whose concentrations are proportional to x, the statistical factor in the transition probability will be proportional to x^2. In this case the slope of log(KM) against log x should be 2.0. Fig. 35 shows spectra of $K_2(Nb,Zr)Cl_6$ for x = 1.0, 0.36 and 0.057. As the zirconium salt absorbs somewhat at the higher energies the baseline for niobium absorption rises rather sharply in the diluted preparations. For this reason we have attempted to estimate

Fig. 34: Visible spectrum of $NbCl_4$ in concentrated hydrochloric acid.

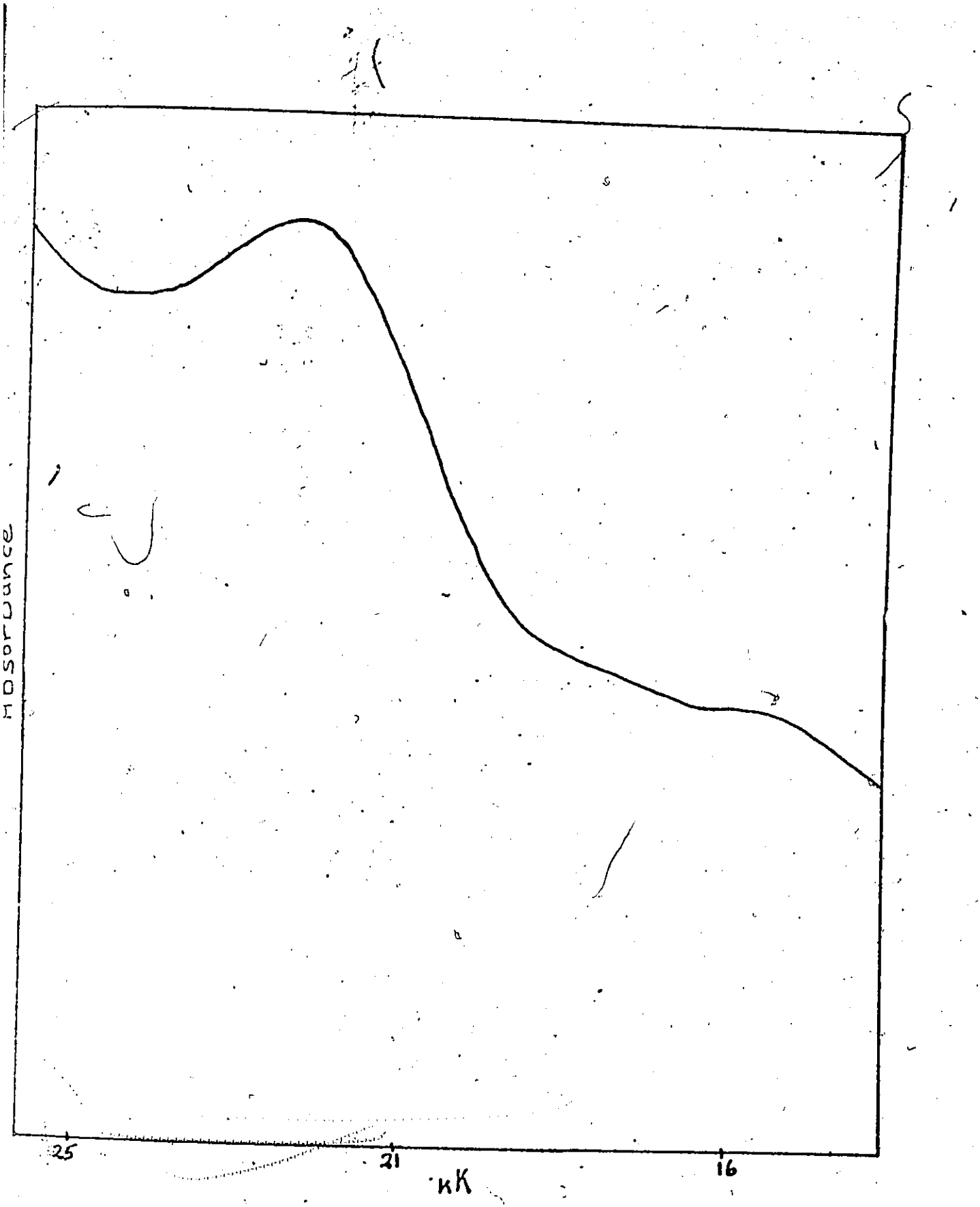
Absorbance
25
21
16
kK

Fig. 35: Diffuse reflectance spectra of $K_2(Nb,Zr)Cl_6$ system.

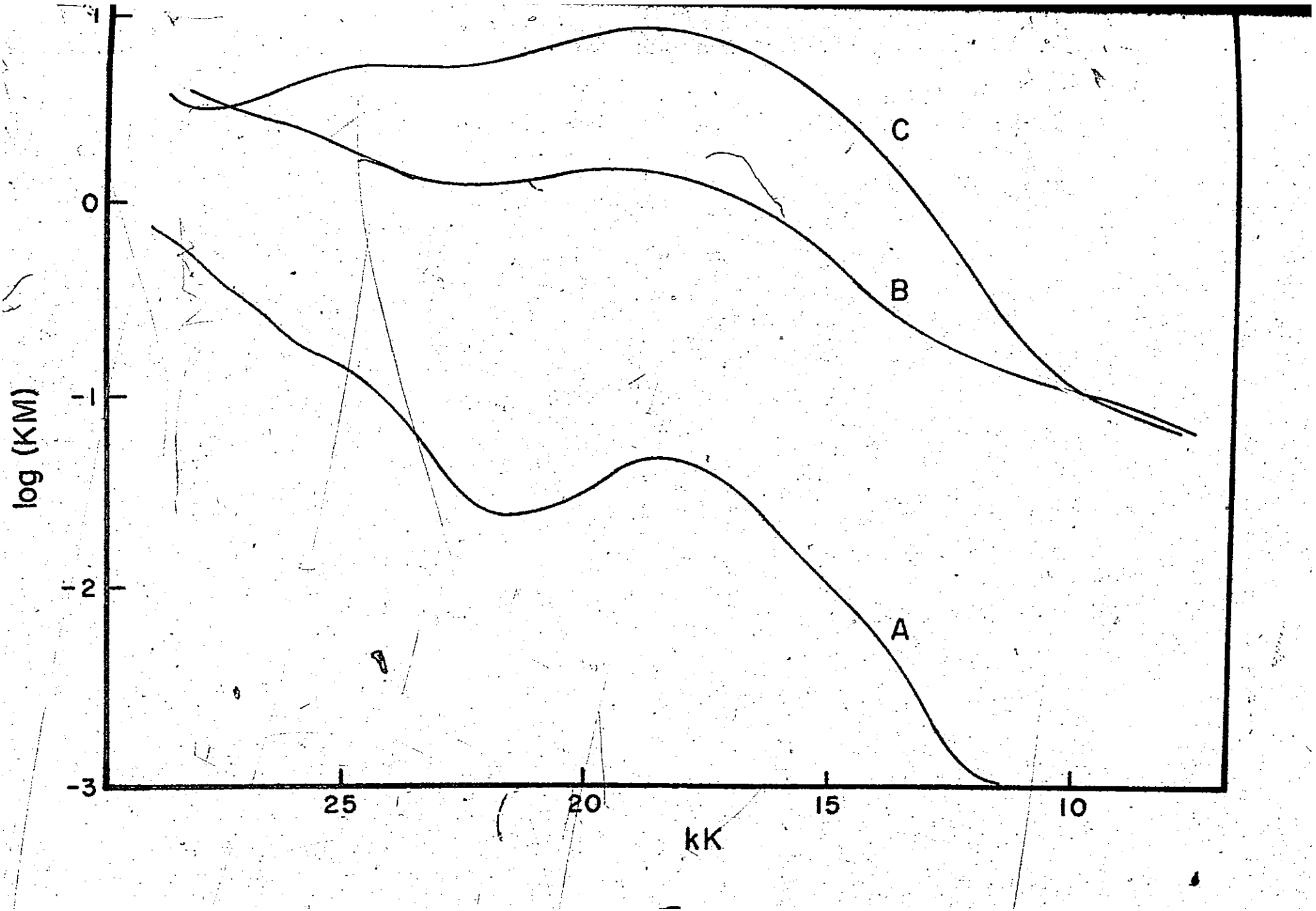
log (KM)
1
0
-1
-2
-3
25
20
15
10
kK
C
B
A

the intensities for the lower transition only. The plot, showing the relation between intensity and concentration appears in Fig. 36. The plot is a straight line with a slope of 1.8. The lack of curvature is verification of the fact that the reflection spectra in this case are quantitative. Because we have taken intensities directly from the curves without allowing for the possible influence of charge transfer absorption in $ZrCl_6^{2-}$ at ~19 kK, the values of log(KM) at the lower concentrations may be somewhat too high. In this case the true slope would be greater than 1.8. In any event the observed slope is considered to be a good indication that the band is not due to a d-d transition.

In spite of the foregoing arguments, the author does not consider the origin of the band at 19 kK as proved. Against the proposal that it is an intervalence electron transfer band is the fact that in the 300°C preparation of Cs_2NbCl_6 for which the magnetic behaviour suggests the absence of large amounts of dissolved impurities, the band is still present. Further, one might have expected to observe two or more intervalence transitions. Possibly the best verification of the intervalence transition would be the preparation of alkali hexachloroniobate(IV) which fails to show the band. We did not succeed after several attempts in eliminating or even weakening the band.

Fig. 36: Plot of log (KM) against log x for the $K_2(Nb,Zr)Cl_6$ system.

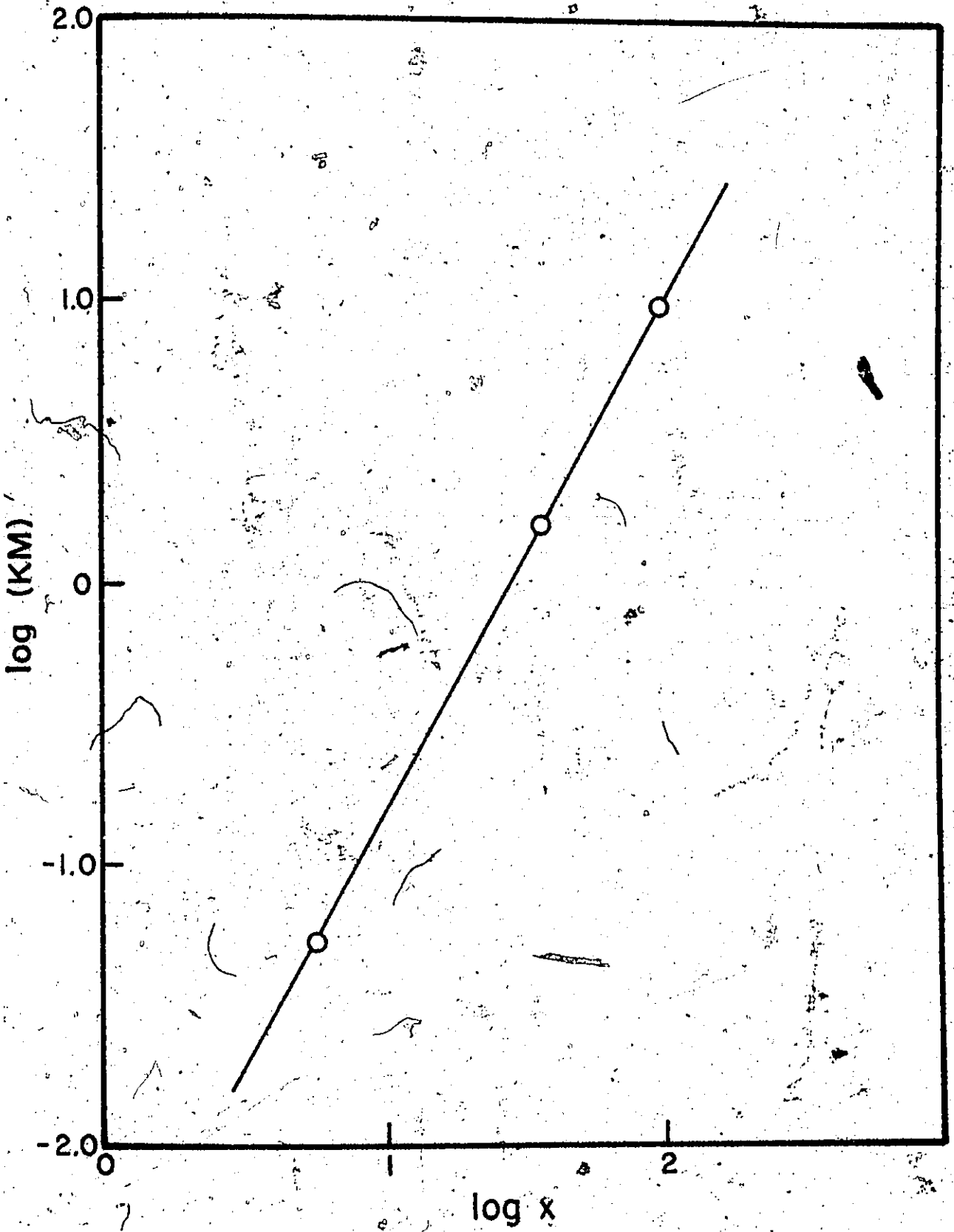
2.0
1.0
0
-1.0
-2.0
log (KM)
0
1
2
log x

Miscellaneous electronic spectra

K_2TaCl_6

The spectrum of K_2TaCl_6 (Fig. 37) shows two bands: a very intense band at 19 kK and a shoulder at 24 kK. Thus the value of 10Dq and the Jahn-Teller splitting are 21,500 cm^{-1} and 5000 cm^{-1} respectively. This spectrum is qualitatively and quantatively similar to K_2NbCl_6.

Cs_2NbI_6

The spectrum of Cs_2NbI_6 (Figures 38(a) and 38(b)) contains broad absorption bands over the entire visible-ultraviolet region. The peaks are due to normal charge transfer transitions of the ligand-metal type. Because iodide is the most oxidizable of the halide ligands, it should produce charge transfer transitions that extend into the visible region. Table XXVII shows absorption maxima in this region.

TABLE XXVII

Band Maxima for Cs_2NbI_6 (kK)

This Work	Torp
10.0	10.70
15.0	15.04
21.0	20
23.8	23.53

Fig. 37: Diffuse reflectance spectrum of K_2TaCl_6

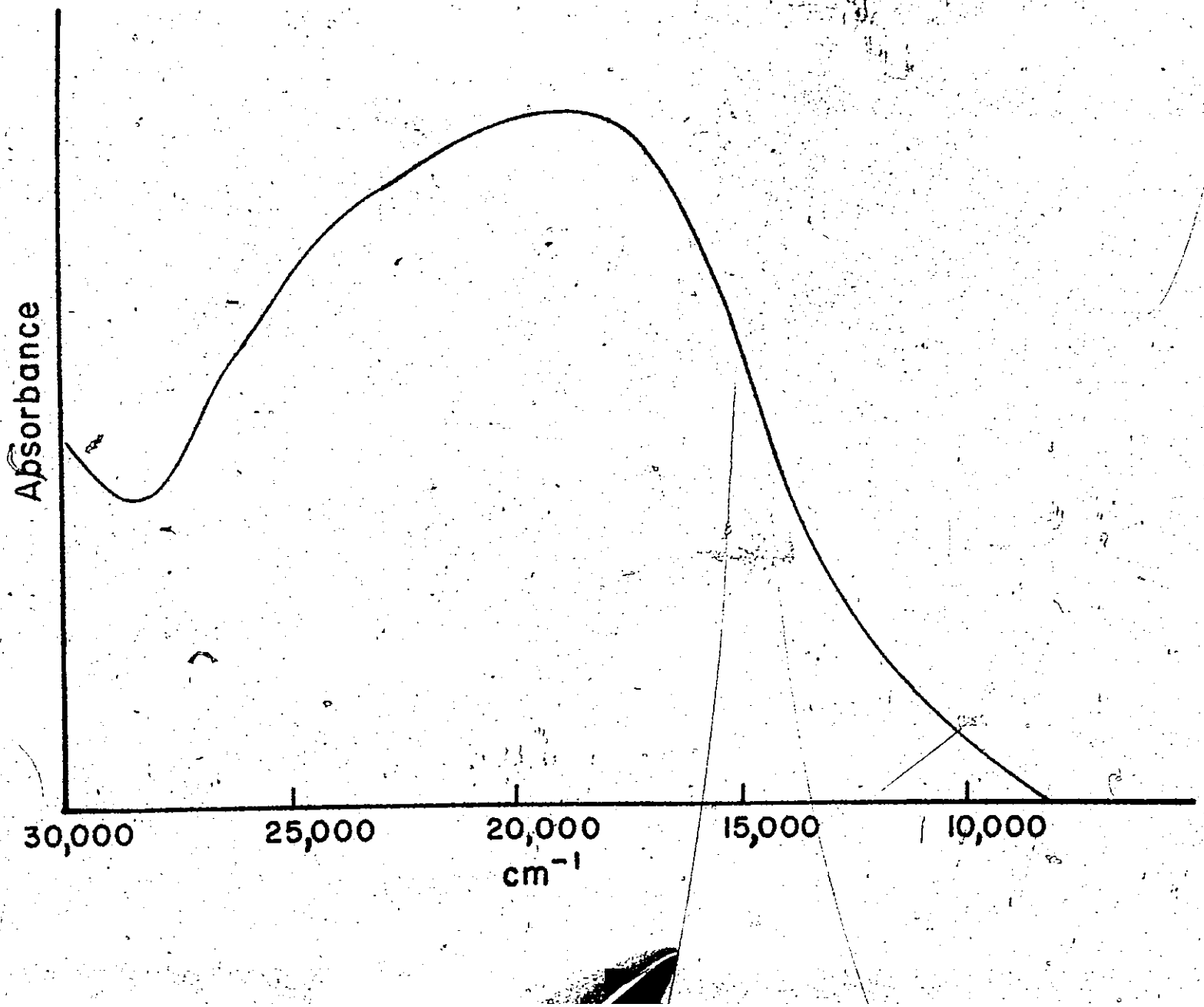
Absorbance
30,000
25,000
20,000
15,000
10,000
cm⁻¹

Fig. 38 : Diffuse reflectance spectrum of Cs_2NbI_6

(a) Cs_2NbI_6 (400° preparation)

(b) Cs_2NbI_6 (high temperature preparation)

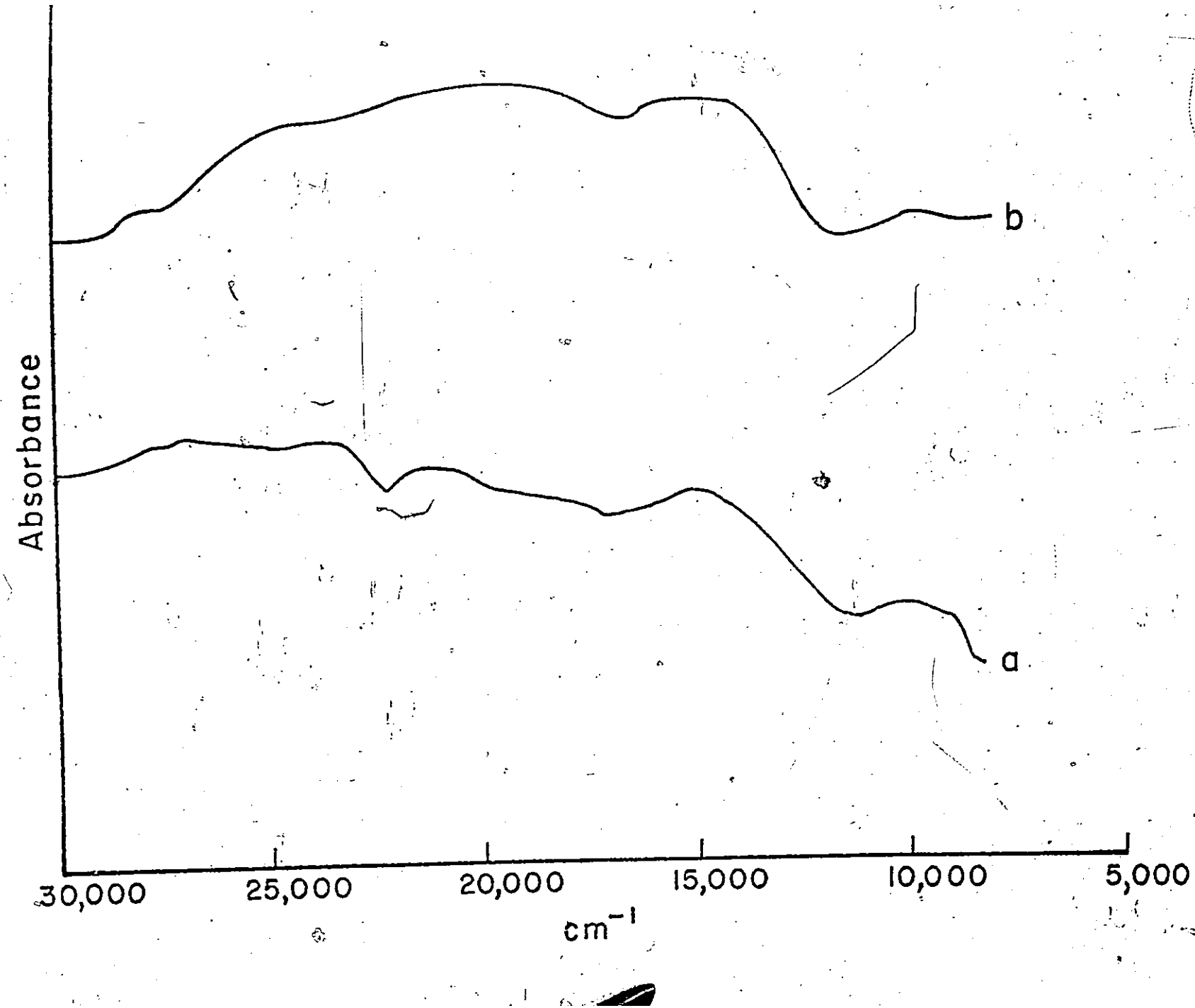
Absorbance
b
a
30,000
25,000
20,000
15,000
10,000
5,000
cm⁻¹

The agreement between the two sets of data is good in spite of the difference in colour of this complex recorded by Torp (brown) and by us (black). Also there is close agreement in positions of band maxima observed for high and low temperature preparations.

Charge transfer bands

Normal charge transfer bands were also observed for other A_2MX_6 complexes. The low apparent intensities of the high energy absorptions do not throw their assignment as charge transfer bands into question as one might think. It is a characteristic of reflection spectra that, because of scattering, the intensity of absorption falls off drastically with decreasing wavelength. A sample of such a spectrum for K_2NbCl_6 is seen in Fig. 39 and positions of the band maxima are recorded in Table XXVIII for K_2NbCl_6 and K_2TaCl_6. Values obtained by Torp are also given in this table for comparison.

Fig. 39 . Diffuse reflectance spectrum of K_2NbCl_6 showing normal charge transfer bands.

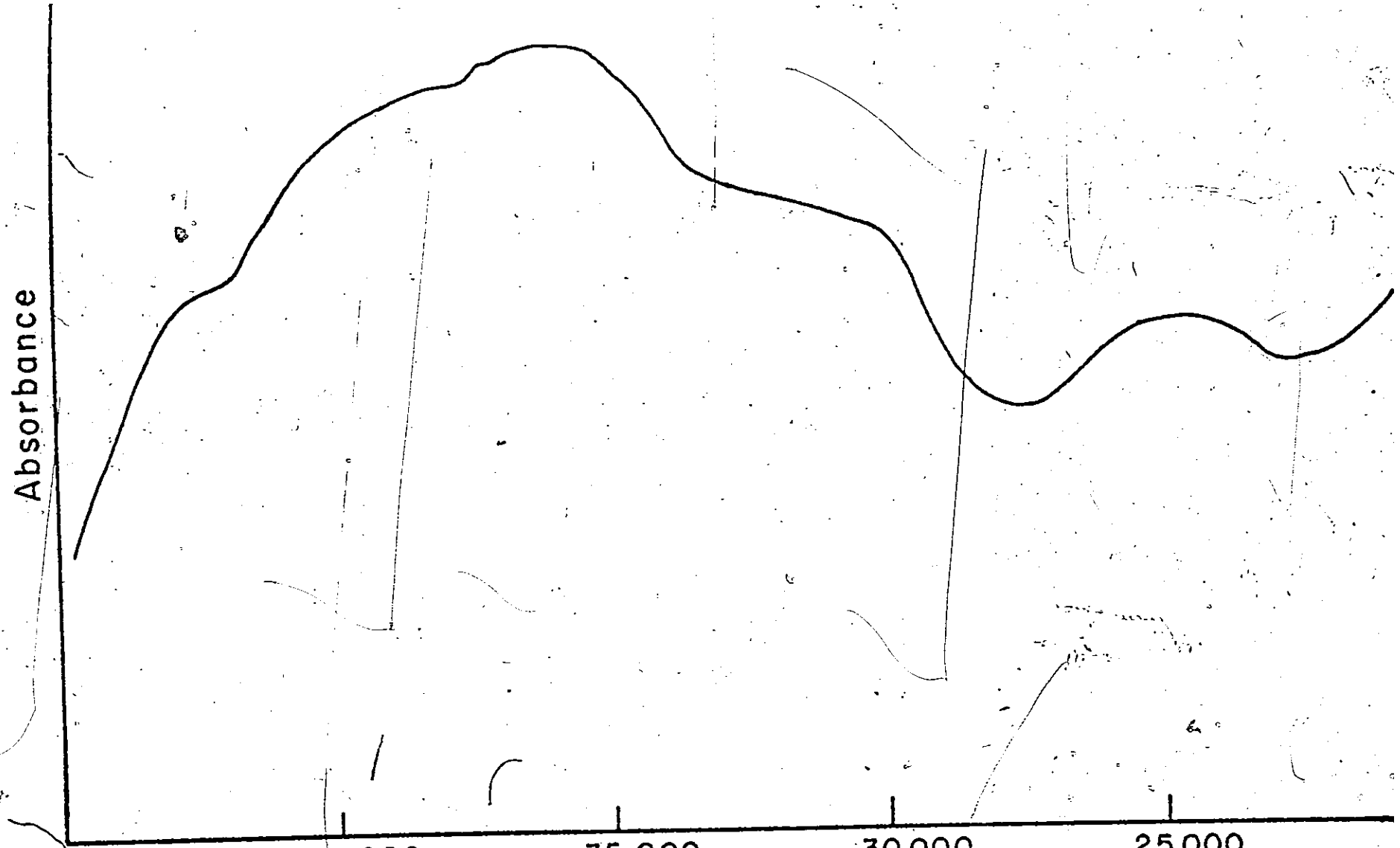
Absorbance
50,000
40,000
35,000
30,000
25,000
cm⁻¹

TABLE XXVIII

Charge Transfer Bands

Complex	Ref.	Band Maxima (kK)		
K_2NbCl_6	Our work	31.0	36.0	42.5
	Torp	33.9	37.74	42.55
K_2TaCl_6	Our work	33.8	37.0	40.0
	Torp	40.0		45.45

Torp (21), Fowles (28) and Horner (27) have attributed the occurence of these bands to charge transfer from ligand to the metal: the charge transfer most likely takes place from the non-bonding or filled t_{1u}, t_{1g} and t_{2g} orbitals localized mainly on the ligands to the predominantly metal t^*_{2g} orbital. In the spectra of A_2NbX_6 (X=Cl, I) the charge transfer peaks are shifted towards lower energies when the chloride ligand is replaced by iodide. This is to be expected since the iodide ion is more easily oxidized than chloride.

(c) Infrared Spectra

The infrared spectra of only two hexahaloniobate(IV) complexes have appeared in the literature (27). Fig. 40 show these spectra and the ν_3 band only is discussed.

It is notable that band A in Fig. 40(a) is not symmetrical and one may suspect that the band consists of at least two components, one appearing as a shoulder.

Fig. 40: The infrared absorption spectra reported by Horner et al. (ref. 27). (A) Cs_2NbCl_6, (B) Cs_2NbBr_6

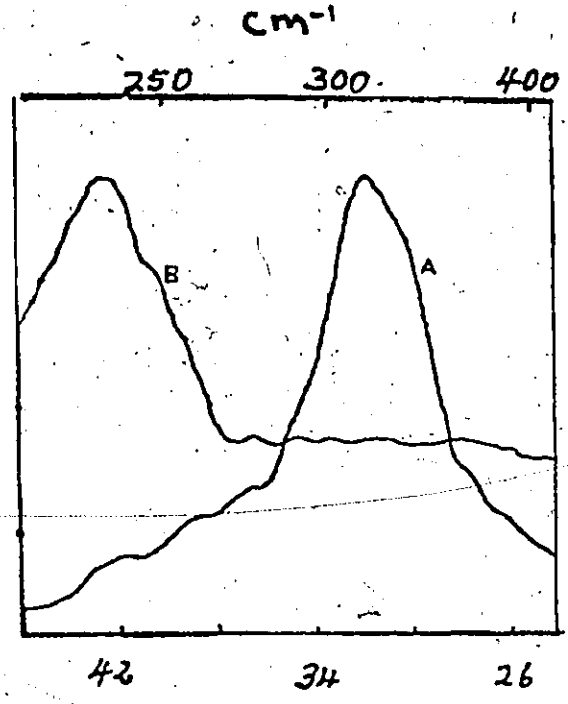

(a)

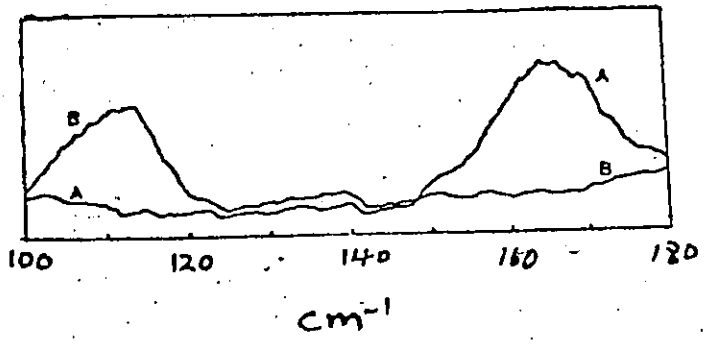

(b)

Figure 41 shows the spectra of some of the complexes studied in this thesis. Results obtained from Nujol mulls between CsI disks were identical to those obtained from CsI pressed pellets.

The infrared spectrum of powdered single crystals of K_2NbCl_6 is shown in Fig. 42. Like the spectra above, it appears to consist of a principle peak at $\sim 310\ cm^{-1}$ with possibly some evidence of weak shoulders on both high and low frequency side, i.e. at $\sim 330\ cm^{-1}$ and at $\sim 290\ cm^{-1}$ respectively. There is an irregularity at $280\ cm^{-1}$ but this coincided with grating change mechanism in the instruments operation. The spectra were repeated several times using both CsI and polyethylene plates in an effort to determine whether these shoulders were genuine features of the spectrum. Although they appeared consistently, the case for their genuiness is not strong. However the shoulders appear rather clearly at the same frequencies in the spectrum reported by Horner et al. and reproduced here in Fig. 40.

The cluster ion $Nb_6Cl_{18}^{4-}$ absorbs at $280\ cm^{-1}$ and $331\ cm^{-1}$ (111) and so the shoulders might well be attributed to this species. There is no doubt that the cluster species contributes to the absorption shown in curve B for Fig. 41. However the single crystal of K_2NbCl_6 appeared from its electronic spectrum to be quite free of this impurity. If this is so, and if the shoulders are real, they must be attributed to absorption by dissolved Nb(V) and Nb(II) or Nb(III) species.

Only one absorption band is expected in this region for octahedral complexes. Such a molecule has six normal modes of vibration: three of these are Raman active while only two

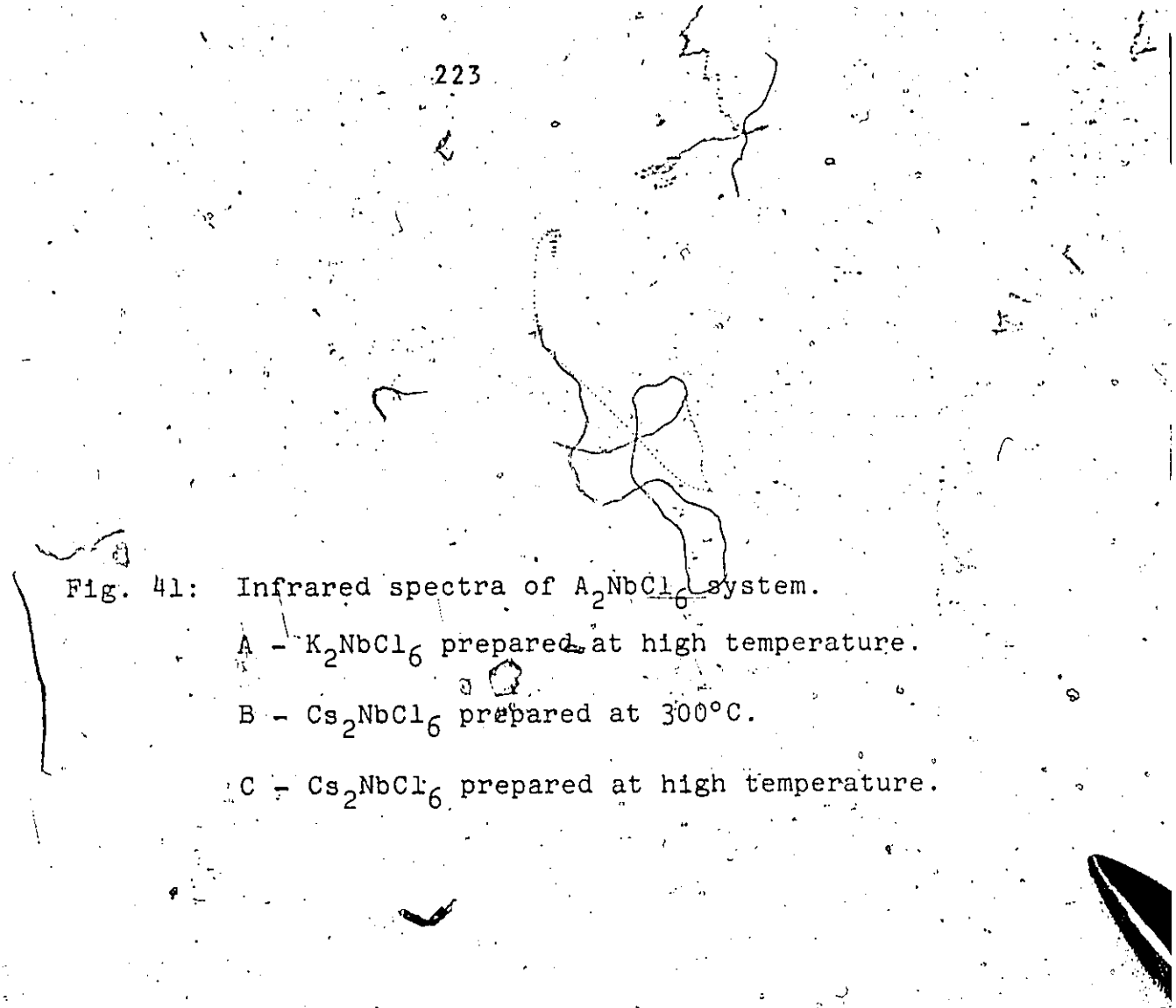

Fig. 41: Infrared spectra of A_2NbCl_6 system.

A - K_2NbCl_6 prepared at high temperature.

B - Cs_2NbCl_6 prepared at 300°C.

C - Cs_2NbCl_6 prepared at high temperature.

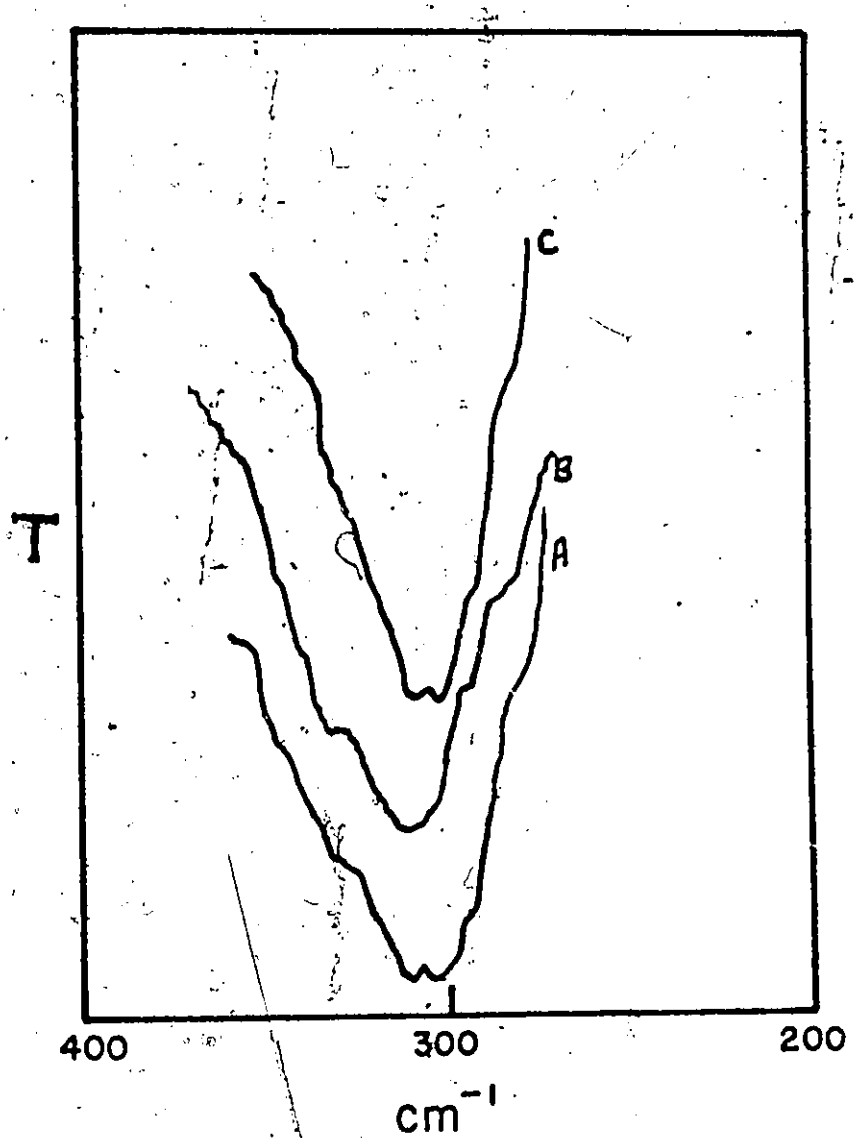
C
B
A
T
400
300
200
cm⁻¹

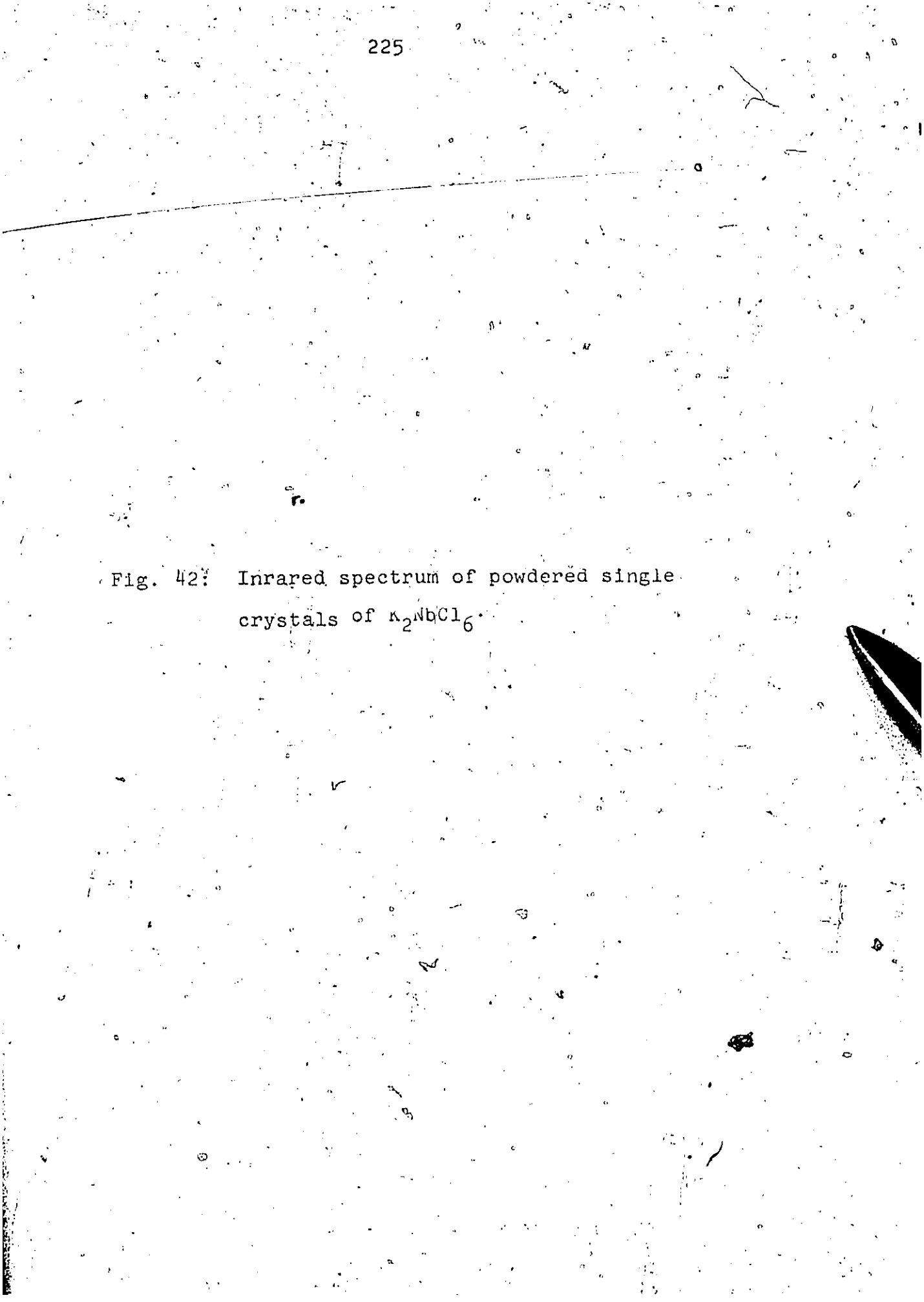

Fig. 42: Inrared spectrum of powdered single crystals of K_2NbCl_6.

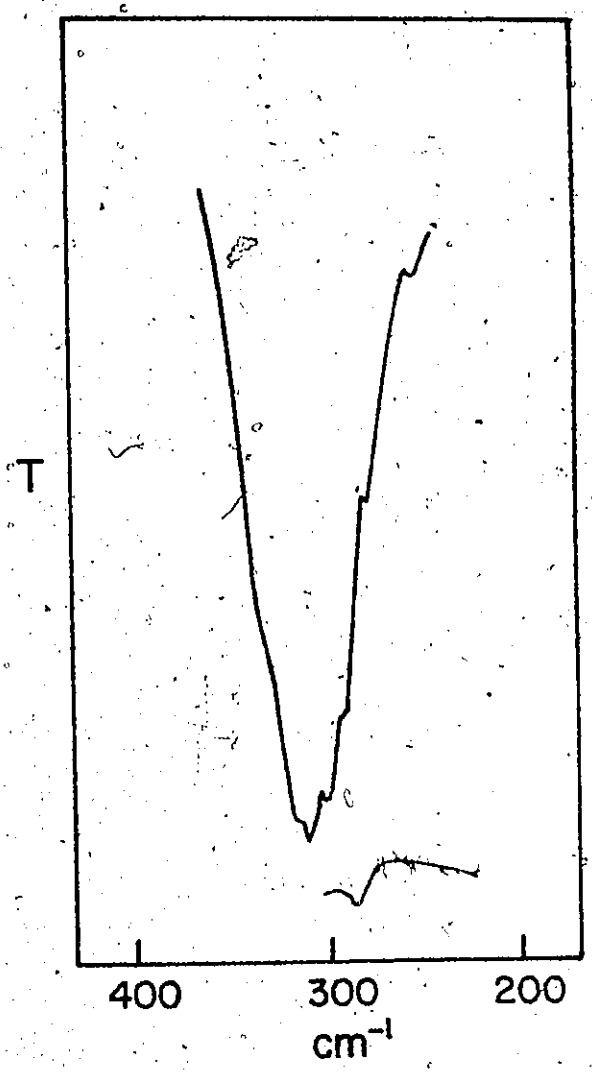
T
400
300
200
cm⁻¹

(ν_3 and ν_4) are infrared active. The ν_6 mode is inactive. The mode ν_3 is due to antisymmetric stretching while ν_4 is the antisymmetric bending vibration. For MCl_6^{2-} complexes, where M is a metal from the second or third transition series, ν_4 occurs at much lower frequency than does ν_3 as shown in Table XXIX.

TABLE XXIX

ν_4 Frequencies of Some Halocomplexes of Transition Metals

Complex	ν_4 (cm^{-1})	Ref.
Cs_2NbCl_6	165	(27)
Cs_2NbBr_6	112	"
Cs_2TaCl_6	160	"
$IrCl_6^{2-}$	168	(112)
$PtCl_6^{2-}$	182	(")

The ν_4 frequencies were outside the range of the spectrometers available to us and therefore the ν_3 mode is the only one recorded here.

In transition metal complexes, the frequency of the ν_3 vibration increases considerably with increasing

oxidation number of the metal implying that the metal-halogen force constant is greater the higher the oxidation number of the metal. This has been demonstrated for a number of complexes as shown in Table XXX.

TABLE XXX

Variation of ν_3 with Oxidation Number

Complexes	ν_3 (cm^{-1})	Ref.
$[Ir^{II}Cl_6]^{3-}$	296	(112)
$[Ir^{IV}Cl_6]^{2-}$	333	"
$[W^{IV}Cl_6]^{2-}$	308	"
$[W^{V}Cl_6]^{-}$	317	"
$[Pt^{II}Cl_4]^{2-}$	325	"
$[Pt^{IV}Cl_6]^{2-}$	344	"

Thus the effect of raising the oxidation state of a transition element from four to five is to increase ν_3 by 10-20 cm^{-1}. The peak at 305-310 cm^{-1} common to all of the A_2NbCl_6 complexes is very probably the Nb(IV)-Cl ν_3 mode.

Horner et al. (27) have reported the value 314 cm^{-1} for this mode. The Nb(V)-Cl ν_3 frequency can be expected at around 330 cm^{-1}. In $CsNbCl_6$ (27) it has been observed at 335 cm^{-1}.

On the other hand ν_3 mode for Nb(II)-Cl stretching may be expected in the range 20 cm^{-1} to 40 cm^{-1} below 310 cm^{-1}. Thus the shoulder at 290 cm^{-1} could correspond with the suggestion that either Nb(II) or Nb(III) is present in the A_2NbCl_6 phases.

The possibility that the side features were chlorine isotope peaks was also considered. However the observed peaks represent too large a spread ($\tilde{\sim}$ 50 cm^{-1}) to be accounted for by the chlorine isotopic splitting.

It appears from our observation that the ν_3 stretching mode in the alkali salts is essentially independent of the cation. Shifts of frequency are often observed for a complex in different crystal environments, i.e. ν_3 for octahedral A_2MCl_6 complexes sometimes shows a quite substantial decrease as the size of the atom A is increased (112). The ν_3 stretching mode for $[(C_2H_5)_4N]_2NbCl_6$ reported by Fowles (28) occurs at 305 cm^{-1} agreeing with the trend mentioned above.

3. Calorimetric Studies

The heats of formation of A_2NbCl_6, K_2TaCl_6 and A_2ZrCl_6 were studied by solution calorimetry.

There were two reasons for the choice of 6.20N hydrochloric acid solution as the calorimetric liquid:

(i) a sufficiently high concentration of acid was required to prevent excessive hydrolysis of the materials. Hydrolysis is accompanied by the evolution of a large quantity of heat. In the interest of attaining good reproducibility, only a slight degree of hydrolysis could be permitted.

(ii) it was essential that the acid concentration remained constant for long periods and evaporation of acid of this concentration has little effect on its normality.

The heats of solution of alkali metal halides, the tetrahalides of niobium, tantalum and zirconium and of the hexahalometallates(IV) of niobium, tantalum and zirconium were determined as described in the Experimental Section.

All samples except the tetraiodide dissolved rapidly. In most cases it took no more than three minutes

for the sample to dissolve completely. This can be seen from the temperature-time curves shown in Figures 43 to 46.

The heat of solution of KCl in water was determined as a check on the accuracy of the calorimeter. The value obtained was 4.22 kcal. $mole^{-1}$ which is in good agreement with published values of 4.21 kcal. $mole^{-1}$ (86) and 4.20 kcal. $mole^{-1}$ (113).

The following partial reactions were used to calculate the heats of complexing. The heat of complexing of K_2NbCl_6 was chosen as an example. The square brackets in the various equations denote solution compositions.

(1) $2KCl(c) + [H_2NbCl_6 + 580\ HCl] = [2KCl + H_2NbCl_6 + 580\ HCl]$ ..... ΔH_1

(2) $NbCl_4(c) + [2KCl + 582\ HCl] = [2KCl + H_2NbCl_6 + 580\ HCl]$ ..... ΔH_2

(3) $[2KCl + H_2NbCl_6 + 580\ HCl] = K_2NbCl_6(c) + [582\ HCl]$ ..... ΔH_3

(4) $[2KCl + H_2NbCl_6 + 1162\ HCl] = [2KCl + 582\ HCl] + [H_2NbCl_6 + 580\ HCl]$ ..... ΔH_4

(5) $[2KCl + H_2NbCl_6 + 580\ HCl] + [582\ HCl] = [2KCl + H_2NbCl_6 + 1162\ HCl]$ ..... ΔH_5

Fig. 43. Temperature-time curve for dissolution of KCl in 6.20N HCl. The temperature scale shows the unconverted Helipot reading. The black dots are experimental points.

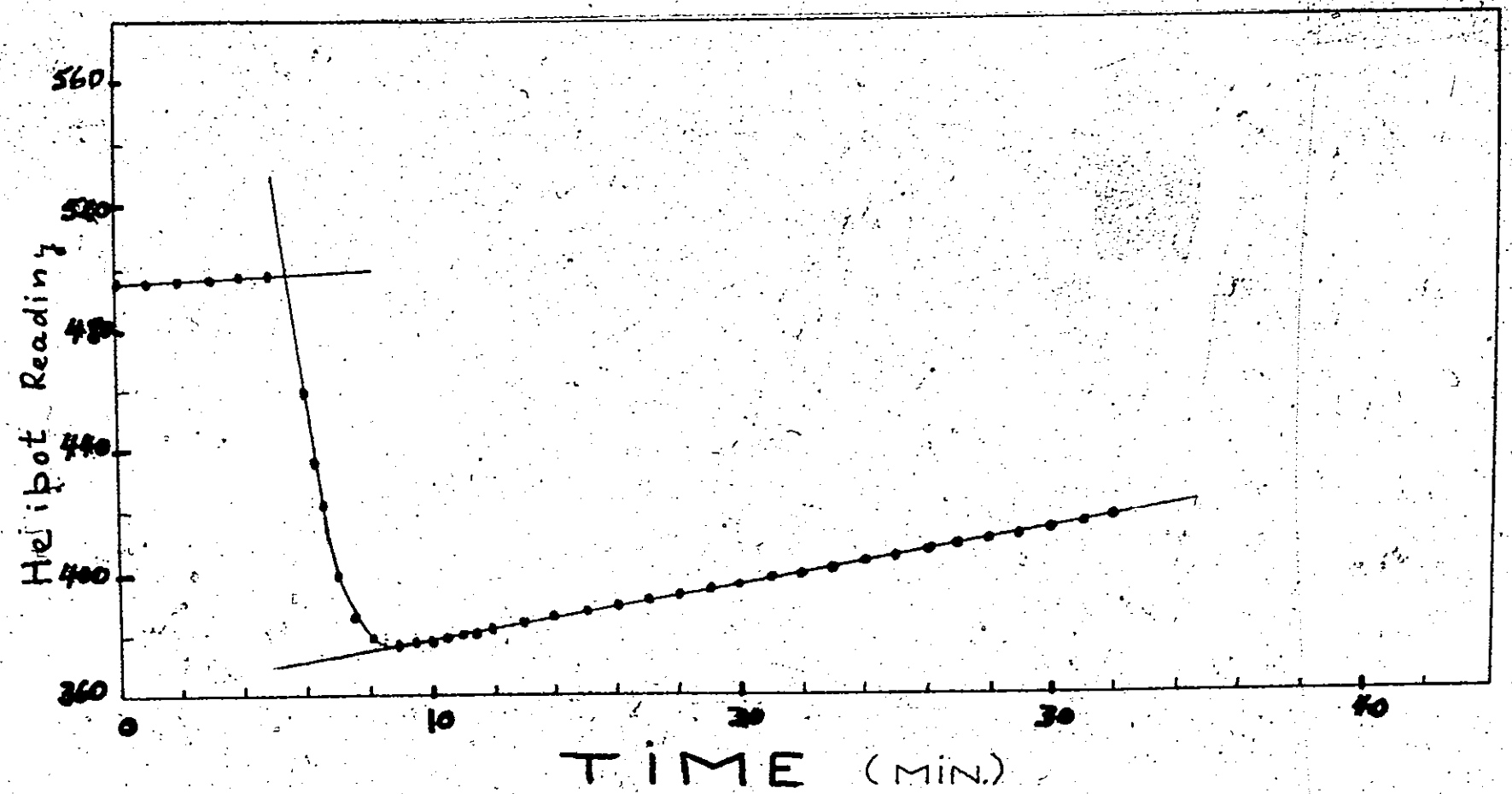
560
520
480
440
400
360
Hellbot Reading
0
10
20
30
40
TIME (MIN.)

Fig. 44: Temperature-time curve for dissolution of $NbCl_4$ in 6.20N HCl. The temperature scale shows the unconverted Helipot reading. The black dots are experimental points.

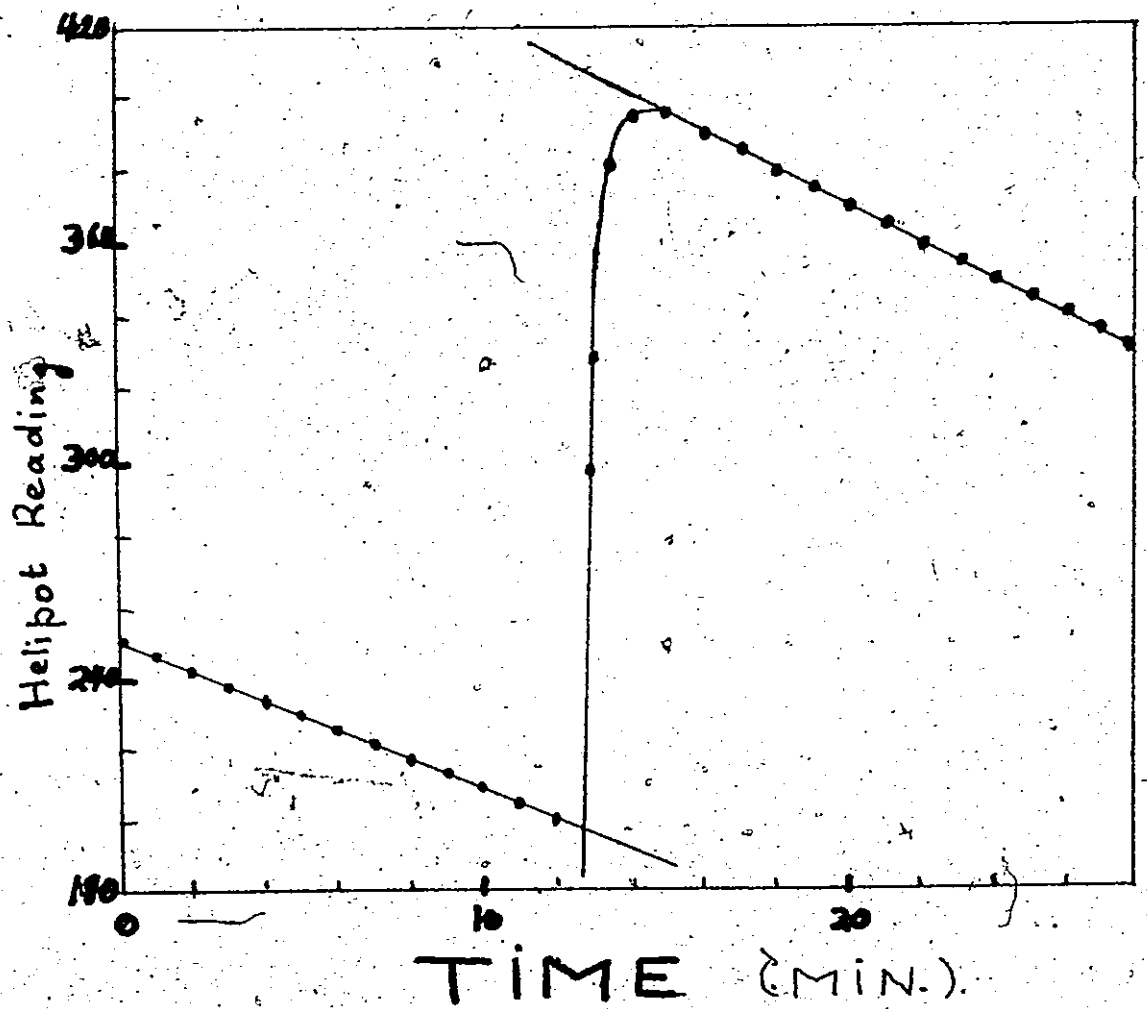
420
360
300
240
180
Helipot Reading
0
10
20
TIME (MIN.)

Fig. 45: Temperature-time curve for dissolution of K_2NbCl_6 in 6.20N HCl. The temperature scale shows the unconverted Helipot reading. The black dots are experimental points.

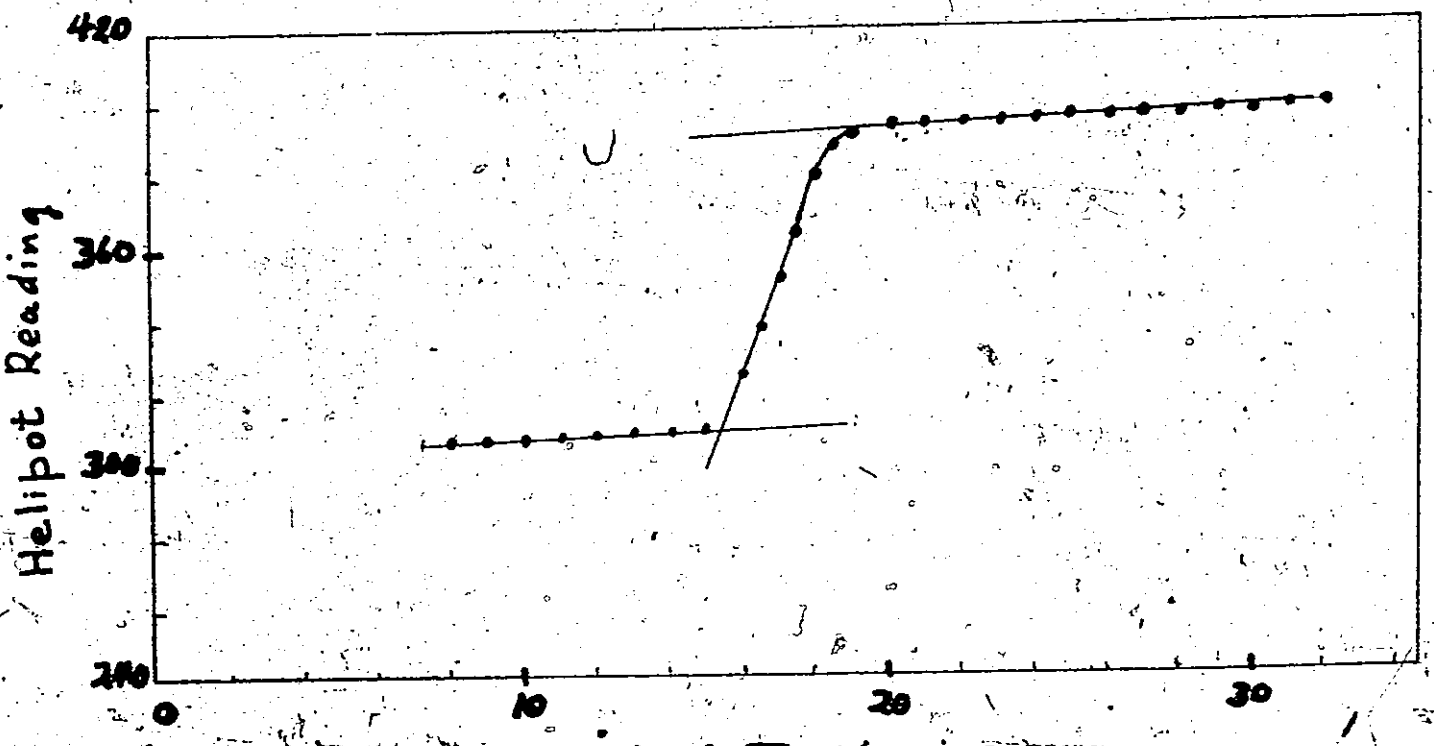
420
360
300
240
Helibot Reading
0
10
20
30
TIME (MIN.)

Fig. 46: Temperature-time curve for dissolution of NbI_4 in 6.20N HCl. The temperature scale shows the unconverted Helipot reading. The black dots are experimental points.

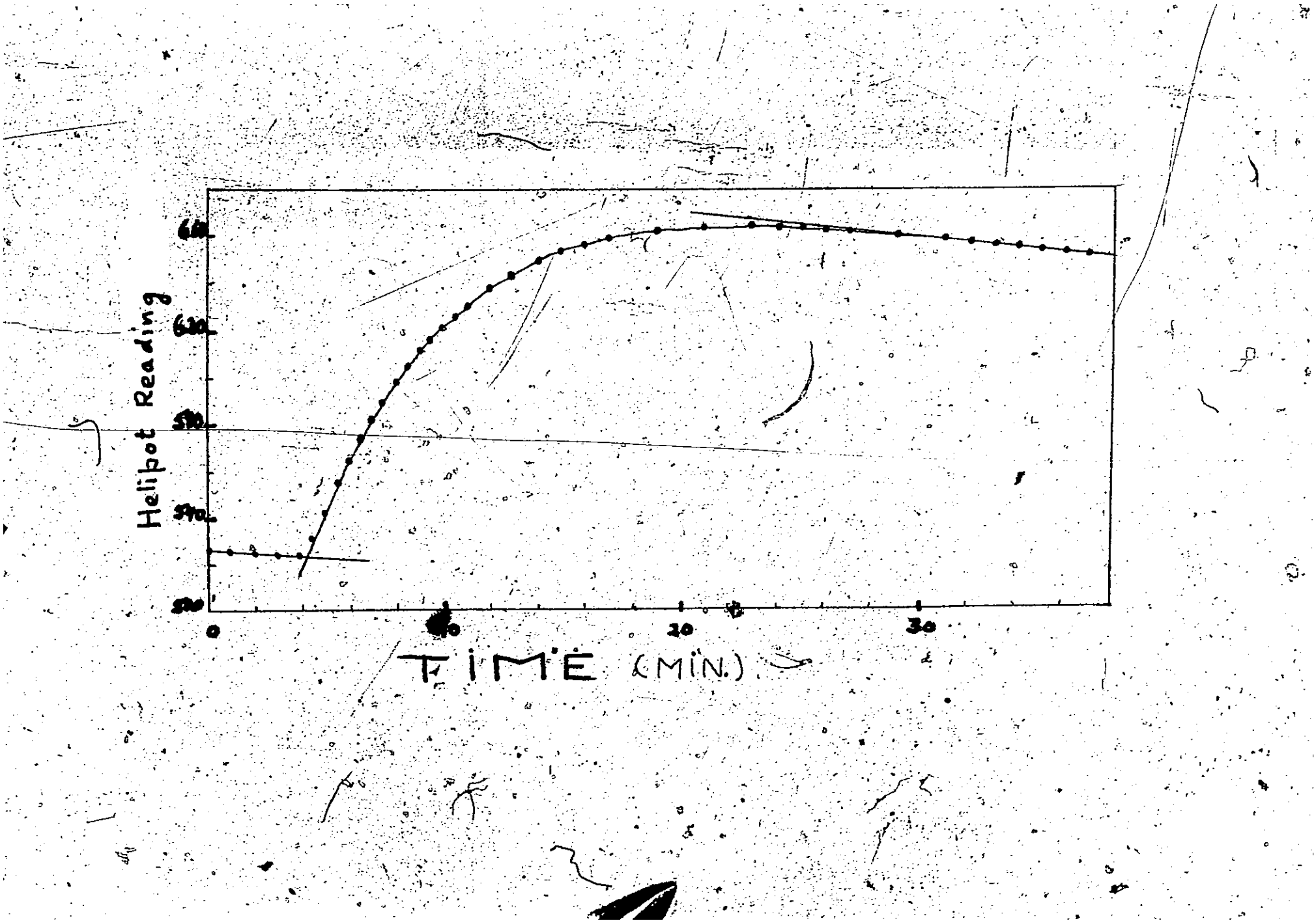
Helipot Reading
0
20
30
TIME (MIN.)

From which we obtain:

$$2KCl(c) + NbCl_4(c) = K_2NbCl_6(c)\ldots\ldots, \quad \Delta H_c = \sum_{i=1}^{i=5} H_i$$

ΔH_4 and ΔH_5, representing heats of mixing, are assumed to be zero or negligible with respect to other quantities. The quantities appearing in the equations are based on the typical example of 0.5 grams of $NbCl_4$ being dissolved in 200 ml. of 6.20N HCl.

The heats of solution, ΔH_1, ΔH_2 and ΔH_3 are recorded in Tables XXXI to XXXIII.

The heats of complexing, ΔH_c, for the complexes calculated from data in Tables XXXI to XXXIV are given in Table XXXIV. Results obtained by other workers are also given for comparison.

It is obvious from Table XXXIV that there is considerable disagreement between the data obtained in this work and those reported by other workers. In view of this disagreement we shall review the data recorded in Table XXXIV.

Comparison of results

The heat of complexing of K_2TaCl_6, reported by Tsintsius and Smirnova (35), was determined calorimetrically

TABLE XXXI

Heats of solution of alkali metal halide ΔH_1

Compound	Wt. of sample (grams)	Calorimeter constant (cal./u*)	ΔH_1 (kcal mole^{-1})	Mean ΔH_1 (kcal mole^{-1})	Mean ΔH_1 (Kilojoules mole^{-1})
KCl	1.24677	0.288	4.60	4.58	19.2
	1.34068	0.295	4.56		
RbCl	1.45779	0.207	3.64	3.64	15.2
	1.41854	0.307	3.64		
CsCl	1.65703	0.198	2.74	2.80	11.7
	1.57375	0.205	2.85		
CsBr	1.61870	0.201	4.62	4.58	19.2
	1.58013	0.205	4.53		
CsT	1.35132	0.266	6.75	6.65	27.8
	1.31931	0.297	6.55		

* The symbol "u" in Tables XXXVII to XXXIX refer to the number of unit change observed on the recorder dial.

Heats of solution of tetrahalides ΔH_2

Compound	Wt. of sample (grams)	Calorimeter constant (cal/u)	ΔH_2 (kcal mole^{-1})	Mean ΔH_2 (kcal mole^{-1})	Mean ΔH_2 (Kilojoules mole^{-1})
$NbCl_4$	0.37542	0.225	-29.5	-29.5	-123
	0.57391	0.219	-29.7		
	0.51705	0.197	-29.6		
	0.34781	0.203	-29.1		
$NbBr_4$	0.81040	0.215	-34.4	-34.2	-143
	0.74902	0.230	-34.1		
	1.03539	0.217	-34.2		
NbI_4*	1.22540	0.215	-17.3	-18.1	-75.7
	1.26449	0.216	-18.1		
	1.84934	0.219	-19.2		
	1.13889	0.209	-17.6		
$TaCl_4$	0.24585	0.241	-52.8	-52.7	-220
	0.25930	0.286	-52.7		
	0.25929	0.283	-52.6		
$ZrCl_4$	0.45593	0.198	-50.7	-50.7	-212
	0.61678	0.199	-50.5		
	0.30445	0.221	-50.7		

* Refer to the discussion when considering the values given for NbI_4.

TABLE XXXIII

Heats of solution of the complexes ΔH_3

Compound	Wt. of sample (grams)	Calorimeter constant (cal/u)	ΔH_3 (kcal mole^{-1})	Mean ΔH_3 (kcal mole^{-1})	Mean ΔH_3 (Kilojoules mole^{-1})
K_2NbCl_6	0.52941	0.240	-14.3	-14.2	-59.4
	0.58779	0.243	-14.3		
	0.29403	0.221	-13.9		
Rb_2NbCl_6	1.26983	0.237	- 7.12	-7.02	-29.4
	1.21958	0.220	- 6.79		
	0.76885	0.235	- 7.14		
Cs_2NbCl_6	1.04684	0.252	+ 1.38	+1.35	+5.65
	1.18365	0.237	+ 1.37		
	1.35988	0.238	+ 1.30		
Cs_2NbCl_6 (300°)	0.54086	0.242	0.0	0.00	0.00
	0.69735	0.240	0.0	0.00	0.00
Cs_2NbCl_6 (Aqueous)	.40461	0.238	0.0	0.00	0.00
	1.17601	0.271	0.0	0.00	0.00
Cs_2NbBr_6	1.86370	0.237	- 1.28	-1.47	-6.15
	1.66961	0.223	- 1.57		
	1.57671	0.225	- 1.56		

TABLE XXXIII CONT

Compound	Wt. of sample (grams)	Calorimeter constant (cal/u)	ΔH_3 (kcal mole^{-1})	Mean ΔH_3 (kcal mole^{-1})	Mean ΔH_3 (Kilojoules mole^{-1})
Cs_2NbI_6	0.74638	0.217	-14.3		
	0.63410	0.222	-15.3	-14.9	-62.3
	0.75321	0.227	-15.2		
K_2TaCl_6	0.12604	0.228	-27.3		
	0.34460	0.266	-27.0	-27.2	-114
	0.30012	0.238	-27.3		
K_2ZrCl_6	0.45570	0.211	-23.7		
	0.51421	0.186	-23.6		
	0.46802	0.203	-23.9	-23.7	-99.6
Cs_2ZrCl_6	0.29962	0.262	-11.7		
	0.23295	0.213	-11.5	-11.7	-49.0
	0.32132	0.18890	-11.7		

TABLE XXXIV

Heats of complexing ΔH_c

Complex	K_2NbCl_6	Rb_2NbCl_6	Cs_2NbCl_6 (High Temp.)	Cs_2NbCl_6 (300°)	Cs_2NbCl_6 (Aqueous)	Cs_2NbBr_6	K_2TaCl_6	K_2ZrCl_6	Cs_2ZrCl_6
This work (kcal mole^{-1})	-6.14 ±0.4	-15.2 ±0.4	-25.3 ±0.2	-23.9 ±0.2	-23.9 ±0.2	-23.6 ±0.2	-16.3 ±0.2	-17.8 ±0.2	-33.4 ±0.2
This work (Joules mole^{-1})	25.7	-63.6	-106	-100	-100	-98.7	-68.2	-74.5	-140
Other workers (kcal mole^{-1})							-25.9 (35)	-52.0 (51) -48.5 (52)	-52.0 (51)

The numbers in parenthesis are references.

using 0.03% hydrogen perioxide solution as a calorimetric liquid. There is a difference of ~ 10 k. cal. between Tsintsius' results and those reported here. Our experience shows that tetrahalides and complexes of the type being studied give gels when treated with water or hydrogen peroxide solutions. We feel that gels are unsuitable products in calorimetry. The compounds studied in the present work dissolved in 6.2N hydrochloric acid to give clear solutions in every case.

Morozov and coworkers (51) have measured the heats of complexing of A_2ZrCl_6 (A=Na, K, Cs) by decomposition methods. It was intended that the decomposition should occur according to the equation:

$$A_2ZrCl_6 \longrightarrow 2ACl + ZrCl_4$$

The vapour pressure of zirconium chloride over the compound A_2ZrCl_6 was determined by the flow method, with chlorine as the carrier gas. The results are summarized in Table XXXV.

TABLE XXXV

Data from reference (51)

Complex	ΔH decomposition ($kcal.mole^{-1}$)	Temperature Range (°C)
Na_2ZrCl_6	25.8	432 - 630
K_2ZrCl_6	52.0	650 - 790
Cs_2ZrCl_6	52.0	700 - 800

Earlier, the same workers had reported phase equilibrium studies of chlorozirconates (50). It is clear that the thermochemical experiments were performed above the eutectic temperature. However free energies of formation of pure compounds can be obtained only at temperatures below the corresponding eutectic temperatures, as this is the only range where the thermodynamic equilibrium constant may be equated to a reaction pressure. For example, when measuring the reaction pressure of pure A_2ZrCl_6, some free alkali metal chloride will always be produced because of its decomposition. Measurements taken at temperatures higher than the corresponding eutectic of the $ACl-A_2ZrCl_6$ binary system would therefore represent saturated solutions of liquidus composition. It is evident that the thermodynamic properties of pure compounds cannot be obtained in this range; instead the data may be

used to calculate the partial molar properties of the solution (53). We are forced to conclude that the values of heats of complexing reported by Morozov and his group (51) are in error. Zvara and Tarasov (52) have reported heats of formation of chlorozirconates obtained by radioactive tracer methods. The experimental procedure involved the chlorination of the oxide in one end of a quartz tube. The $ZrCl_4$ formed was led by a carrier gas (Cl_2) to a hot dense bed of KCl. A controllable temperature gradient was set up along the bed by means of a furnace which had sectional windings. Depending on the initial partial pressure of chloride vapour in the gas and on the mechanism of its reaction with KCl, the volatile chloride was retained in different parts of the KCl bed, that is, at regions of differing temperatures. After discontinuing the reaction, the distribution of radioactivity along the KCl bed and the residual activity in the boat containing the oxide were measured, and thus the location and intensity of the chloride distribution were determined.

The partial pressures of $ZrCl_4$ (e.g. 0.049 m.m. Hg at 525°C) were so low that traces of water vapour could have interfered. It has been the authors experience that passing good quality nitrogen over $ZrCl_4$ frequently gave $ZrOCl_2$.

Moreover the authors themselves pointed out that $ZrCl_4$ readily reacts with SiO_2. This may have introduced considerable error.

Evaluation of experimental data

Our experimental results for A_2NbCl_6 complexes show that the thermodynamic stability of alkali-metal hexachloroniobates(IV) increases from potassium to caesium, which is normal for ternary complexes.

The values for the heat of complexing of Cs_2NbCl_6 prepared at 300° and that prepared at higher temperatures differ by $\sim$ 1 kcal $mole^{-1}$. This difference is not surprising in view of the fact that the 300° preparation was impure. Values of Cs_2NbCl_6 precipitated from concentrated hydrochloric acid gave results which were similar to those for 300° preparation. The infrared spectrum of this compound showed that it was slightly hydrolysed.

The apparent value of +10 kcal $mole^{-1}$ for the heat of complexing of the iodo complex is anomalous. This appears to be due to a rather small heat of solution of NbI_4. From Fig. 46, it is clear that NbI_4 dissolved quite slowly. There could be several reasons for this behaviour:

(i) the product of dissolution of NbI_4 in the hydrochloric acid solution is probably not the same as that of Cs_2NbI_6. This may have come about if the metal-metal bonds in the tetraiodide did not break to give mononuclear dissolved species.

(ii) dissolving of A_2NbI_6 in HCl solution is probably accompanied by ligand substitution:

$$NbI_6^{2-} + 6Cl^- \longrightarrow NbCl_6^{2-} + 6I^-$$

The slow dissolution of NbI_4 suggests that a corresponding substitution of iodo groups does not occur readily. It is therefore possible that NbI_6^{2-} and NbI_4 do not reach an equilibrium position in this substitution process. In this case the thermochemical data derived from temperature-time plots would be meaningless. Our attempts to catalyse the dissolution of NbI_4 with activated charcoal failed.

Our results show that K_2TaCl_6 is much more stable than its niobium analogue. The origin of this difference could be explained as follows: the effective nuclear charge of the tantalum atom should be somewhat greater than that for niobium owing to the presence of the 4f subshell in the former atom. The tantalum atom would therefore have a greater affinity for the corresponding halide ion.

Like the niobium complexes, the stability of alkali metal hexachlorozirconates(IV) increases with increasing size of the alkali metal ion. This may be accounted for by the consideration of the following reactions:

$$(a)\quad A_2MCl_6(s) = 2A^+(g) + MCl_6^{2-}(g) \qquad (+ U_{A_2MCl_6})$$

$$(b)\quad MCl_6^{2-}(g) = MCl_4(g) + 2Cl^-(g) \qquad (+ \Delta H_D)$$

$$(c)\quad 2A^+(g) + 2Cl^-(g) = 2ACl(s) \qquad (- 2U_{ACl})$$

By adding (a), (b) and (c), we obtain the overall reaction

$$(d)\quad A_2MCl_6(s) = 2ACl(s) + MCl_4(s) \qquad (\Delta H_R)$$

and

$$\Delta H_R = \Delta H_D - (2U_{ACl} - U_{A_2MCl_6})$$

$U_{A_2MCl_6}$ and U_{ACl} represent respectively lattice energies of A_2MCl_6 and ACl. ΔH_D is the heat of dissociation

of the complex anion MCl_6^{2-} and ΔH_R is the experimentally measured heat of decomposition of the solid A_2MCl_6.

The difference in the lattice energy $(2U_{ACl} - U_{A_2MCl_6})$ is always positive because of the smaller size of the Cl^- anion as compared to the size of the MCl_6^{2-} ion. This difference should increase in going from a large to a smaller cation. As the heat of dissociation of the MCl_6^{2-} ion is common to all three hexachlorometallates, it follows that the heat of decomposition of ΔH_R for hexachlorometallates should increase with increasing ionic radius. This is a general result for halometallates.

Gas phase enthalpies

The enthalpy of complexing, i.e. for the reaction $MX_4 + 2X^- \longrightarrow MX_6^{2-}$, can be assessed easily only when the reactants and products are gaseous. In other cases, lattice energies and/or heat of solvation are involved in reaction heats and simple relationships are obscured.

The cycle below may be used to calculate the enthalpy of formation when the reactants are gaseous.

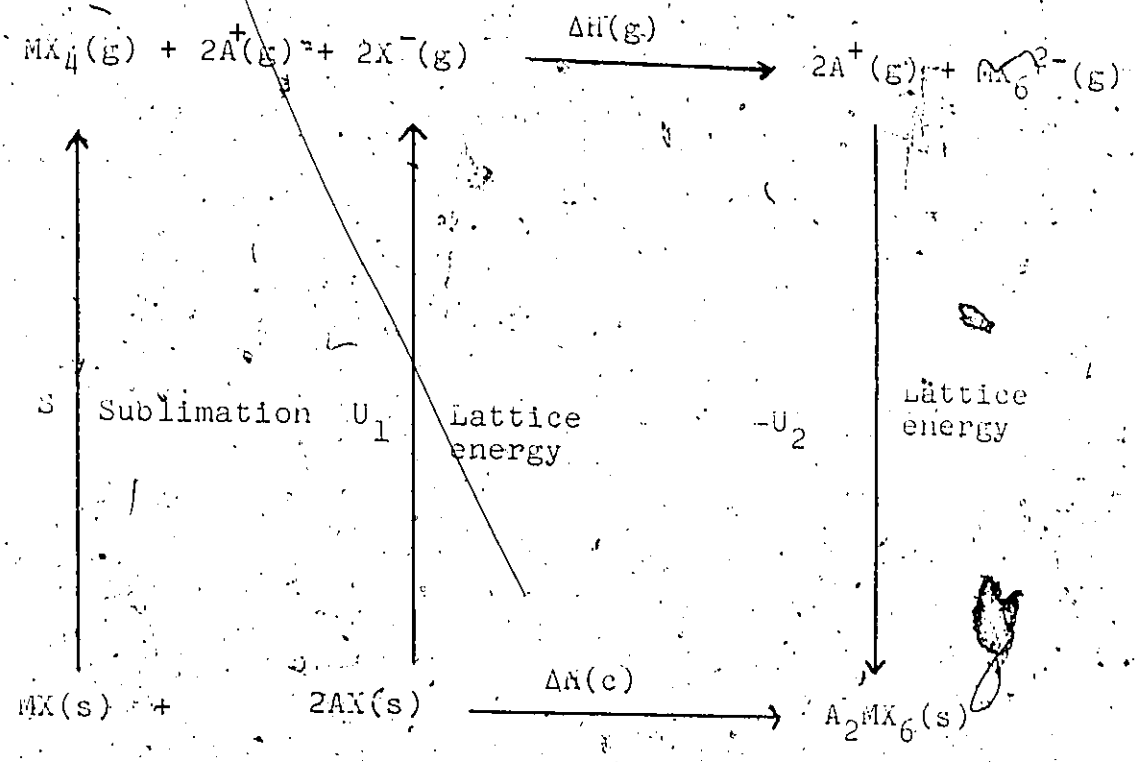

It would be very desirable to compare the reactions:

$$NbCl_4(g) + 2Cl^-(g) \longrightarrow NbCl_6^{2-}(g)$$

$$NbBr_4(g) + 2Br^-(g) \longrightarrow NbBr_6^{2-}(g)$$

By so doing, it would be possible to ascertain whether niobium exhibits any class (b) character. A class (b) metal might show a definite preferential bonding to the larger halide ion. Unfortunately, the lattice energies of Cs_2NbCl_6 and Cs_2NbBr_6 are not accurately known. Moreover, the enthalpy of sublimation of $NbBr_4$ is not recorded in the literature, but an attempt was made by the author to measure it. (See Experimental Section). As the experimental difficulties proved to be very great this project was abandoned. Instead, it was decided to estimate the required enthalpy as follows. The enthalpy of sublimation of $ZrBr_4$ is greater than that of $ZrCl_4$ by 2.5 kcal $mole^{-1}$ (37; 114). If we ignore the metal-metal bonding in NbX_4 (X=Cl and Br), we may assume a similar difference in the enthalpies of sublimation of $NbBr_4$ and $NbCl_4$.

If metal-metal bonding is taken into account, we conclude that the additional enthalpy required to break this bond should be greater for the chloride as the Nb-Nb

distance is presumably less in this compound. These considerations put a maximum value of 34 kcal $mole^{-1}$ on the enthalpy of sublimation of $NbBr_4$.

The lattice energies of Cs_2NbCl_6 and Cs_2NbBr_6 were estimated by the method of Yatsimirskii (115). If the difference in strength of the metal-metal bonds in $NbCl_4$ and $NbBr_4$ be ignored, we obtain the estimate of heats complexing given in Table XXXVI.

TABLE XXXVI

Gas phase data for Cs_2NbCl_6 and Cs_2NbBr_6 (kcal $mole^{-1}$)

Complex	X-Ray Density ($gm\ cm^{-3}$)(37)	S(37,114)	U_1(113)	U_2(114)	$-\Delta H_c$	$-\Delta H_g$
Cs_2NbCl_6	2.522	31.4	155.3	367.6	25.3	0.6
Cs_2NbBr_6	4.216*	34	149.1	356.4	23.6	0.4

*estimated

Thus the difference in the gas phase enthalpies of Cs_2NbCl_6 and Cs_2NbBr_6 is negligible. However it might be expected that the bromo complex should exhibit a much less negative enthalpy of formation (ΔH_g) (since most elements exhibit class

(a) character). Since this is not so, Nb(IV) must be capable of class (b) character.

However, the preference shown toward bromide, which is implied by these results, would be reduced if it were shown that the enthalpy of sublimation of $NbBr_4$ is significantly less than 34 kcal mole^{-1}.

Enthalpies for complexing from gaseous reactants for salts of $NbCl_6^{2-}$ and $ZrCl_6^{2-}$ ions are given in Table XXXVII for comparison. There are several conclusions that can be drawn from the data in this table.

(i) By comparison of ΔH_c for pairs of chlorozirconates and chloroniobates it appears that chlorozirconates are more stable; however the difference is small. The trend observed could be rationalized if we assume that the central atoms in these complexes engage in strong Cl $\rightarrow$ M π-bonding. Nb(IV) has one t_{2g} electron which would diminish somewhat the tendency for Nb(IV) to accept p electrons from Cl in a π-type interaction. Although Nb(IV) will have a greater effective nuclear charge than Zr(IV), it appears that the specific character of the π-interaction is of greater importance in

TABLE XXXVII

Enthalpies of complexing from gaseous reactants (kcal $mole^{-1}$)

Complex	$S_{(37,114)}$	$F_1(116)$	$V_1(87)$	ΔH_c	$-\Delta H_{(g)} + (V_2+F_2)$
K_2NbCl_6	31.4	6.41	39.0	-6.14	128.2
K_2ZrCl_6	24.7	6.41	39.0	-17.7	133.2
Cs_2NbCl_6	31.4	3.61	38.2	-25.2	140.2
Cs_2ZrCl_6	24.7	3.61	38.2	-33.4	141.7

determining the relative heats of complexing. This π interaction would decrease in going from d^o to d^6 ions, i.e. towards the right, in the periodic table for M^{4+} ions. This is further evidence for our claim that these are not simple class (a) type elements.

(ii) The niobium complexes form less exothermically than the zirconium analogue especially when the reactants are in their standard states. This is in part attributable to the heat of metal-metal bond breaking in the sublimation of $NbCl_4$. The metal-metal bond is presumed to be broken when $NbCl_4$ is volatilized ($NbCl_4$ vapour is assumed by Schäfer (34) to be monomeric). Thus some of the difference in stability of the complexes, when referred to standard states, is

attributable to the metal-metal bond in $NbCl_4$.

It should be noted that molecular dimensions and charges are very similar for the pair of atoms under discussion. For example, the lattice constant for K_2NbCl_6 is 9.97 Å (21) while that for K_2ZrCl_6 is 10.08 Å (82).

Calculated heats of complexing of $AX_{(c)} + MX_{4(c)}$

Heats of complexing were calculated by the method used by Tsintsius and Smirnova (35).

The heat of formation of K_2NbCl_6 from the elements can be determined from the equation:

$$\Delta H^\circ_f [K_2NbCl_6] = 2\Delta H^\circ_f [KCl] + \Delta H^\circ_f [NbCl_4] - 6.14$$

and has the value -380.5 kcal $mole^{-1}$. The heats of formation of KCl (113) and $NbCl_4$ (37) are -104.18 kcal $mole^{-1}$ and -166 kcal $mole^{-1}$ respectively.

From the published (20,58) density data and values of heats of formation of the corresponding gaseous alkali metal ions (113), we calculated the lattice energies of the chloro complexes K_2NbCl_6, Rb_2NbCl_6 and Cs_2NbCl_6 and the enthalpies of formation

of Rb_2NbCl_6 and Cs_2NbCl_6. The values of the lattice energies were estimated by Kapustinskii's formula, modified slightly by Yatsimirskii (115).

$$U = \frac{287.2 \sum n.Zc.Za}{r_c + r_a} \left(1 - \frac{0.345}{r_c + r_a}\right) + 2.5 \sum n.Zc.Za \quad [24]$$

where

$\sum n$ = number of ions forming a molecule of the salt.

Zc and Za = charges on the ions.

$r_c + r_a = r_z$ = inter-ionic distance A°

According to Yatsimirskii $r_z = \frac{11.85}{\sqrt[3]{J}}$ [25]

where J is the concentration of ions in one litre of the solid salt. Further,

$$J = \frac{1000.d.\sum n}{M} \quad [26]$$

where d is the density of the substance and M is its molecular weight. Using the equation $U_{M_2A} = -\Delta H_{M_2A} + 2\Delta H_{M^+} + H_{A^{2-}}$ transformed for two salts of the same type with a common anion and different cations the following relationship is obtained:

$$\Delta H°_{Rb_2NbCl_6} = \Delta H°_{K_2NbCl_6} + 2(\Delta H°_{Rb^+} - \Delta H°_{K^+}) + U_{K_2NbCl_6} - U_{Rb_2NbCl_6}$$

The calculated thermochemical data are given in Table XXXVII

TABLE XXXVIII

The calculated thermochemical data

Complex	Density (g cm^{-3})	Σr_o (Å)	U (kcal $mole^{-1}$)	$\Delta H°$ formation M^+ (kcal $mole^{-1}$)	ΔH formation from elements (kcal $mole^{-1}$)
K_2NbCl_6	2.54	4.38	378	123.07	-380.05
Rb_2NbCl_6	3.04	4.43	374	118.30	-386
Cs_2NbCl_6	3.39	4.54	366	110.08	-395

From the above data heats of complexing of Rb_2NbCl_6 and Cs_2NbCl_6 were calculated and the results are recorded in Table XXXIX From the density and lattice energy data given by Tsintsuis (35) for A_2TaCl_6 complexes and the heat of complexing for K_2TaCl_6 obtained by us, heats of complexing for Rb_2TaCl_6 and Cs_2TaCl_6 were also calculated and these are recorded in Table XXXIX.

TABLE XXXIX

Calculated heats of complexing

Complex	ΔH_c from solid chlorides	Complex	ΔH_c from solid chlorides
K_2NbCl_6	-6.14 (experimental)	K_2TaCl_6	-16.3 (experimental)
Rb_2NbCl_6	-14	Rb_2TaCl_6	-24
Cs_2NbCl_6	-22	Cs_2TaCl_6	-34

There is reasonable agreement between these calculated values and experimental values given in Table XXXIV for niobium complexes. This lends support to the experimental data for A_2NbCl_6 complexes and shows that it is fairly accurate providing there is no systematic error.

It should be noted that the method used to calculate lattice energies is very approximate but since we are interested only in obtaining differences, the exercise appears to be justified.

4. Decomposition Pressure Measurements

It was stated earlier that there is a lack of thermochemical data for bromides of less familiar elements such as niobium and tantalum. For instance, there is considerable

disagreement in the literature regarding the melting point of $NbBr_5$. Whether this variation is due to impurities in the various samples or other experimental errors is not clear.

The tetrahalides of niobium undergo thermal disproportionation (75, 117) to the corresponding pentahalide and a lower halide at elevated temperatures according to the equation:

$$(5-x)NbBr_4(s) \rightleftharpoons NbBr_x(s) + (4-x)NbBr_5(g)$$

where x may vary between the limits 2.67 and 3.03 (117). Thus a knowledge of equilibrium pressures of NbX_5 is desirable for work with these compounds at elevated temperatures. In the preparation of NbX_4, it is necessary to maintain a high pressure of NbX_5 by having an excess of NbX_5 present as a liquid. Such decomposition pressures of tetrahalides of niobium and tantalum have another important application. We have talked about "loss of individual properties" of these metals in the earlier part of this thesis. Indeed separation of these metals from each other is a challenge to the extraction metallurgist in view of the importance of these metals in modern technology. A knowledge of decomposition pressures is

extremely important in the difficult separation of the elements.

Schäfer, Bayer and Lehmann (34) have measured the decomposition pressures of $NbCl_5$ over $NbCl_4 + NbCl_x$ by vapour dew point measurements. This elegant method had been used by Hargreaves (116) as far back as 1939 to measure the vapour pressure of zinc in a brass alloy. It has also been applied to measurement of titanium tetrachloride pressure (87) in the reactions:

$$2TiCl_3 \rightleftharpoons TiCl_2 + TiCl_4$$

We have used the technique to measure the equilibrium dissociation pressures of $NbBr_5$ over mixtures of $NbBr_4$ and $NbBr_x$. The dew point method, in this study, permits the determination of pressure of the major component in a gaseous mixture of $NbBr_5$, $NbBr_4$ and $NbOBr_3$.

The dew point measurements were carried out as described in the experimental section. The results are given in Table XL and Fig. 47. The results of two different samples show excellent agreement. In Fig. 47 the two segments of the plot corresponding to solid and liquid condensed phases intersect at the melting point of $NbBr_5$. Table XLI gives the melting points obtained by various workers.

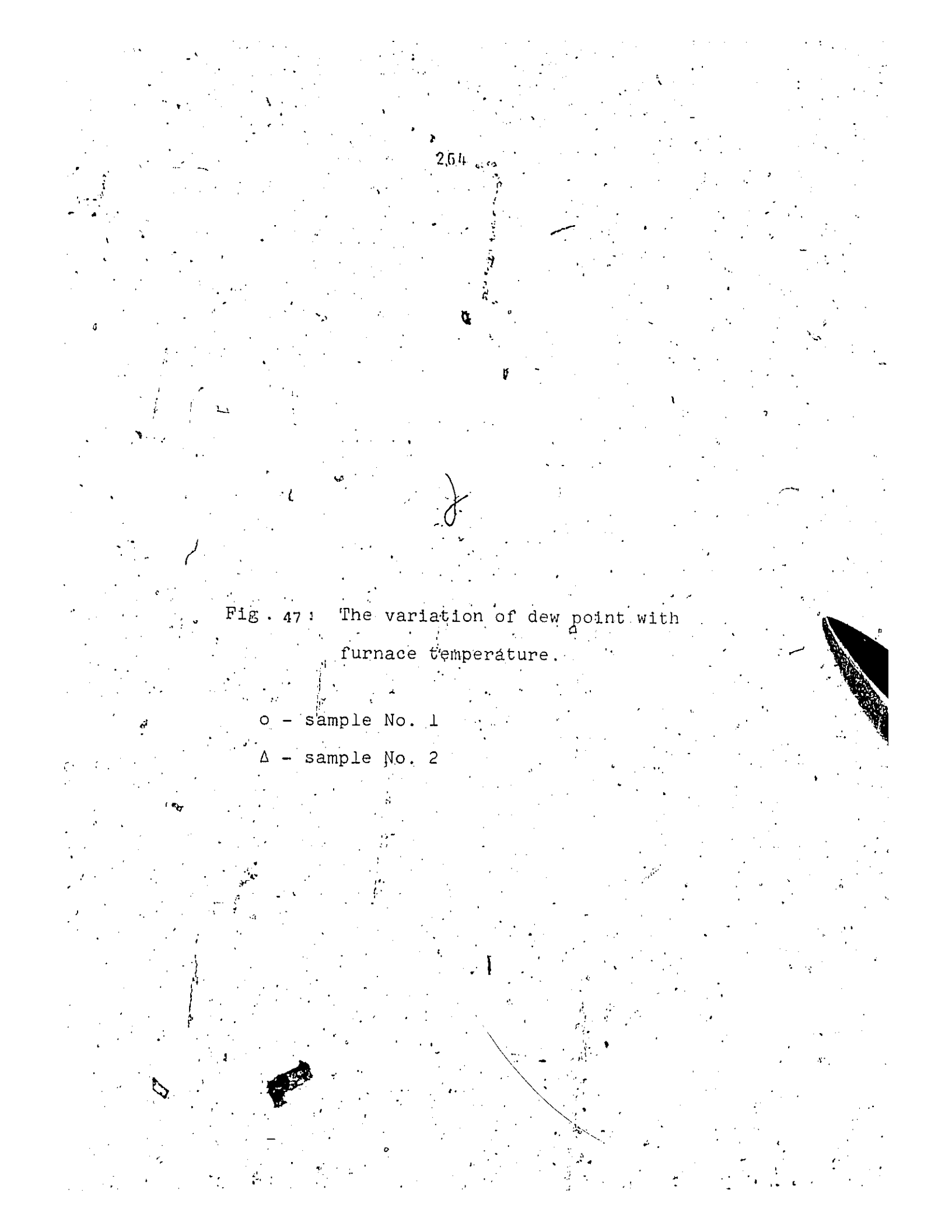

Fig. 47 : The variation of dew point with furnace temperature.

o - sample No. 1

Δ - sample No. 2

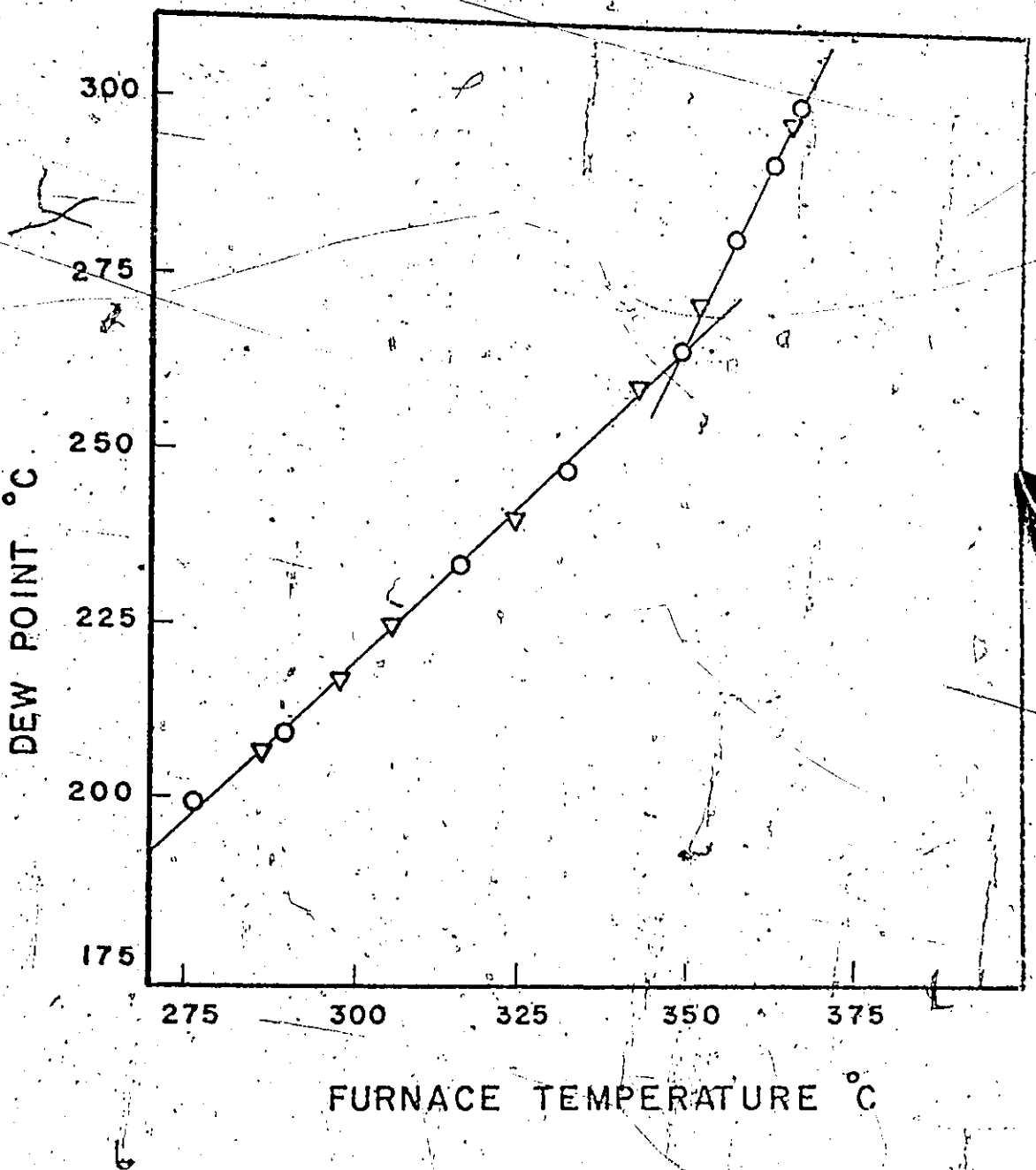
300
275
250
225
200
175
DEW POINT °C
275
300
325
350
375
FURNACE TEMPERATURE °C

TABLE XL

Equilibrium Decomposition Data

Furnace (T°K)	Dew Point (T°K)	Furnace $\frac{10^3}{T°K}$	log p (mm Hg)
549.0	474.0	1.821	0.162
559.2	479.0	1.788	0.300
562.0	482.0	1.779	0.375
570.7	490.3	1.752	0.587
579.5	497.2	1.725	0.775
588.5	506.2	1.699	0.987
597.2	513.2	1.674	1.150
604.7	520.0	1.653	1.300
614.7	532.6	1.626	1.587
621.7	537.7	1.608	1.700
624.5	546.5	1.601	1.837
630.2	555.7	1.586	1.962
636.5	566.7	1.571	2.100
639.3	573.2	1.564	2.162

TABLE XLI

Melting Point Data for $NbBr_5$

Melting Point (°C)	References
254	(119)
255	(120)
267.5	(121)
265.2	(122)
264.5	This work

To utilize the dew point data, saturation pressures of $NbBr_5$ were needed. Two previous investigations of the vapour pressures of $NbBr_5$ have been reported. Alexander and Fairbrother (121) employed a static method using a Bourden type gauge. We evaluated their data for temperatures above 239° by the method of least squares and obtained the following equations for the temperature dependence of vapour pressure:

$$\log_{10} p = 13.17 \pm 0.15 - (6.17 \pm 0.01) \frac{10^3}{T} \quad [27]$$

(239-269°C)

$$\log_{10} p = 9.30 \pm 0.06 - (4.08 \pm 0.01) \frac{10^3}{T} \quad [28]$$

(270-360°C)

Berdonosov et al. (119) obtained pressure data by employing a radioactive tracer technique in a static method. They give the following equations for the dependence of vapour pressure on temperature:

$$\log_{10} p = 12.52 \pm 0.33 - (5.782 \pm 0.158) \frac{10^3}{T} \quad [29]$$

(205-252°C)

$$\log_{10} p = 9.784 \pm 0.260 - (4.347 \pm 0.147) \frac{10^3}{T} \quad [30]$$

(252-350°C)

There is reasonably good agreement between the two sets of results only for the higher temperatures. Berdonosov et al. certainly report many more experimental points at low temperatures. However, our melting point value differs considerably from that given by Berdonosov et al. but agrees well with that of Alexander and Fairbrother. For this reason and also because Alexander and Fairbrother used direct pressure measurements, we have chosen to use their data.

Decomposition pressures of $NbBr_4$

Saturation pressures of $NbBr_5$ at the dew point correspond to the decomposition pressures of $NbBr_4$. The decomposition pressures are given in Table XI and are plotted in Fig. 48. The following equation for the temperature dependence of decomposition pressures was obtained by the method of least squares:

$$\log_{10} p = 15.02 \pm 0.38 - (8.25 \pm 0.03) \frac{10^3}{T} \qquad [31]$$

Here p is the pressure of $NbBr_5$ over $NbBr_4$ and $NbBr_x$ in mm of Hg. The straight line in Fig. 48 was obtained by the use of the above equation.

Fig. 48 : Equilibrium decomposition pressures of $NbBr_5$ over $NbBr_4$

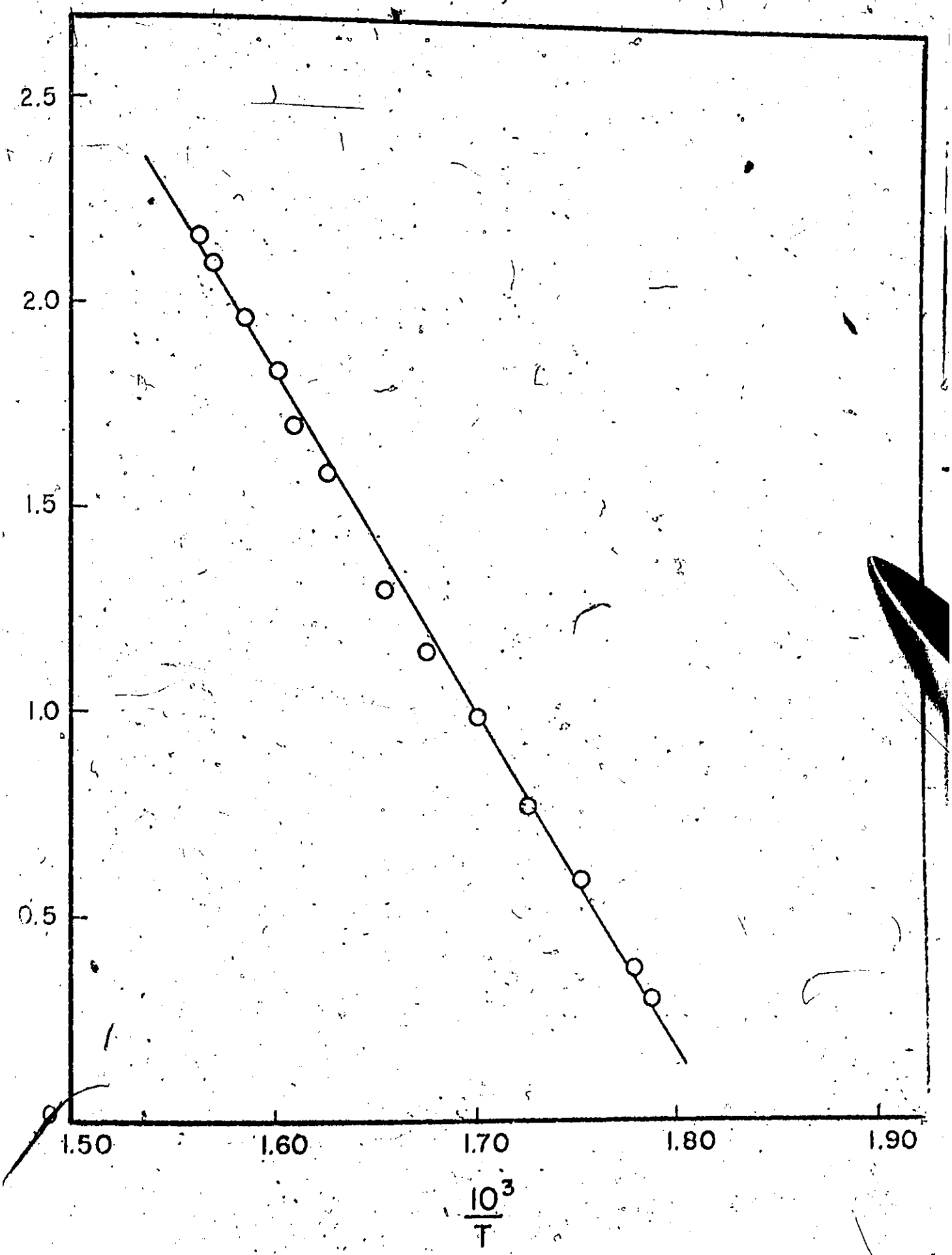
2.5
2.0
1.5
1.0
0.5
1.50
1.60
1.70
1.80
1.90
10³/T

Fig. 49 shows the existence region of solid $NbBr_4$. Line AB is the dissociation pressure curve obtained in this work. Below this line $NbBr_x$ and $NbBr_5$ vapour do not react to form $NbBr_4$. The line BCD is the vapour pressure curve for solid and liquid $NbBr_5$. Thus the tetrabromide phase is stable only within the conditions bounded by the figure ABCD. The maximum temperature at which the solid $NbBr_4$ can exist is found from Fig. 49 to be approximately 454°. It is assumed in the diagram that $NbBr_4$ is insoluble in liquid $NbBr_5$. One would expect as in the chloride system (31) that $NbBr_4$ is soluble in liquid $NbBr_5$. This would cause some reduction in the vapour pressure of liquid $NbBr_5$ and the line BC would be slightly depressed. Consequently, the quadruple point would also be somewhat lower than the point indicated. That this is not too serious an error is seen from the melting point data for $NbBr_5$ in Table XLI which indicates that the solubility of $NbBr_4$ in liquid $NbBr_5$ is not substantial.

A comparison of the $NbBr_4$ and the $NbCl_4$ decompositions indicate that the bromide is much more stable compound. For instance at 300°, we obtained a pressure of 1.3 Torr for the $NbBr_5$ pressure while Schäfer *et al.* (34) obtained 230 Torr for the pressure over $NbCl_4$ at 300°.

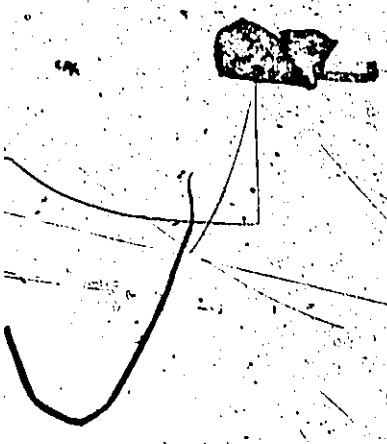

Fig. 49 : Existence regions of various niobium bromide phases.

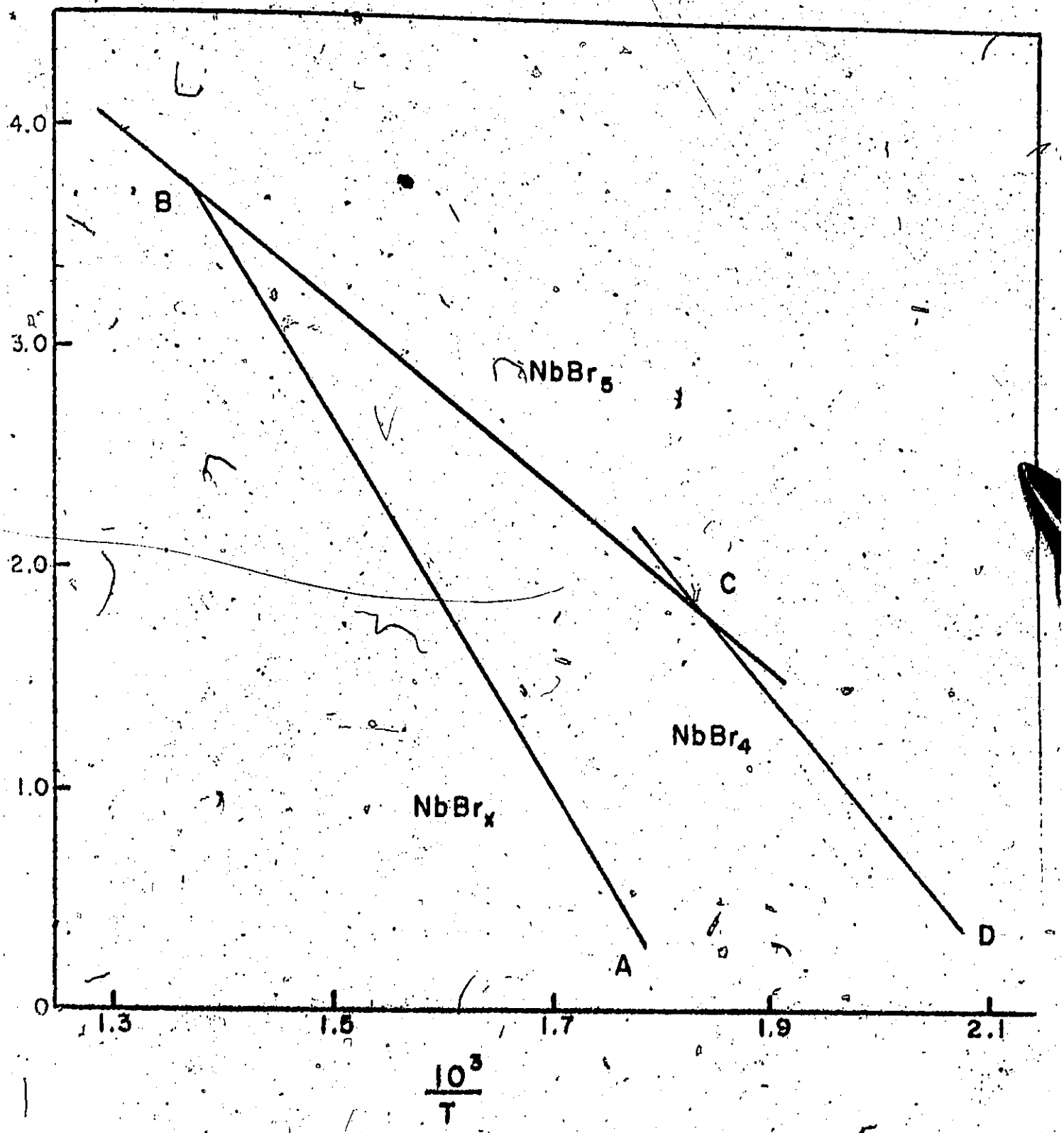
4.0
3.0
2.0
1.0
0
B
NbBr5
C
NbBr4
NbBrx
A
D
1.3
1.5
1.7
1.9
2.1
10³/T

The coefficient of the temperature dependent term in the equation for the log p leads to a value of 37.8 kcal. for the heat of the decomposition reaction producing 1 mole of $NbBr_5$ vapour. This corresponds to the decomposition of $\frac{5-x}{4-x}$ moles of $NbBr_4$. At the temperature at which this experiment was carried out, it is expected that the lower bromide phase should be close to the upper limit of the homogeniety range i.e. x should be about 3.03 (117). However as x may vary somewhat with temperature, its value remains uncertain and the reaction is not precisely defined. The above value for the heat of reaction should be understood accordingly.

It should be noted that the changes in the vapour pressure with temperature were too great to be accounted for by the temporary Boyles' Law expansion. For instance a rise of 3° in furnace temperature gives a rise of 3° in dew point which corresponds to a rise of about 10 percent in vapour pressure of $NbBr_5$. However a rise of 3° would in fact elevate the vapour pressure by only 1 percent.

REFERENCES

1. C. Marignac, Ann. Chim. Phys., (4), 13 (1868).
2. C.H. Warren, Chem. News, 94, 298 (1906).
3. F.D. Metzger and C.E. Taylor, Z. Anorg. Chem., 62, 383 (1909).
4. W.D. Treadwell, Analyst, 47, 533 (1922).
5. W.D. Treadwell, Helv. Chim. Acta, 5, 806 (1922).
6. D. Cozzi and S. Vivarelli, Z. Anorg. Allg. Chem., 279, 165 (1955).
7. H.G. Schnering, H. Wohrle and H. Schäfer, Naturwissenschaften, 48, 159 (1961).
8. H.S. Harned, J. Amer. Chem. Soc., 35, 1078 (1913).
9. W.H. Chapin, J. Amer. Chem. Soc., 32, 323 (1910).
10. R.E. McCarley, B.G. Hughes, F.A. Cotton and R. Zimmerman, Inorg. Chem., 4, 1491 (1965).
11. F.A. Cotton and T.E. Haas, Inorg. Chem., 3, 10 (1964).
12. M.B. Robin and N.A. Keubler, Inorg. Chem., 4, 978 (1965).
13. D.C. Bradley and M.H. Chisolm, J. Chem. Soc., (A), (1971), 1511.
14. J.B. Hamilton and R.E. McCarley, Inorg. Chem., 9, 1333, 1339 (1970).
15. G.W.A. Fowles, D.J. Tidmarsh and R.A. Walton, J. Inorg. Nucl. Chem., 31, (1969), 2373.
16. R.J.H. Clark, D.L. Kepert, J. Lewis and R.S. Nyholm, J. Chem. Soc., (1965), 2865.

17. M. Allbutt, K. Feenan and G.W.A. Fowles, J. Less-Common Metals, 6, 299 (1964).

18. B.G. Korshunov and V.V. Safonov, Russ. J. Inorg. Chem., 6, 385 (1961).

19. V.V. Safonov, B.G. Korshunov and Z.N. Shevtsova, Russ. J. Inorg. Chem., 7, 1021, 1019 (1962).

20. V.V. Safonov, B.G. Korshunov, Z.N. Shetsova and L.G. Shadrova, Russ. J. Inorg. Chem., 9, 763 (1964); ibid., 10, 359 (1965).

21. (a) B.A. Torp, Doctoral Thesis, Iowa State University, Ames, Iowa, 1964.
(b) B.A. Torp, Diss. Abstr., 25, 2751 (1964).

22. A.D. Westland and N.C. Bhiwandker, Can. J. Chem., 39, 1284 (1961).

23. A.D. Westland and N.C. Bhiwandker, Can. J. Chem., 39, 2353 (1961).

24. A.D. Westland, Can. J. Chem., 41, 2692 (1963).

25. A.D. Westland, Can. J. Chem., 46, 3591 (1968).

26. S.M. Horner, F.N. Collier and S.Y. Tyree, J. Less-Common Metals, 13, 85 (1967).

27. S.M. Horner, R.J.H. Clark, B. Crociani, D.B. Copley, W.W. Horner, F.N. Collier and S.Y. Tyree Jr., Inorg. Chem., 7, 1859 (1968).

28. G.W.A. Fowles, D.J. Tidmarsh and R.A. Walton, Inorg. Chem., 8, 631 (1969).

29. W.D. Benzinger, Ph.D. Thesis, Pennsylvania State University, Pennsylvania, 1967.

30. H. Schäfer, C. Göser and L. Bayer, Z. Anorg. Allg. Chem., 265, 258 (1951).

31. H. Schäfer and C. Pietruck, Z. Anorg. Allg. Chem., 266, 151, (1951).

32. H. Schäfer and F. Kahlenberg, Z. Anorg. Allg. Chem., 305, 178 (1960).

33. H. Schäfer and K.D. Dohmann, Z. Anorg. Allg. Chem., 311, 139 (1961).

34. H. Schäfer, L. Bayer and H. Lehmann, Z. Anorg. Allg. Chem., 268 (1952).

35. V.M. Tsintsius and E.K. Smirnova, Russ. J. Inorg. Chem., 14, 1729 (1969).

36. E.K. Smirnova and I.V. Vasil'kova, Vestn. Leningrad. Univ., Fiz. Khim., 20, 161 (1965).

37. J.H. Canterford and R. Colton in "Halides of the Second and Third Row Transition Metals". John Wiley and Sons Ltd., New York. 1st Edition (1968).

38. V.N. Fedetov, N.S. Garif'yanov and B.M. Kozyrev, Dokl. Akad. Nauk. SSSR., 145, 1318 (1962).

39. M. Larden and H.H. Günthard, J. Chem. Phys., 44, 2010 (1966).

40. S. Maniv, W. Low and A. Gabay, Phys. Lett., A, 29(9), 563 (1969).

41. D.P. Johnson and R.D. Bereman, J. Inorg. Nucl. Chem., 34, 679 (1972).

42. R.D. Brown and C.H. Bruebaker, Inorg. Chem., 8, 2480 (1969).

43. Y.Y. Kharitonov and N.P. Lipatova, Izv. Akad. Nauk SSSR, Neorg. Mater., 3, 405 (1967).

44. J.G. McCullough and L. Meites, J. Electroanal. Chem. Interfacial Electrochem., 18, 123 (1968).

45. I.S. Morozov and L.P. Lipotova, Russ. J. Inorg. Chem., 11 550 (1966).

46. V.V. Safonov and B.G. Korshunov, Izv. Akad. Nauk SSSR, Neorg. Mater., 1, 604 (1965).

47. T.I. Beresenev, G.P. Gosteva, A.N. Ketov, Russ. J. Inorg. Chem., 16, 209 (1971).

48. T.I. Beresenev, G.P. Gosteva, A.N. Ketov, Russ. J. Inorg. Chem., 16, 1284 (1971).

49. A.I. Morozov and I.I. Leonova, Russ. J. Inorg. Chem., 17, 1402 (1972).

50. I.S. Morozov and Sun In'-Chzhu, Russ. J. Inorg. Chem., 4, 307 (1959).

51. I.S. Morozov and Sun In'-Chzhu, Russ. J. Inorg. Chem., 4, 1176 (1959).

52. I. Zvara and L.K. Tarasov, Russ. J. Inorg. Chem., 7, 1388 (1962).

53. R.L. Lister and S.N. Flengas, Can. J. Chem., 43, 2947 (1965).

54. J.E. Dutrizac and S.N. Flengas, Can. J. Chem., 45, 2317 (1967).

55. J.E. Dutrizac and S.N. Flengas, Can. J. Chem., 45, 2313 (1967).

56. S.N. Flengas, J.E. Dutrizac and R.L. Lister, Can. J. Chem., 46, 425 (1968).

57. V.V. Safonov, B.G. Korshunov, Z.N. Shevtsova and S.I. Bakum, Russ. J. Inorg. Chem., 9, 914 (1964).

58. V.V. Safonov, B.G. Korshunov, T.N. Zimina and Z.N. Shevtsova, Russ. J. Inorg. Chem., 11, 488, 1146 (1966).

59. V.V. Safonov, B.G. Korshunov and A.A. Yarovoi, Russ. J. Inorg. Chem., 11, 918 (1966).

60. A. Broll, H.G. von Schnering and H. Schäfer, J. Less-Common Metals, 22, 235 (1970).

61. A. Simon, H.G. Schnering and H. Schäfer, Z. Anorg. Allg. Chem., 361, 235 (1968).

62. P.B. Fleming, L.A. Meuller and R.E. McCarley, Inorg. Chem., 6, 1 (1967).

63. R.A. Mackay and R.F. Schneider, Inorg. Chem., 6, 549 (1967).

64. V.V. Safonov, B.G. Korshunov, T.N. Zimina and Z.N. Shevtsova, Russ. J. Inorg. Chem., 11, 1148 (1966).

65. H. Schäfer and L. Grau, Z. Anorg. Allg. Chem., 275, 198 (1954).

66. H. Schäfer, R. Gerken and H. Scholz, Z. Anorg. Allg. Chem., 335, 96 (1965).

67. R.E. McCarley and J.C. Boatman, Inorg. Chem., 4, 1486 (1965).

68. P.W. Seabough and J.D. Corbett, Inorg. Chem., 4, 76 (1965).

69. P.J. Kuhn and R.E. McCarley, Inorg. Chem., 4, 1482 (1965).

70. G.F. Knox and T.M. Brown, Inorg. Chem., 8, 1401 (1969).

71. A.I. Vogel, "A Textbook of Practical Organic Chemistry including Qualatative Organic Analysis", Longmans, Green and Co., London, 2nd Edition, 1948.

72. H. Schäfer and K. Dohmann, Z. Anorg. Allg. Chem., 300, 1 (1959).

73. C.H. Bruebaker and R.C. Young, J. Amer. Chem. Soc., 73 4179 (1951).

74. Parr Manual, No. 121, Parr Instrument Co., Moline, Illinois, U.S.A.

75. R.E. McCarley and B.A. Torp, Inorg. Chem., 2, 540 (1963).

76. R.E. McCarley and J.C. Boatman, Inorg. Chem., 2, 547 (1963).

77. S.S. Berdonosov, A.V. Lapitskii and L.G. Vlasov, Russ. J. Inorg. Chem., 7, 1125 (1962).

78. H. Schäfer and C. Pietruck, Z. Anorg. Allg. Chem., 264, 1, (1951).

79. S.A. Shchukarev, J.V. Vasil'kova and B.N. Sharupin, Vestn. Leningrad. Univ., Fiz. Khim., 20, 72 (1959).

80. R.F. Rolston, J. Amer. Chem. Soc., 79, 5409 (1957).

81. H. Schäfer, Angew. Chem., (1955), 67, 748.

82. R.L. Lister and S.N. Flengas, Can. J. Chem., 42, 1102 (1964).

83. W. Kiefer and H.J. Bernstein, Appl. Spectrosc., 25, 609 (1971).

84. H. Lux, "Anorganische Chemische Experimentierkunst", Johann Ambrosius Barth, Verlag, Leipzig (1959), p. 443.

85. H. Schäfer and C. Pietruck, Z. Anorg. Allg. Chem., 267, 174, 180 (1951).

86. N.N. Greenwood and P.G. Perkins, J. Inorg. Nucl. Chem., (1957), 4, 291.

87. O. Kubaschewski, E.Ll. Evans and C.B. Alcock, "Metallurgical Thermochemistry", Pergamon Press, London, England. 4th Ed. (1965).

88. P. Langevin, J. Phys., 4, 678 (1905).

89. J.H. van Vleck, "Electric and Magnetic Susceptibilities", Oxford University Press, London, 1932.

90. K.W.H. Stevens, Proc. Roy. Soc. (London), A219, 542 (1953).

91. M. Gerloch and J.R. Miller, Progr. Inorg. Chem., 10, 1 (1968).

92. M.J. Kotani, J. Phys. Soc. Jap., 4, 293 (1949).

93. A.D. Liehr, J. Phys. Chem., 64, 43 (1960).

94. A. Earnshaw, B.N. Figgis, J. Lewis and R.S. Nyholm, Nature, 179, 1121 (1957).

95. H. Kamimura, S. Koide, H. Sekiyama and S. Sugano, J. Phys. Soc. Jap., 15, 1264 (1960).

96. A.D. Westland, Can. J. Chem., 50, 1468 (1972).

97. T.M. Dunn, Trans. Faraday Soc., 57, 144 (1961).

98. T.M. Dunn, J. Chem. Soc., 1959, 623.

99. A. Earnshaw, "Introduction to Magnetochemistry", Academic Press, New York, 1st Ed. 1968.

100. B.N. Figgis, "Introduction to Ligand Fields", John Wiley and Sons, New York, 1st Ed. (1964), Chapter 10.

101. P.W. Selwood, "Magnetochemistry", Interscience Publishers, Inc., New York, 2nd Ed. (1956).

102. R.S. Nyholm, Pure Appl. Chem., 17, 1 (1968).

103. J.H.E. Griffiths, J. Owen, J.G. Park and M.P. Partridge, Proc. Roy. Soc. (London), A250, 84 (1959).

104. P. Kubelka and F. Munk, Z. Tech. Physik., 12, 513 (1931).

105. H. Bethe, Ann. Physik [5], 3, 133 (1929).

106. J. Owen, Proc. Roy. Soc. (London), A 227, 183 (1955).

107. C.J. Ballhaussen, "Introduction to Ligand Field Theory", Interscience Publishers, Inc., New York, 1st Ed. (1962).

108. F.A. Cotton and G. Wilkinson, "Advanced Inorganic Chemistry", Interscience Publishers, Inc., New York, 2nd Ed. (1962).

109. T.M. Dunn, "Modern Co-ordination Chemistry", Interscience Publishers, Inc., (1960)., Chapter 4.

110. P. Day, Inorg. Chem., 2, 452 (1963).

111. P.M. Boorman and B.P. Straughan, J. Chem. Soc., (1966), A, (1954).

112. D.M. Adams, "Metal-Ligand and Related Vibrations", Edward Arnold (Publishers) Ltd., London, England (1967).

113. F.D. Rossini, Nat. Bur. Stand., Circular 500, (1952).

114. E.M. Larsen, Adv. Inorg. Chem. Radiochem., 13, 1 (1970).

[illegible] A.B. Yastomirskii, Russ. J. Inorg. Chem., 6, 918 [illegible]

[illegible] Handbook of Chemistry and Physics, The Chemical Co., Cleveland, Ohio, 50th ed., 1969-1970.

[illegible] H. Schäfer, C. Göser and L. Bayer, Z. Anorg. Allg. Chem., 265, 258 (1951).

[illegible] A. Hargreaves, J. Inst. Metals, 1939, 64, 119.

[illegible] B.G. Berdonosov, A.V. Lapitskii and E.N. Yakov[illegible], Zh. Neorg. Khim., 10, 173 (1965).

[illegible] E.A. Nisolison and [illegible] Dokl. Akad. Nauk SSSR, Inorg. Chem., 9, 1117 (1964).

[illegible] A.M. Alexander and F. Fairbrother, J. Chem. Soc., 1319 (1949).

[illegible] G. Brauer (ed.), Handbook of Preparative Inorganic Chemistry, Vol. 2, Academic Press, New York, N.Y., 1965, p. 1313.